Charles University
Faculty of Science

Study programme: Biology

Branch of study: Immunology

Bc. Peter Holíček

Activation and regulation of cell death in senescent cancer cells

Aktivace a regulace buněčné smrti v senescentních nádorových buňkách

Master thesis

Supervisor: RNDr. Ladislav Anděra, CSc.

Prague 2018

Prehlásenie:

Prehlasujem, že som záverečnú prácu spracoval samostatne a že som uviedol všetky použité informačné zdroje a literatúru. Táto práca ani jej podstatná časť nebola predložená k získaniu iného alebo rovnakého akademického titulu.

V Prahe, 12.8.2018

Podpis

Acknowledgements

Here, I would like to thank to my supervisor RNDr. Ladislav Anděra, CSc. for guiding my diploma project, for his help and his support. I would also like to thank to Prof. Ing. Jiří Neužil, CSc. for having me in his Laboratory of Molecular Therapy and to all members of his laboratory who were willing to help anytime I needed. Additionally, I would also like to thank to MUDr. Zdeněk Hodný, CSc. for his help with my project and to Mgr. Tomáš Zikmund, Ing. Galina Kislik and MUDr. Lukáš Lacina, Ph.D. as they helped me with data gathering.

Lastly, but not less importantly I want to say big thanks to my family as I can always rely on them.

Abstract

Cellular senescence is a distinct cell state, characteristic by cessation of cell proliferation and it is accompanied by specific morphological and biochemical alterations. Increasing and persisting incidence of senescence cells has been shown to have detrimental effect on an organism largely contributing to its ageing. Senescent cells also positively support tumour growth and can even stimulate carcinogenic transformation of surrounding cells. Moreover, senescence can be induced even in tumour cells spontaneously or by chemotherapy. Regardless of an initial stimuli and type of cells, there are two main senescence inducing pathways p16/pRb and p53/p21. Both senescent cells as well as senescent cancer cells seems to have modified apoptotic signalling at the level of mitochondria and Bcl-2 family proteins. In this study, we aimed to analyse effect of senescent state as well as pre-senescent (growth arrested state) induced by p16/pRb and p53/p21 signalling pathways on the response of H28 mesothelioma cancer cells-derived clonal cultures to various cell death-inducing stimuli. By inducible expression of p16 and p21 proteins in doxycycline-dependent manner, we forced cells to acquire senescent-like phenotype, which we detailly characterised. Our results showed that senescent-like phenotype, manifests same phenotypical features regardless of employed signalling pathway p16/pRb or p53/p21, however, with varying intensity and efficacy. We documented that p16-expressing cells acquire weaker senescent-like phenotype, proliferate and produce less reactive oxygen species and have less mitochondria then senescent p21-expressing cells. P16- and p21-expressing cells in arrested and especially in senescent-like state have increased levels of Bcl-2 and antioxidant defence proteins. Bioenergetic analysis revealed increased respiration and glycolytic rates in both arrested and senescent-like cells, again to lesser extent in p16-expressing cells. Interestingly, despite differently pronounced phenotypes and bioenergetic profiles, p16 and p21 senescent like cells altered their responses to selected death-inducing stimuli to similar levels, while in arrested state they did not manifested any alterations compared to their proliferative counterparts. We also showed that senescent-like cancer cells are more resistant to ROS-mediated cell death by mitoVES and also to TRAIL-induced apoptosis enhanced by homoharringtonine. Moreover, they became more sensitive to drug ABT-737, which inhibits Bcl-2/BcL-

XL/Bcl-W, thus triggers intrinsic apoptotic pathway. Our results confirmed and extended knowledge about altered response of senescent cells to death inducing stimuli and at the same time they imply, that these altered responses are consequences intracellular biochemical changes associated with senescent-like phenotype independently of the terminal cell cycle arrest.

Abstrakt

Bunková senescencia je špecifický bunkový stav charakteristický zastavením proliferácie, sprevádzaný typickými morfologickými a biochemickými zmenami. Narastajúci a pretrvávajúci výskyt senescentných buniek v organizme sa ukázal ako škodlivý a prispievajúci k jeho starnutiu. Senescentné bunky podporujú rast nádoru a dokonca aj stimulujú nádorovú transformáciu. Senescencia môže byť navyše indukovaná aj v samotných nádorových bunkách a to napríklad spontánne alebo chemoterapiou. Vzhľadom na prvotný stimul a na druh buniek, existujú dve hlavné senescenciu-indukujúce signálne dráhy sprostredkované proteínami p16/Rb a p53/p21. Senescentné, tak ako aj rakovinné senescentné bunky, sa zdajú mať pozmenené apoptotické signálne dráhy na úrovni mitochondrií a proteínov rodiny Bcl-2. V tejto štúdii sme sa zamerali na analýzu vplyvu senescentného a pre-senescentného (v proliferácii zastaveného) stavu v klonálnych kultúrach mezoteliomálnej rakovinnej línie H28, indukovaného buď signálnou dráhou p16/Rb alebo p53/p21 na odpoveď voči smrť-indukujúcim stimulom. Prostredníctvom doxycyklín-závislej inducibilnej expresie proteínov p16 a p21 sme bunkám navodili senescenciu-podobný fenotyp, ktorý sme podrobne charakterizovali. Zdokumentovali sme, že p16-exprimujúce bunky získajú slabší senescenciu-podobný fenotyp, proliferujú, produkujú menej reaktívnych foriem kyslíka (ROS) a majú menej mitochondrií v porovnaní s p21-exprimujúcimi bunkami. p16- aj p21-exprimujúce bunky, tak ako v senescencii-podobnom tak aj v pre-senescentnom stave, majú zvýšenú úroveň Bcl-2 proteínov a taktiež proteínov antioxidačnej odpovede. Bioenergetická analýza u týchto buniek taktiež ukázala zvýšenú respiráciu a glykolytickú hladinu, aj keď u p16-exprimujúcich buniek v nižšej miere. Pozoruhodne, napriek rozdielne intenzívne prejaveným fenotypom a bioenergetickým profilom, p16 a p21 bunky v senescencii-podobnom stave, zmenili mieru bunečnej smrti na podobnú úroveň voči vybraným srmť-indukujúcim stimulom, zatiaľ čo bunky v pre-senescentnom stave nevykazovali žiadne zmeny v porovnaní s proliferujúcimi protikladmi. Ukázali sme, že p16 a p21 bunky v senescencii-podobnom stave sú viac rezistentné voči ROS-mediovanej bunečnej smrti prostredníctvom látky mitoVES a taktiež voči TRAIL-indukovanej homoharringtoninom zefektívnenej apoptóze. Naproti tomu sme u týchto buniek preukázali zvýšenú citlivosť ku chemikálii ABT-737, ktorá

inhibuje proteíny Bcl-2/BcL-XL/Bcl-W a spúšťa vnútornú apoptotickú dráhu. Naše výsledky potvrdili a rozšírili znalosti o odpovedi senescentných buniek voči smrť-indukujúcim látkam a implikujú, že tieto pozmenené odpovede sú skôr výsledkom samotných biochemických zmien súvisiacich so senescentným fenotypom, a to nezávisle od terminálnej zástavy bunečného cyklu.

Kľúčové slová: regulovaná buněčná smrt, apoptóza, senescencia, nádorové buňky, buněčný cyklus, mitochondrie

Table of contents

List of Abbreviations

ABB	Annexin V binding buffer
ANT2	Adenine Nucleotide Translocase 2
ATM	Ataxia-telangiectasia-mutated kinase
ATR	Ataxia Telangiectasia and Rad3-related kinase
BSA	Bovine Serum Albumin
CAD	Caspase-activated DNase
CCCP	Carbonyl Cyanide m-chlorophenyl hydrazone
CDK	Cyclin Dependant Kinase
CDKi	Cyclin Dependant Kinase inhibitor
DAPI	4′,6-Diamidino-2-phenylindole dihydrochloride
DED	Death Effector Domain
DD	Death Domain
ddH_2O	double distilled H_2O
DDR	DNA Damage Response
DMEM	Dulbecco´s Modified Eagle´s Media
DNA	Deoxy-ribonucleotide Acid
Doxy	Doxycycline
DR	Death Receptors
ECAR	Extracellular Acidification Rate
ETC	Electron Transport Chain
FACS	Fluorescence-activated Cell Sorting
FBS	Fetal Bovine Serum
ICAD	Inhibitor of Caspase-activated DNase
IMM	Inner Mitochondrial Membrane
IMS	Intramembrane Mitochondrial Space
MDM2	Mouse Double Minute 2 homolog
MOMP	Mitochondrial Outer Membrane Permeabilization
OCR	Oxygen Consumption Rate

OMM	Outer Mitochondrial Membrane
PCNA	Proliferating cell nuclear antigen
PBS	Phosphate-Buffered-saline
PBST	Phosphate-Buffered-saline Tween 20
PcG	Polycomb group Protein
PFA	Paraformaldehyde
PINK1	PTEN-induced putative kinase 1
RCD	Regulated Cell Death
RNA	Ribonucleic Acid
ROS	Reactive Oxygen Species
RPMI	Roswell Park Memorial Institute medium
RS	Replicative Senescence
Sa-β-Gal	Senescence Associated Beta Galactosidase
SAHF	Senescent Associated Heterochromatin foci
SASP	Senescence Associated Secretory Phenotype
SAMD	Senescent Associated Mitochondrial Dysfunction
SBM	Seahorse Base Media
γH2AX	phosphorylated version of histone H2AX

1 Introduction

Cellular senescence is a distinct cell state in which cells stop to proliferate, despite having all nutrients, growth factors and enough space. Cells enter senescent state either after specific number of divisions or under various stressful conditions (metabolic stress, excessive DNA damage etc.) as their further proliferation would be undesirable. Cellular senescence is very important fail-safe mechanism preventing transformation of pre-malignant cells and has also many physiological roles in wound healing and embryogenesis.

Senescent cells secrete large amounts of factors affecting neighbouring cells (inflammatory cytokines, growth factors etc.) thus long-term presence of senescent cells cause deterioration of organism by promoting age-related pathologies. Many chemotherapeutic drugs that fail to induce cell death due to e.g. low local drug concentration can drive cancer cells instead into senescence state. Initially, senescence-inducing side effects of chemotherapeutic treatments were considered as a positive outcome as they stop proliferation of malignant cancer cells. However, it turned out, that in long term, senescence cancer cells residing in tumour micro-environment have negative role, promoting tumour growth and invasiveness.

For successful cancer treatments, as well as for preventing senescence-driven pathologies, it would be beneficial to eliminate these cells from the organism. Senescent cells alter their response toward pro-apoptotic agents and it is therefore important to analyse specific changes in their apoptotic signalling, that could eventually be exploited in therapeutic approaches.

2 Literature review

2.1 Cellular senescence

Cellular senescence is a state of cells defined as irreversible cell cycle arrest with characteristic morphological and biochemical alterations. It has been firstly described as finite proliferative/replicative potential of human fibroblast in vitro, despite having all necessary nutrients, sufficient space and growth factors (Hayflick and Moorhead 1961). This phenomenon is now known as replicative senescence (linked to telomeres erosion) and finite proliferative capacity is referred Hayflick limit. Cells with specific senescent phenotype have been since then also observed in vivo (Dimri et al. 1995; Krishnamurthy et al. 2004) and it has been documented that their accumulation correlates with increasing age in primates (Jeyapalan et al. 2007). Senescence is triggered by different stress stimuli including DNA damage, oncogene activation, telomere shortening, metabolic perturbation and others. It serves mostly as intrinsic fail-safe system to prevent carcinogenic transformation of pre-malignant cells in case of apoptotic failure with other roles in tissue formation and remodelling.

2.1.3 Physiological roles of cellular senescence

As already mentioned, cellular senescence is important mechanism that prevents pro-cancerous cellular transformation (Serrano et al. 1997) and participates in clearance of unwanted structures, such as scars or tissues that are no longer needed, leading to organismal rejuvenation and tissue remodelling. Many of these effects are orchestrated by senescent associated secretory phenotype (SASP) and executed by immune system.

For example, oncogene-mediated transformation can be avoided by oncogene-induces cellular senescent program thus suppressing tumorigenesis and promotes subsequent clearance of senescent (pro)cancer cells in SASP-mediated immune clearance fashion.

Cellular senescence also has a profound role in embryogenesis removing unnecessary cells from tissues by SASP-mediated recruitment of macrophages (Muñoz-Espín et al. 2013) and enhancing wound healing by secreting PDGF-AA and thus depletion of

senescent cells can impair healing process (Demaria et al. 2014). Moreover, presence of cells with increased expression of CDKN2A/B (p16INK4a, ARF, and p15INK4b) locus has been shown to negatively corelate with progression of atherosclerotic plaque (Harismendy et al. 2011).

2.1.3.1 SASP

Senescence cells produce and secrete number of proteins with different functions including proinflammatory cytokines, chemokines, growth factors, and proteases. This distinctive secretome is called senescence associated secretory phenotype or SASP and its composition slightly varies in cell type-depending manner. SASP is interconnected with DNA damage in senescent cells, which is inflicted either directly by stress stimuli or through increased ROS production by dysfunctional mitochondria (Passos et al. 2010). Despite different ways of triggering senescence, SASP is conserved and is regulated by Nuclear factor κB (NF-κB) and CCAAT/enhancer binding protein beta (Acosta et al. 2008). SASP is composed of interleukins, chemokines (e.g. - TNF-α, IFN-γ, IL-6, IL-7, IL-1a, -1b, IL-13, IL-15, IL-8, TGFβ, MMPs, MCP-1, RANTES, MCP-2, MCP-4, MIP-1α, β, MIP-3α, GM-CSF), and growth factors (EGF, HGF, VEGF, Angiogenin and others). These secreted molecules cause autocrine and paracrine signalling in neighbouring cells with both beneficial and detrimental effects as mediating clearance of senescent cells by cells of the immune system, activation of innate and adaptive immunity, carcinogenesis, induction of senescence in surrounding environments, remodelling of extracellular matrix and others.
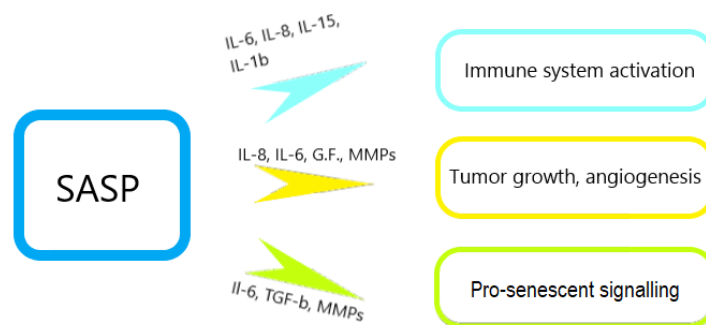
Figure 1. Pleiotropic functions of SASP in autocrine or paracrine fashion. SASP is composed of variety of cytokines, growth factors and metalloproteinases which orchestrate and propagate different physiological and pathophysiological functions.

2.1.3.2   Immunosurveillance of senescence

Regulation of senescent cell presence is not fully understood yet, however it seems that immune surveillance is one of the major mechanisms. Senescent cells express adhesion molecules and produce SASP comprising interleukins and cytokines, which results into intensive cross talk between senescent cells and immune system.

One of the first evidences supporting immunosurveillance, came from studying mouse model of hepatocellular carcinoma whereas upon restoration of endogenous p53, tumour cells entered senescent state and were subsequently eliminated by macrophages, neutrophils and NK cells.

NK cells – express different chemokine receptors such as CCR2, CCR5, CXCR1, CXCR3, and CX3CR1. Senescent cells produce many cytokines including IL-12, IL-15 and chemokines (MCP-1, RANTES, MCP-2, MCP-4, MIP-1α, β) by which they attract and stimulate NK cells. Subsequent recognition of senescent cells is mediated by RAE1ε, MICA and ULBP2, ligands of NKG2D receptor of NK cells and their engagement is vital for efficient removal of senescent cells (Iannello et al. 2013; Iannello and Raulet 2013; Sagiv et al. 2016)

NK cells kill their target either by cytolytic granule exocytosis or by activation of death receptors (DR) and they are capable to use both these mechanisms for the elimination of senescent cells. It has been shown that NK cells are able to eliminate senescent hepatic stellate cells (HSCs) from liver by perforin/granzyme-mediated mechanism. This clearance was accompanied by decline of fibrosis and subsequent tissue regeneration (Krizhanovsky et al. 2008; Sagiv et al. 2013). Senescent cells also upregulate FasR and are very sensitive to Fas mediated apoptosis (Crescenzi et al. 2011) which makes them a suitable target for elimination via activation of death receptors by NK cells.

Monocytes/Macrophages – also express various chemokine receptors sensitive to MCP-2, MCP-3, MCP-4, RANTES, MIP-1α, MIP-1β, that are also secreted by senescent cells, thus attracting them to their site. Senescent HSCs in diseased liver also secrete IFNγ and IL-6 (SASP) which induce and attract M1 type of macrophages into their site and subsequently eliminate them (Lujambio et al. 2013). M1 macrophages are part of

Th1 immune response, exerting anti-tumour activities and as documented, they are also capable of attacking senescent cells. Interestingly, p53-deficient HSCs that could not enter senescence, secrete high levels of M2 macrophages activating IL-4 (Lujambio et al. 2013). M2 macrophages are immune-suppressive with wound healing abilities preferring tumour progression and metastasis (Mantovani et al. 2013) suggesting that even mere senescence induction can have positive effect on organism .

Th1 CD4+ T cells – are also attracted to the site of senescent cells by SASP (Kang et al. 2011). They do not exert direct cytolytic actions, however they are antigen specific and reinforce Th1 response by secreting Th1 polarizing cytokine (IFNγ, IL-12) enhancing function of M1 Macrophages and Dendritic cells, which are also involved in Th1 response against senescent cells. Existence and presence of senescence epitope-specific CD4+ T cells was documented in NrasG12V-induced senescent mouse model (Kang et al. 2011). Interestingly CD8+ T cells, despite being part of Th1 response with direct cytolytic functions, apparently do not participate in immunosurveillance of senescent cells, despite being part of Th1 response with direct cytolytic functions.

2.1.3 Pathophysiological roles of cellular senescence

Persisting presence of senescent cells in organism has largely negative effects. These effects include accelerated aging, promoting age-related diseases and autoimmune chronic inflammations such as hypertension, diabetes 2, arthritis, cancer and others (Ovadya and Krizhanovsky 2014). Under physiological conditions senescent cells are usually effectively and rapidly cleared out from organism by immune system (Demaria et al. 2014). The age-dependent accumulation of senescent cells is partly due to their higher resistance to apoptosis and can be also accounted to age-related, attenuated efficiency of the immune system (Wang 1995). Therefore, selective elimination of senescent cells might rejuvenate aged organism (Baar et al. 2017), indicating that clearance of senescence cells can be a therapeutic approach to combat negative aspects of ageing.

Although the cellular senescence is being considered as a fail-safe system to prevent carcinogenesis, it can paradoxically promote or enhance cancer growth by secreting proinflammatory cytokines, growth factors (Krtolica et al. 2001) and by metabolic bi-products of autophagy released into microenvironment (Capparelli et al. 2012). All these substances have been shown to increase tumour mass in vivo. Also, paracrine signalling of TGF-β induces senescence in ROS dependent manner in its surroundings(Hubackova et al. 2012). Senescent cells not only enhance tumour growth but can also promote its invasiveness (Kim et al. 2017).

2.1.4 Induction of senescence

Cellular senescence can be induced by many different stimuli including telomere attrition, DNA damage, oncogene activation, epigenetic factors, mitochondrial stress, drug cytotoxicity, oxidative stress, irradiations, bacterial toxins, viruses and others. Pro-senescence stimuli can be divided into two major subgroups that are a) developmentally programmed senescence and b) stress/damage-induced premature senescence (SIPS) that can be further subdivided into several subgroups such as oncogene-induced senescence (OIS), DNA damage-induced senescence, drug-induced senescence and others. Despite many different inducing stimuli, downstream of an initial insult there are two prominent signalling pathways p53/p21 and p16/Rb pathways causing irreversible growth arrest. Proteins p16 and p21, cyclin dependant kinases inhibitors (CDKIs), are main effectors of the cell cycle arrest and subsequent cellular senescence (Fig. 2). Their specific roles and regulations will be further discussed in following chapters.
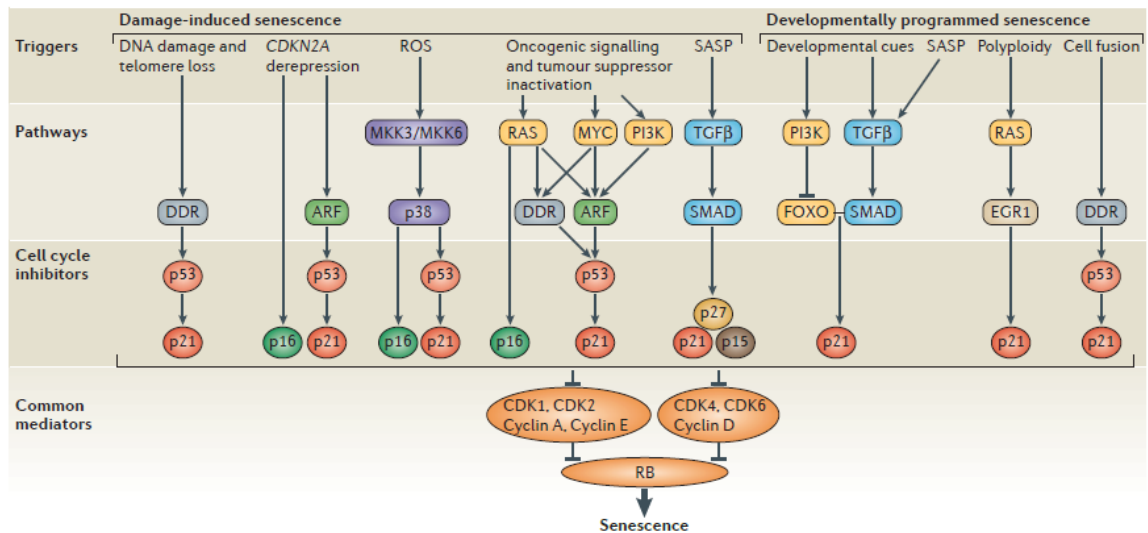
Figure 2. Overview of senescence inducing pathways. Majority of the initial pro-senescence triggers converge on CDKIs p16 and p21 resulting in dephosphorylation of Rb protein. DNA damage caused by various stimuli results DDR-triggered activation of the p53/p21 axis. Epigenetic repression of cyclin-dependent kinase inhibitor 2A (*CDKN2A)* locus coding for p16 and ARF get de-repressed resulting in their expression. ROS trigger p16 and p21 expression via activation of MKK3 and 6-induced activation of p38 stress kinase. Oncogenic signalling together with tumour suppressor inactivation induce p16 and p21 expression through DDR and ARF-mdm2-p53 axis. TGF-β that is part of SASP activates CDKIs p21, p27, p15 through SMAD signalling. Developmental cues activate p21 through PI3K and TGF-β pathways. Polyploidy and cell fusion induce p21 via DDR and by RAS induced expression of the transcription factor early growth response protein 1 (EGR1). (Muñoz-Espín and Serrano 2014)

Protein p53 is not only indirect inducer of senescence but also regulator other signalling pathways including apoptosis. Initially puzzling question was how cell decides to enter senescence or to die by apoptosis. This cellular decision is in normal cells closely related to the intensity of acquired stress stimuli and thus efficacy of the activation of p53 pathway (Li et al. 2012). This fine tuning is mediated acetylation of different lysines of p53. When stress exceeds certain threshold, acetylation switches between lysines K161, K162 to K117, resulting in activation p53 signalling leading to expression of pro-apoptotic genes such as NOXA, PUMA, Bax, Bak, Caspase-2, and even DNMT3A that actively suppress transactivation pro-senescent genes (Fig. 3) (Li et al. 2012; Zhang et al. 2011).
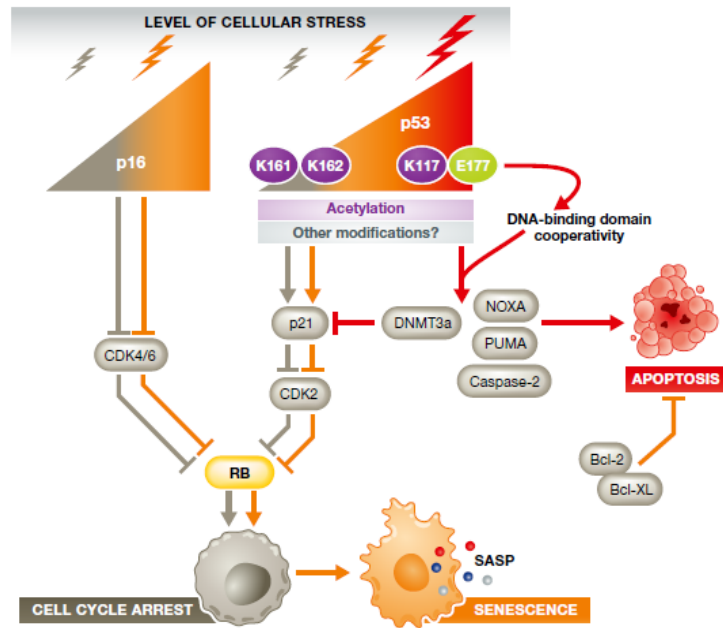
Figure 3. Fine tunning between apoptosis and senescence. At lower level of cellular (e.g. DNA damage) stress acetylation of p53 at lysins K161 and K162 enhances p53-mediated transactivation of p21 CDKi, which together with enhanced p16 expression shifts affected cells towards senescence. Upon stronger stress stimuli, K117 of p53 is acetylated, inducing transcription of pro-apoptotic genes such as BH3-only proteins Puma or Noxa (Childs et al. 2014)

There were discussions about evolutionary reason behind programmed especially in a context of readily available apoptosis. One of the clues might be that apoptosis does not always have to be the best solution to deal with damaged cell as it could be potentially harmful for organogenesis and other essential processes in embryogenesis. Other downside of apoptosis is that it terminally removes cells from the tissue and when it happens in large extend, it may lead to organ dysfunction and eventually death of an organism. In contrast, senescence, as already discussed, induces regenerations and wound healing, thus preserving tissue function.

2.1.4.1   Role of DDR, Mitochondria, Mitophagy and ROS in induction of senescence

Mitochondria, ROS and DNA damage signalling (DDR) are crucial components of both p53/p21 and p16/Rb pathway of senescence induction. They seem to be the main effectors of senescent phenotype establishment (Correia-Melo et al. 2016; Korolchuk et al. 2017). Senescent cells, regardless of inducing stimuli and downstream signalling were shown to have significantly increased, though damaged mitochondria with

decreased mitochondrial membrane potential, producing significantly elevated levels of ROS. Damaged mitochondria are another characteristic feature of senescent cells and this phenomenon is called Senescence-associated Mitochondrial Dysfunction (SAMD) (Korolchuk et al. 2017). ROS produced by SAMD, cause DNA damage that triggers DDR. DDR itself is required for establishment and maintenance of senescence state and at the same time DDR stimulates expression of SASP genes which further by autocrine signalling reinforce senescent phenotype (Passos et al. 2010). It has been shown that DDR signalling in senescent cells is active even when no DNA damage was inflicted by initial senescence-inducing stimuli (Pospelova et al. 2009), suggesting that DDR is widely preserved mechanism. This "pseudo-DDR" could be linked to generally increased ROS levels in senescent cells which is capable of directly activating ATM kinase, creating positive feedback loop.

Apparently, damaged mitochondria have an important role in this positive feedback loop during senescence establishment due to their continuous production and replenishment of ROS.

SAMD has been shown as one the major driver and maintenance of cellular senescent. However, the reasons behind SAMD and an exact mechanism is still not fully understood. So far there are only many observations mapping changes in mitochondria.

During SAMD the level of gatekeeper enzyme, protein pyruvate dehydrogenase (PDH) increases, leading to higher usage of pyruvate in Krebs cycle, NADH synthesis and thus to elevated respiration and ROS production (Kaplon et al. 2013). Mitochondria also undergo fission and fusion which are important processes participating in regulation of mitochondrial dynamics in order to preserve their functionality under cellular stress. In senescent cells, fission mediators Drp1 and Fis1 are downregulated, which correlates with attenuated mitochondrial dynamics resulting in formation of large inter-connected mitochondria, which are too enormous for being degraded by autophagy (Dalle Pezze et al. 2014).

Process called autophagy degrades and recycles damaged cell organelles and cellular structures. During the establishment of senescence, autophagy has been shown to have pleiotropic effect on this process in different cellular models. Specific subtype of autophagy eliminating damaged mitochondria is called mitophagy. Under physiological

conditions, damaged mitochondria with decreased membrane potential are marked with polyubiquitin chains through action of PTEN-induced putative kinase 1 (PINK1) and E3 ligase Parkin, and are recognized by autophagy related receptor proteins and subsequently engulfed in autophagosome and degraded (Korolchuk et al. 2017). However, this process is being defective in senescent cells (both in vitro and in vivo), thus further contributing to SAMD (Dalle Pezze et al. 2014). There are couple of mechanisms that may drive a decline in mitophagy. Indirect explanation for this event could be elevated activity of mTORC1, a negative regulator of the initiation steps in autophagy, which is observed in senescent cells suppressing overall autophagy, thus affecting also mitophagy (Correia-Melo et al. 2016). Another anti-mitophagic signalling can be related to blockage of Parkin-mediated mitophagy by cytoplasmic p53 that accumulates in senescent cells (Ahmad et al. 2015) . Senescence-imposed mitochondrial changes can be also affected by DNA damage signalling through phosphorylation cascade ATM, Akt and mTORC1 resulting in activation of the master regulator of mitochondria biogenesis PGC1-β (Correia-Melo et al. 2016). As previously mentioned SASP induces and reinforces senescent phenotype and is part of positive senescence feedback loop. Besides SASP contributing to DDR, there is additional link between SAMD and SASP. Dysfunctional mitochondria release ROS and mtDNA, which are recognized by immune system as danger associated molecular patterns (DAMPs). These DAMPs activate intracellular NOD-like immune receptors, especially NLRP3, which in turn initiate inflammasome assembly, resulting in processing and activation of important pro-inflammatory cytokines IL-1β and IL-18 (Salminen, Kaarniranta, and Kauppinen 2012). Interestingly, fully functional mitophagy abolish NLRP3 activation (Nakahira et al. 2011). However, dysfunctional mitochondria alone, without pro senescent signalling, are incapable of inducing senescent phenotype as has been shown by disruption of mitochondrial function by depletion of mtDNA, mitochondrial sirtuins or by inhibition of the mitochondrial electron transport chain ETC (Wiley et al. 2016). All these data demonstrate, that mitochondria, ROS and mitophagy are the key regulators and enhancers of senescence, cooperating together in positive loop manner, causing DDR, thereby maintaining pro-senescent stimuli.
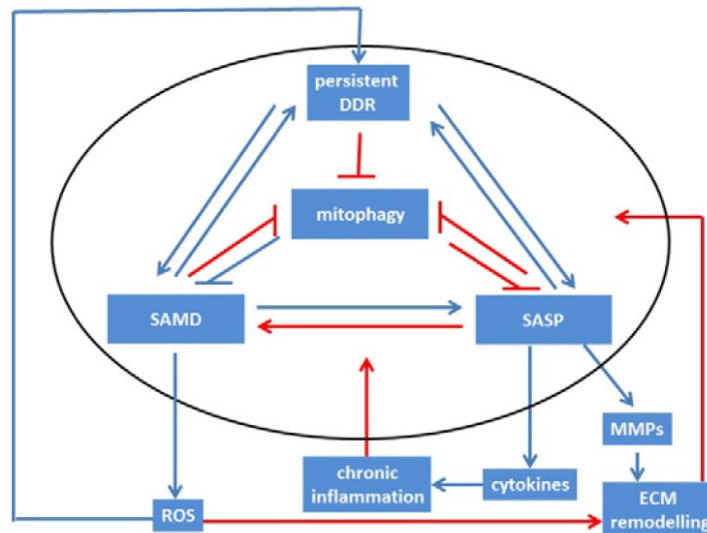
Figure 4. Interconnected pro-senescent signalling network. Persistent DDR leads to SAMD via p38MAPK and TGFβ and SASP via NF-κB and C/EBPβ resulting in production of ROS and pro-inflammatory cytokines further reinforcing DDR. DDR also inhibits mitophagy, that leads to further promoting SAMD and SASP, which in turn also contribute to block of mithophagy, creating additional positive feedback loop. Red arrows indicate yet incompletely understood mechanisms (Korolchuk et al. 2017).

2.1.4.2 p16/Rb pathway and its regulations

p16/Rb pathway is one of the main pathways inducing senescence. Initially, p16/Rb signalling leads to cell cycle arrest in G1 phase and subsequently triggers establishment of senescence. Protein p16[INK4a] is a tumour suppressor, encoded by CDKN2A gene, which functions as the inhibitor of Cyclin dependant kinases 4 and 6 (CDK4/6). Those kinases are specifically active in G1 phase of cell cycle and their main role is to inactivate Retinoblastoma protein (Rb) which upon phosphorylation-mediated inactivation releases E2F transcription factor. Release of E2F induces expression of proteins required for DNA synthesis and progression through cell cycle. Thereby, inhibition of CDK4/6 by p16 prevents cells from entering S phase.
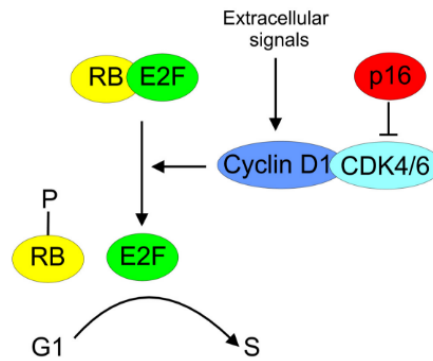
Figure 5. p16/Rb pathway. CDK4/6 in conjunction with Cyclin D1 phosphorylates protein Rb, which then releases transcription factor E2F resulting in cell cycle progression. Protein p16 blocks this whole cascade by inhibiting CDK4/6 (Akin et al. 2014)

Connection between expression of p16 and subsequent senescence induction is not fully understood yet. As discussed in the previous chapter, ROS plays an important role in triggering and maintaining DDR, hence reinforcing pro-senescent signalling. Pathway p16/Rb induces increased production of ROS (H_2O_2 in this case), which seems to be mediated by upregulated mitochondrial super oxide dismutase (MnSOD). Upregulation of MnSOD is a consequence of imposed inhibitory effect of p16 protein on E2F/DP1 signalling. Subsequent increase of ROS activates protein kinase C- δ (PKC-δ) (Takahashi et al. 2006). Active PKC-δ, then in turn stimulates further production of ROS (Takahashi et al. 2006) likely through activating NADPH-oxidase via p47[xphos] phosphorylation (Bey et al. 2004), thus creating positive feedback loop. Irreversibility of the cell cycle arrest mediated by p16/Rb pathway, may also be partially due to downregulation of mitotic exit network kinase, termed WARTS (required for cytokinesis) (Takahashi et al. 2006). Prolonged presence of ROS was shown to irreversibly downregulate levels of WARTS, indicating that this might be partially responsible for blocked cytokinesis in senescent cells.
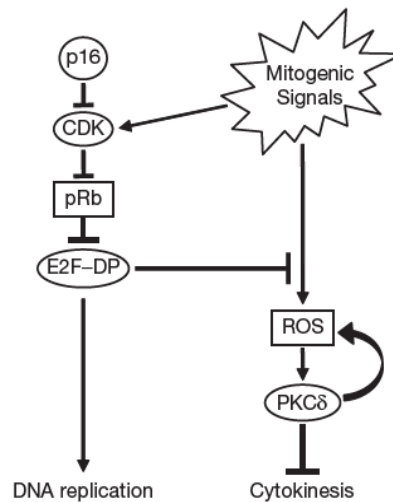
Figure 6. Interplay between ROS and p16/Rb pathway. Mitogenic signals stimulate ROS and activates CDK. Inhibition of CDK results in inhibition of E2F that normally helps to combat ROS induced by mitogenic signal. Accumulated ROS activates PKC δ that in turn blocks cytokinesis (Takahashi et al. 2006).

Moreover, it is known that p16 positives cells accumulate with age (Krishnamurthy et al. 2004) and this accumulation is telomere and p53/p21 axis independent (Garbe et al. 2009). Activation of p16 expression is regulated mostly by de-repression of its loci. Protein p16 is normally repressed by epigenetic modifications of histones such as H3 lysine 27 methylations (H3K27Me3), by Polycomb Repressive Complex 2 (PRC2) and further enforced by Polycomb Repressive Complex 1 (PRC1) (Bracken et al. 2007). De-repression is carried out by different stimuli such as by decline of BMI1 and CBX7 proteins, parts of PRC1. Downregulation of BMI1 and CBX7 correlate with activation of p16 expression during cellular senescence. (Gil et al. 2004; Itahana et al. 2003).

Decline of Polycomb Group proteins (PcG) result in expression of p16 that is partly mediated by SA-miRNAs (SA-miRNA-26b, 181a, 210, 424). Expression of SA-miRNA suppress PcG proteins and it even further propagate their self-expression, hence creating positive feedback loop.

Activated oncogenes such as Ras, Raf, are also capable of inducing senescence, which is mediated via activation of p16 expression through demethylation of K3K27 by histone demethylase JMJD3, then by downregulation of methyl transferase Ezh2 (Barradas et al. 2009) and by activating Ets transcription factors via RAS-MAP kinase signalling, which promotes transcription of p16 gene (Ohtani et al. 2001)

2.1.4.3   p53/p21 pathway

P53 is tumour suppressor protein, that is induced and activated either by DNA damage via DDR signalling, comprising both ATM/ATR kinases or by ARF mediated degradation of murine minute 2 (MDM2), which normally ubiquitinylates p53 targeting it for degradation. ARF (p14^{ARF}) is a product of alternative reading frame of CDKN2A gene, which also codes for ^{p16INAK4} and is activated as a response to elevated mitogenic stimuli by for example RAS or MYC as already mentioned in previous chapter. Active p53 then transactivates expression of CDKi p21, which is encoded by CDKN1A gene. Expressed p21, then inhibits CDKs resulting in cell cycle arrest and subsequent senescent establishment.
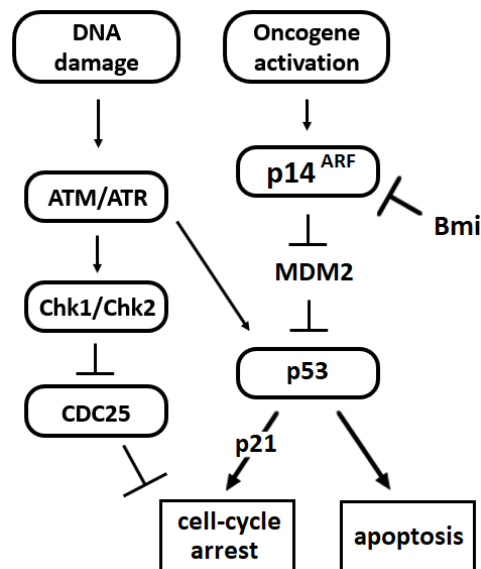
Figure 7. The p53/p21 pathway. Activation of tumour suppressor protein p53 proceeds via p14 mediated degradation of MDM-2 or by DNA damage signalling comprising ATM/ATR kinases. Cell cycle arrest is subsequently executed by either CDKi p21 or by inhibition of phosphatase CDC25. Activity of CDC25 is controlled by kinases Chk1/Chk2. Adapted from (Bringold and Serrano 2000).

Similarly to p16/Rb pathway, p53/p21 also targets CDKs. As CDKi p21$^{WIF1/CIP}$ can unlike p16^{INK4A} suppress activity of multiple CDKs (CDK1/2/4/6) throughout the cell cycle including important CDK1-cyclin b complex, which is a master regulator of mitosis. p21$^{WIF1/CIP}$ can in addition to blocking cell cycle possess specific ability to inhibit proliferating cell nuclear antigen (PCNA) (Xiong et al. 1993) and interaction of p21 with PCNA can induce cycle arrest in G2 phase (Cayrol, Knibiehler, and Ducommun 1998). In

this case p21 prevents the interaction between PCNA and CDC25, which is required for subsequent CDC25 mediated activation of CDK1/cyclin B (Ando et al. 2001). P21 is therefore capable of arresting cells in both G1 and G2 phases.

Interestingly, DDR can arrest cells even in p53-independent way, by activating Chk1/Chk2 kinases which in turn inhibit CDC25 phosphatase. Such an inhibition of CDC25 is sufficient for triggering cell cycle arrest (Bringold and Serrano 2000).

As described in chapter 2.1.4.1, mitochondria seem to be crucial for induction of senescent state and there is strong link between p53/p21 pathway and generation of malfunctional mitochondria and ROS. In senescent model induced by irradiation has been shown, that activated p53 indirectly activates PGC-1β via murine double minute 2 (MDM-2) mediated degradation of hypoxia induced factor 1α (HIF-1α) resulting in free PGC-1β (Bartoletti-Stella et al. 2013). HIF-1α is also inducer of mitophagy (Allen et al. 2013) and thus p53 can both downregulate mitophagy and increase mitochondrial biogenesis thus significantly contributes to accumulation of mitochondria. p21 itself can also induce ROS production via interaction with GADD45 that trigger downstream signalling cascade GADD45-MAPK14-GRB2-TGFBR2-TGFβ, which ultimately results in elevation of ROS levels (Passos et al. 2010).

There are also evidences that p21 inhibits PCNA-dependant DNA replication and impairs mismatch repair in vitro (Umar et al. 1996), which contributes to elevated DDR in senescent cells as well.

2.1.5 Senescent cancer cells

Though tumour cells often exhibit inactivation or attenuation of p53/p21 and p16/Rb signalling pathways, they are still capable to enter senescence-like state triggered e.g. by DNA damage. It was shown that cancer cells can acquire senescent phenotype via targeting by different chemotherapeutic drugs and cancer treatments as cisplatin (Wang et al. 1998), doxorubicin (Chang et al. 1999), 5-bromodeoxyuridine (Michishita et al. 1999), gamma irradiation (Gewirtz, Holt, and Elmore 2008) and others which rather navigate drug-resistant cells to senescence-like phenotype then to cell death. However, cell cycle arrest in tumour senescent cells, seems to be reversible and it was documented that this can happen either spontaneously both in vitro and in vivo (Roberson et al. 2005) or when exposed to apoptotic stimuli like ABT 737 or Camptothecin. These senescent revertants continuously exhibits markers of senescent while still proliferating (Yang, Fang, and Chen 2017).

In cancer treatment, cellular senescence is initially considered as positive therapeutic outcome (at least in early stages of cellular transformation) resulting in tumour stasis and shrinkage of tumour volume through SASP-mediated immune-clearance. However, in advanced tumours the therapy-accompanying cancer cells senescence is considered pro-cancerous enhancing local inflammation. Moreover, though in vitro the senescent revertants exhibit reduced proliferative rate, in vivo they have increased invasion potential and enhanced tumorigenic abilities, which could contribute to phenomenon of cancer therapy-induced progression (Yang et al. 2017). Induction of tumour senescence, despite having short term beneficial effects, seems to be generally unfavourable, promoting secondary tumorigenesis and metastasis(Milanovic et al. 2018).

2.2 Programmed/Regulated cell death

Regulated cell death (RCD) represents inducible and controlled process mediated by inner programs ultimately leading to elimination of affected cell(s). RCD is crucial mechanism for multicellular organisms assuring its proper functions during development and at stress/danger situations. RCD comprises both caspase-dependant modes of death: apoptosis, pyroptosis, e.g. and caspases-independent modes of death: necroptosis, autosis and others. Programmed cell death (PCD) is mainly triggered by developmental clues and proceeds mainly through apoptosis.

Apoptosis is a most common mode of programmed cell death. It is mainly non-immunogenic and predominantly caspase dependent**.** (apoptosis is further addressed in chapter 2.2.1)

Necroptosis is a necrotic mode of RCD triggered in apoptosis-resistant cells through activated death receptor, toll-like receptors etc., which relies on activation (phosphorylation) of mixed lineage kinase domain-like protein (MLKL) by receptor-interacting serine-threonine kinase 3 (RIPK3) or by RIPK3/RIPK1 complex also called necrosome. Activated, oligomerized MLKL is then translocated to cell membrane and permeabilizes it, which results in cellular destruction (Wang et al. 2014)

Pyroptosis is an inflammatory necrotic-like type of cell death induced by a strong activation of pro-inflammatory caspases like caspase 1. It is triggered by many microbial infections and non-infectious stimuli and requires processing of Gasdermin D by activated inflammatory caspases (Liu et al. 2016), Gasdermin D subsequently forms pores in cell membrane resulting in release of pro-inflammatory cytokines IL-1β and IL-18, DAMPs and necrotic-like cell death.

Ferroptosis is a regulated caspase-independent iron dependent cell death, characteristic with accumulation of lipid peroxidation products and massive levels of ROS (Dixon et al. 2013). Dysregulation of ferroptosis has been linked many pathophysiological states such as neurotoxicity, neurodegenerative diseases and others (Skouta et al. 2014).

Autosis is autophagy gene-dependent, Na$^+$,K$^+$-ATPase-regulated mode of cell death with characteristic features such as swelling of perinuclear space, loss of endoplasmic reticulum (Liu et al. 2013)**.** Autosis is activated when cell lacks oxygen, nutrients or when they are exposed to autophagy-inducing peptides.

2.2.1 Apoptosis

Apoptosis is specific largely non-immunogenic, mainly caspase-dependent mode of RCD, firstly defined as "Mechanism of controlled cell deletion" (J. F. R. KERR* 1972). Once cell dies by apoptosis, the cell remnants are engulfed by phagocytes, leaving no trace in an organism, which is in sharp contrast to necrosis. Hallmarks of apoptosis are cellular shrinkage and blebbing, chromatin fragmentation and condensation, activation of caspases and phosphatidyl serine (PS) exposure at the cell surface. The classical, caspase-dependent apoptosis can be triggered by either endogenous or exogenous stimuli (intrinsic or extrinsic pathway), and it is initiated and executed by caspases family of proteases. Caspases (cysteine-dependent aspartate-directed proteases) are divided into several functional subgroups:

Initiator caspases: Caspase-2, 8, 9 and 10 initiate apoptotic signalling

Executioner caspases: Caspase-3, 6 and 7 execute massive proteolysis leading to cell demise

Inflammatory caspases: Caspase1, 4, 5, 11, 12 have role in inflammatory processes and in pyroptosis
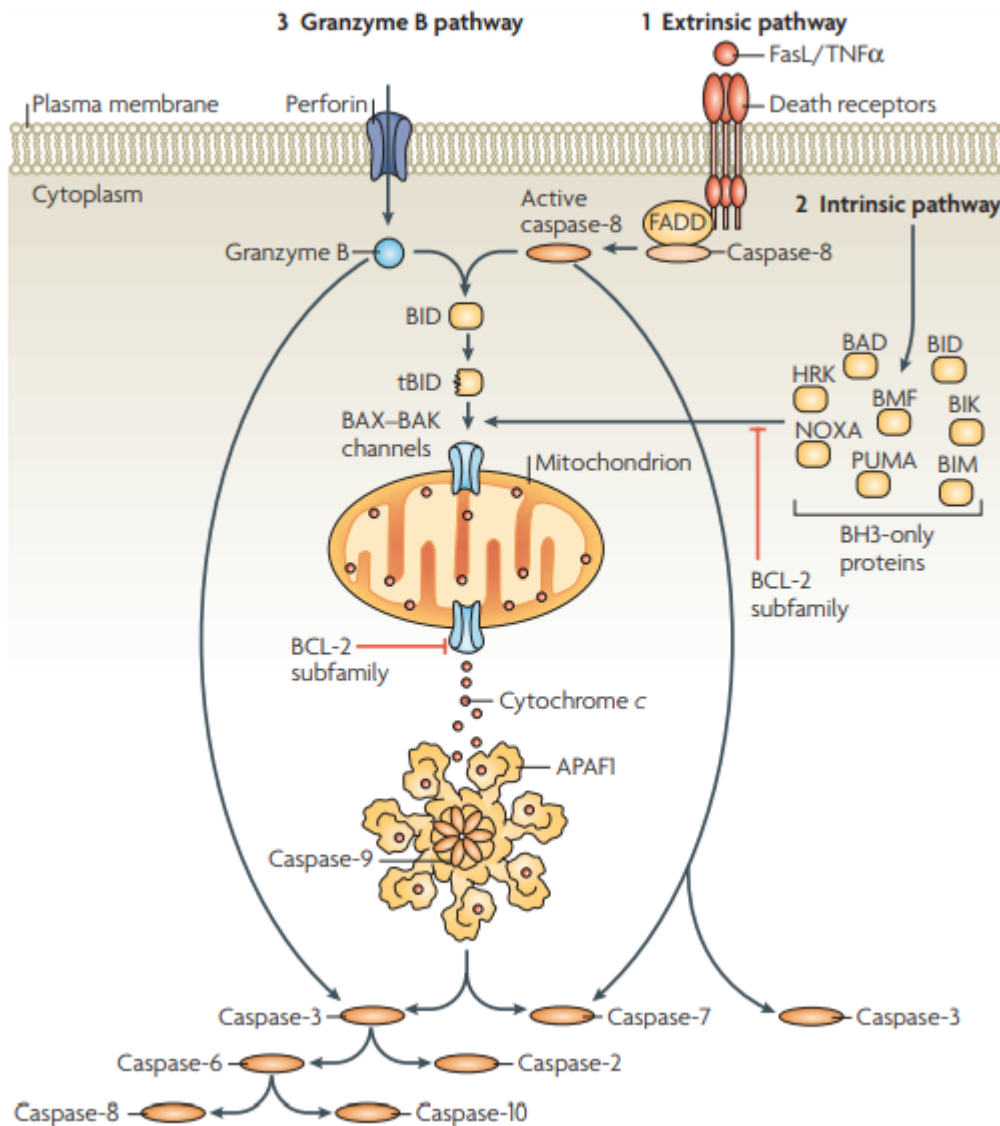
Figure 8. Overview of Intrinsic and Extrinsic apoptotic pathways. **Intrinsic pathway (2):** BH3-only proteins activate pro-apoptotic Bcl-2 proteins BAX/BAK. Those subsequently form pores into OMM resulting in cytochrome C release and assembly of apoptosome from APAF1 subunits. Apoptosome is a platform for activation of Caspase-9 which in turn activate Caspase-3. Intrinsic pathway is negatively regulated by anti-apoptotic Bcl-2 proteins **1,3 Extrinsic pathways**: a/ Death receptors activate Caspase 8, which then either directly activate Caspase-3 or cleave Bid into active tBid form. tBid then employ mitochondrial pathway of apoptosis induction, through tBid-mediated activation of BAX/BAK. **b/ Granzyme B pathway:** granzyme b enters cell through perforins and then it can directly activate/process Caspase-3 and cleaves Bid thus engaging also mitochondria pathway of caspase 3 activation. (Taylor, Cullen, and Martin 2008)

2.2.1.1   Intrinsic apoptotic pathways

Intrinsic apoptotic pathways can be triggered by sensors of damaged organelles, DNA damage, oxidative stress and others. Intrinsic pathways rely on mitochondria and activate process called mitochondrial outer membrane permeabilization (MOMP) that enables release of several pro-apoptotic proteins from the mitochondrial inter-membrane space. Among those proteins a prominent one is cytochrome c, which in cytosol forms with Apoptotic protease activating factor 1 (Apaf-1) and caspase-9 apoptosome – ATP-dependent caspase-9 self-processing/activation complex. MOMP is mediated by oligomerized pro-apoptotic effector B-cell lymphoma 2 proteins (Bcl-2) Bak and Bax, which form protein-permeable pores in the outer mitochondrial membrane. Their function is negatively regulated through their inhibition by anti-apoptotic proteins of Bcl-2 family such as Bcl-2, Bcl-XL, Bcl-W and Mcl-1.

Anti-apoptotic Bcl-2 proteins are further regulated/suppressed by other pro-apoptotic initiator/BH3 only protein such as NOXA, Bad, Bmf, Bid, Bim through interaction of their BH3 domains with these anti-apoptotic Bcl-2 proteins (see Fig. 9 for overview of Bcl-2 mutual interactions). BH3 only proteins serve as sensors of cellular stress and stimulate apoptosis by blocking Bax/Bak-inhibitory effect of anti-apoptotic Bcl-2 proteins. Proteins Bim and Bid also directly binds to Bak and Bax and change their conformation, which results in their activation (Chen et al. 2005) on mitochondria and subsequent MOMP (Fig. 10 – mechanism of Bax-mediated MOMP). Both initiator and executioner caspases can be inhibited by proteins of IAPs family such as XIAP, c-IAP1 (Deveraux and Reed 1999). During MOMP, along with cytochrome-c, Smac/DIABLO and HtrA2/Omi are released into cytosol and they supress activity of IAPs protein, hence enhancing caspase activity (van Loo et al. 2002; Verhagen et al. 2000).
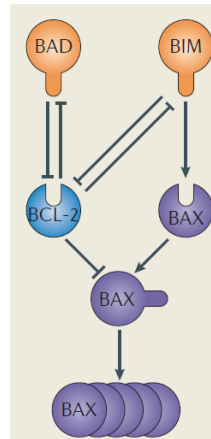
Figure 9. Overview of mutual interactions among Bcl-2 proteins. BAD and BIM are BH3 proteins activating BAX/BAK either directly or indirectly, through inhibition of anti-apoptotic Bcl-2 proteins. Head arrows and bars represent activation and inhibition respectively. Adapted from (Czabotar et al. 2014).
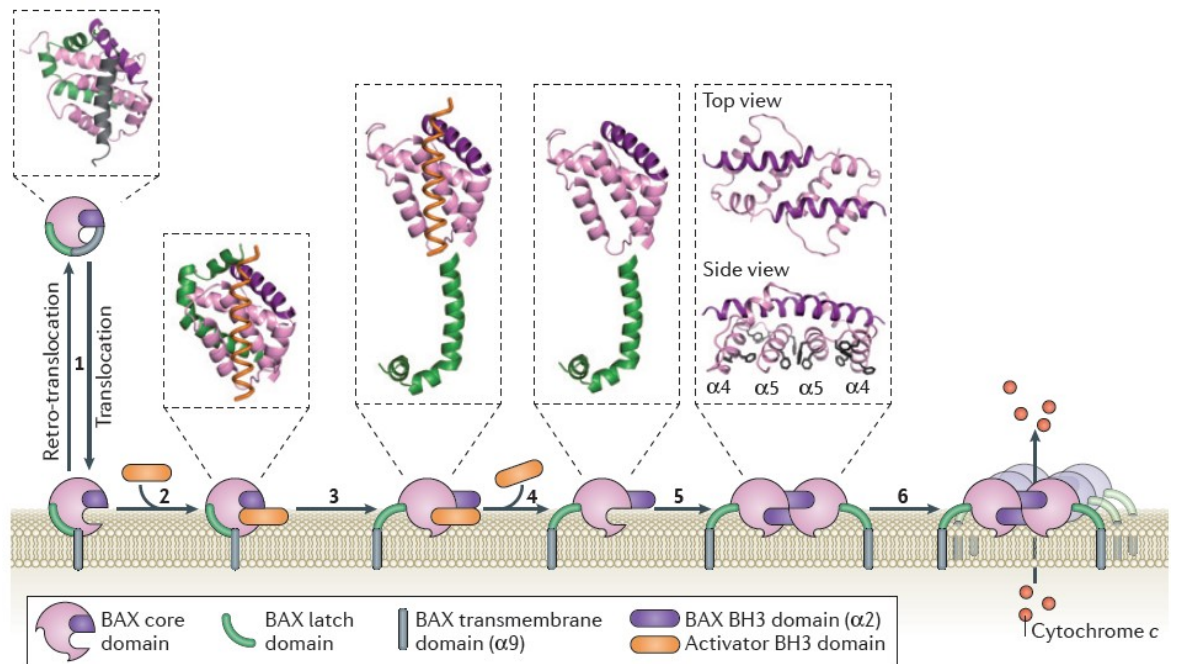
Figure 10. Model for the activation and oligomerization of BAX and BAK. Ilustrative representation of structural transitions during BAX activation and oligomerization. 1) Translocation of BAX from cytosol to the outer mitochondrial membrane. While translocating to mitochondria, BAX releases transmembrane domain which can inserts into the outer mitochondrial membrane. 2) Activators BH3 domain binds into the groove of BAX and 3) triggers release of BAX latch domain and subsequently 4) activator BH3 domain disengage from BAX. Released latch domains changes conformation of BAX 5) resulting in dimerization and exposure of α-helixes with aromatic residues (side view). α-helixes 4, 5 bound mitochondrial membrane induce tension resulting in membrane permeabilization(Czabotar et al. 2014).

**Regulation of intrinsic apoptotic signalling by ROS**

Cardiolipin is phospholipid localized at the outer list of in the inner mitochondrial membrane (IMM), where it interacts with proteins of oxidative phosphorylation including cytochrome-c. ROS oxidizes cardiolipin thus interrupting its interaction with cytochrome-c. Unattached cytochrome-c can then diffuse from intra-cristae space close to the outer mitochondrial membrane (OMM) and eventually exit mitochondria through BAX/BAK channels (Rytomaa, Mustonen, and Kinnunen 1992; Shidoji et al. 1999). Cytoplasmic ROS can also directly trigger conformational changes in BAX protein by forming disulphide bonds between its cysteine residues that stimulate its translocation to the outer mitochondrial membrane (OMM) (D'Alessio 2005).

Moreover, ROS has also indirect role in regulation of pro- and anti-apoptotic Bcl-2 proteins. ROS is known to activate many signalling kinases including p38 MAPK, c-Jun N terminal kinase (JNK), extracellular signal-regulated kinase (ERK), Akt, ATM, glycogen synthase kinase-3β (GSK-3β) and others that affects Bcl-2 protein functions and its expression. For example, as already mentioned, ROS can directly and indirectly (via DNA damage) activate ATM (Guo et al. 2010), which can eventually lead to activation of p53 that transactivate expression of pro-apoptotic Bcl-2 proteins NOXA, PUMA and BAX

2.2.1.2 Extrinsic apoptotic pathway

The canonical extrinsic pathway is triggered upon ligation of "death ligand" to the death receptors (DR) of TNFR family (Tumour necrosis factor receptors) such as FasR(CD95), TNF-related apoptosis-inducing ligand - TRAIL receptors-1/-2(DR3, DR4, DR5) and tumor necrosis factor receptor-1 (TNF-R1). Binding of death ligands to trimeric receptors triggers conformational change of the DR´s intracellular domains, which enables them to recruit the adaptor proteins FADD/TRADD (Fas-associated protein with death domain/Tumor necrosis factor receptor type 1-associated death domain) via common death domains (DD) motif, and subsequently together with procaspase-8, -10 or c-FLIP form death inducing signalling complex (DISC). FADDs incorporated in DISC exposes death effector domain (DED) by which they bind procaspase-8 via their own tandem DED, forming platform for autocatalytic chain activation of caspase-8 (Schleich et al. 2012).

DISC can also recruit protein c-FLIP via DED of FADD, which is able to dimerize with procaspase-8. Procaspase-8/cFLIP dimerization prevents proximity induced catalytic activation of procaspase-8, as c-FLIP is not catalytically active, thus inhibits apoptotic signalling
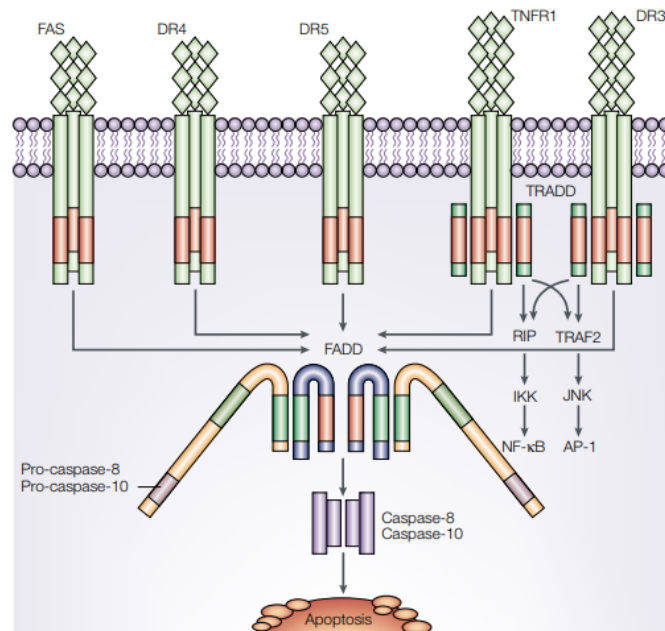
Figure 11. Overview of death receptors and their domains. Death domains, depicted as red rectangles, are parts of intracellular domains of all DRs and they mediate recruitment of adaptor FADD. FADD subsequently binds initiatior procaspases-8 and -10 via DED domains depicted as green rectangles. Induced proximity of procaspases results in their autocatalic cleavage-mediated activation and forming dimers capable of further transducing apoptotic signal leading to cell death. TNFR1 and DR3 can also recruit adaptor TRADD which in turn can activate RIP or TRAF2 kinase leading to activation of transcription factors Nfκb and AP-1. Adapted from (Ashkenazi 2002)

Depending on efficacy of caspase-8 activation, its total amount in a cell and on level of inhibitory IAP proteins, cells can be divided into two categories - type I cells or type II cells. Type I cells are so called mitochondria-independent, which means that direct cleavage-mediated activation of caspase-3 by caspase-8 is enough to induce apoptosis without additional amplification of apoptotic signalling through mitochondria. In type II cells, referred as mitochondria-dependent, direct activation of caspase-3 by caspase-8 is not sufficient to trigger apoptosis and this apoptotic signal is further amplified by caspase-8 processed (truncated) BH3-only protein tBid, which then engage mitochondrial pathway of apoptotic signalling by activation of Bax/Bak.

Perforine/Granzyme (Granzyme B) pathway is an additional mechanism of apoptotsis triggered by exogenous stimuli and can be both caspase dependant and independent. Granzyme B (and granzymes such as A, G, M, …) enters cell via perforin-induced cell membrane repair/permeabilization mechanism of target cells which leads to endocytic uptake of granzymes-containing vesicles and subsequent their release into cytosol via perforin channels (Thiery et al. 2011).

Apoptotis is then initiated by direct activating of caspase-3, -8 and by cleavage of Bid into tBid form activating mitochondrial pathway. Granzyme B can mediate apoptosis even in caspase independent manner which proceeds through the direct cleavage of caspases targets such as Lamin B or ICAD. Perforine/Granzyme pathway is used by cytotoxic lymphocytes and NK cells to eliminate target cells and is necessary for control of T helper cells type 2 expansion (Devadas et al. 2006)

Activation of effector caspases-3, -6, -7 initiate final effector phase of apoptosis characteristic with massive proteolysis. Effector caspases target and degrade all kinds of functional, structural and signalling proteins including: Actin, lamin A/B, gelsolin, β-catenin, Bid, Bad, Bax, XIAP, ICAD, MDM2, PARP, DNA-topoisomerase, PKC, Akt1, p21, pRb and many others. Ultimately, once cells start to disintegrate, apoptotic bodies are formed, and they are eventually engulfed and degraded by phagocytes.

3   Aim of thesis

The main aim of this thesis was to study effects imposed in a model cancer cell line by inducible mid- to long-term expression of well-known, pro-senescent cell cycle inhibitors p16 and p21, especially in respect to apoptotic signalling.

4 Material and methods

4.1 Experimental Material

4.1.1 Experimental cells, cultivation and selection

For all experiments was used H28 adherent cancer cell line derived from mesothelioma stage 4, purchased from ATCC (Manassas, Virginia, United States) that expresses wildtype p53 tumour suppressor protein. Prior to experiments, this cell line was transduced by pLVX tet-ONE puro vector containing transactivator Tet-On 3G alongside with either protein p16^{INK4a} or p21$^{WAF1/Cip1}$ (both of human origin) and puromycin resistance gene or by only empty pLVX tet-ONE puro vector carrying only puromycin resistence gene. Tet-One inducible system is further described in chapter 4.3 Induction of senescent phenotype.

Transduced cells were subjugated to clonal expansion and best performing clones, in terms of p16^{INK4a} or p21$^{WAF1/Cip1}$ genes of interest (GOI) expression, were selected for further experiments. Out of many tested clonal cultures, clones summarized in the Table were selected for further experiments.

Cells were cultured in RPMI 1640 Media (Sigma) supplemented with tetracyclin free 10% FBS (BioWest), antibiotics (streptomycin 100μg/ml, penicillin G 100U/ml) and 2ug/ml puromycin assuring selection of transduced cells. Transduced cells were grown under 5% CO_2 atmosphere in a CO_2 incubator at 37°C, maintained at medium confluency and discarded after 30 days to avoid possible undesired occurrence of GOI non-expressing cells. After each 30days new individual aliquots of clones were thawed. Cells were cultured either with doxycycline (1 μg/ml; experimental samples) or without doxycycline (control samples) in cultivating media (cultivating media +/- doxy).

GoI expressing clones	Clone number	Clone number
p16 expressing	5	34
p21 expressing	33	36
Empty Vector (EV)	Mixed culture	

Table 1. Summary of p16[INK4a] or p21[WAF1/Cip1] expressing H28 clones and EV used in diploma project

Exclaimer: Transduction and clonal expansion was done by former PhD. Student Gita Novaková and preceded my involvement in this project.

4.2 Composition of solutions

- 1x PBS (Phosphate-Buffered Saline**):** NaCl 137.0 mM, KCl 2.70 mM, Na_2HPO_4 10.0 mM, KH_2PO_4 1.80 mM, pH 7.4, in ddH_2O

- 10x Annexin binding buffer: 0.2 μm sterile filtered 0.1 M Hepes (pH 7.4), 1.4 M NaCl, and 25 mM CaCl2, in ddH_2O

- 1x Transfer Buffer for Western blotting: 25 mM Tris, 192 mM glycine, 10% (v/v) methanol, in ddH_2O

- 1x Laemmli electrophoresis running buffer: 25mM M Tris, 192mM M glycine, and 0,1% (w/v) SDS in ddH_2O

- 2x Laemmli lysis buffer: 4% (w/v) SDS, 100 mM Tris-Cl pH 6.8, 20% (v/v) glycerol in double distilled H_2O

- PBST (PBS TWEEN20): 0,1% (v/v) TWEEN20 in 1x PBS

- 40x X-Gal: 40mg/ml 5-bromo-4-chloro-3-indolyl-β-D-galactopyranoside in N,N-dimethylformamide

- 1x X-Gal staining solution: 1 mg/ml X-gal, 0.12 mM $K_3Fe[CN]_6$, 0.12 mM $K_4Fe[CN]_6$, 1 mM $MgCl_2$ in PBS at pH 6.0

- 1x SBM (Seahorse Base Media): 8,3 mg/ml DMEM in ddH_2O,

- Trypsin: 0,05% (w/v) Trypsin, 0,02% (w/v) EDTA

- Ponceau Red: 0,5% Ponceau S, 1% acetic acid in ddH_2O

4.3 Induction of senescent phenotype

Induction of senescent phenotype was imposed by inducible upregulation of two CDKi p16^{INK4a} and p21$^{WAF1/Cip1}$. Ectopic constitutive upregulation of either of these two CDKi was previously used for induction of senescent phenotype/senescence in cancer cells and it is widely accepted (Capparelli et al. 2012; Coppé et al. 2011; McConnell et al. 1998).

Induction of CDKIs expression was triggered by tetracycline analogue doxycycline (D9891, Sigma) via the Tet-One inducible system described in Figure 12. The addition of doxycycline throughout the induction period followed schedule as described below, in the Table 2.

.
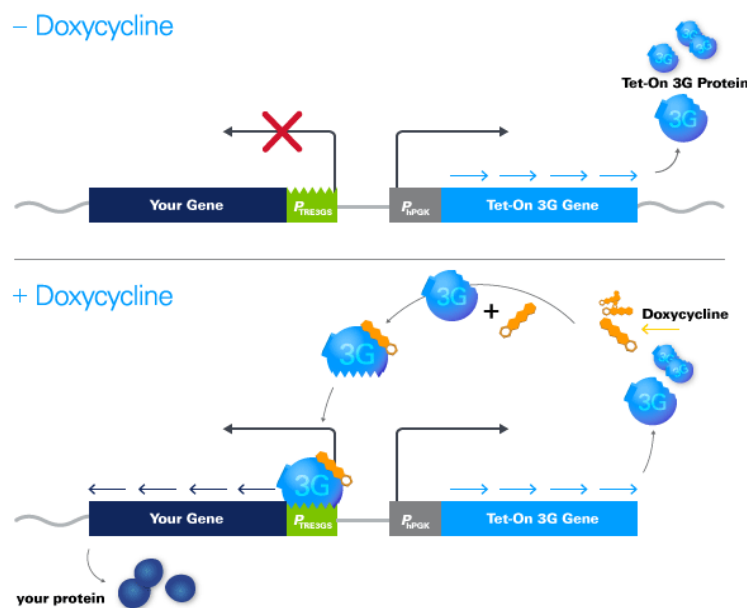
Figure 12. Tetracycline Inducible Expression—Tet-One Systems. Tet-One System is single vector system capable of delivering more than one gene expression in a single vector. Tet-On 3G codes for trans-activator, that is constitutively expressed. Binding of tetra-cyclins (doxycycline) to trans-activator changes its conformation state allowing it to bind to promotor site of target gene and thus trigger its expression. (Clontech,2014)

GoI	-1.Day	0.Day	1.Day	2.Day	3.Day	4.Day	5.Day	6.Day	7.Day
p16	Seeding	Doxy		Doxy			Doxy		doxy
p21	Seeding	Doxy		Doxy			Doxy		*analysis*

GoI	8.day	9.day	10.day	11.day	12.day	13.day	14.day	15.Day
p16		Doxy			Doxy		Doxy	*analysis*

Table 2. Schedule of doxycycline addition into the cell media throughout the induction period. For clones expressing p16[INK4a] protein (marked as p16) was used 15day long induction period prior to analysis. For clones expressing p21[WAF1/Cip1](marked as p21) was used 7day long induction period prior to analysis.

Senescence lacks a single specific marker, thereby it is recommended to use set of biomarkers for its detection and distinguish falsely positive/negative results. Common strategies and markers to detect senescence include enlarged flattened morphology, absence for Ki67 and/or PCNA staining, positivity for p16 and p21, positivity for Sa-β-Gal, positivity for γH2Ax, positivity for SAHF, SASP and positivity for Sudan black. However, not all senescent markers can be assessed in different cells types, tissues, modes of senescence induction and experimental conditions. Some these observed and published discrepancies are specified in following subchapters of 4. Material and Methods, regarding detection of selected senescent markers.

Markers of senescence assessed in this diploma project:

- flattened enlarged morphology (Chen et al. 2000; Sikora, Mosieniak, and Alicja Sliwinska 2016)

- absence of Ki67 (Lawless et al. 2010) which is proliferative marker and is absent in senescence and quiescence states

- positivity for Sa-β-Gal (Dimri et al. 1995)

- positivity of senescent specific yH2AX foci (Lawless et al. 2010; Pospelova et al. 2009)

- assessment of cell cycle arrest. (discussed in chapter 4.6)

Non-used markers of senescence and reasons behind:

- Staining for p16 and p21 – already ectopically overexpressed

- PCNA – substituted with Ki67, as these both markers provide identical results on human and mouse fibroblasts (Lawless et al. 2010)

- Detection of SAHF – Despite its common usage, it is dispensable and not present in all cell types in senescent state (Kosar et al. 2011).

- SASP – Though being characteristic for senescent state (Coppé et al. 2008, 2010) and conserved between cell types (Coppé et al. 2010), it was shown, that it is not produced by cells with senescent phenotype induced by overexpression of p16 and p21 (Coppé et al. 2011), and therefore it was not considered as marker of senescence.

4.4 Induction of arrested phenotype

Arrested phenotype is hereby defined as a cell state, when cells with Doxycycline-induced expression of CDKi significantly hinder proliferation but do not stain positively for Sa-β-Gal, thus lacking one of the crucial senescent markers. This arrested or pre-senescence state of H28 clones was instrumental for the analysis of H28 cellular response to selected apoptogens.

Induction of arrested phenotype followed the same principle as described in chapter 4.3 Induction of senescent phenotype. but was shorter following schedule as described in Table 3.

GoI	-1.Day	0.Day	1.Day	2.Day	3.Day	4.Day	5.Day
p16	Seeding	Doxy		Doxy		Doxy	*analysis*
p21	Seeding	Doxy		*analysis*			

Table 3. Time schedule of pro-arrest doxycycline treatment of p16[INK4a] and p21[WAF1/Cip1] expressing H28 clones. For clones expressing p16[INK4a] protein (marked as p16) was used 5day long induction period prior to analysis. For clones expressing p21[WAF1/Cip1] (marked as p21) was used 2day long induction period prior to analysis.

4.5   Senescent associated Beta Galactosidase staining

Lysosomal β -Galactosidase functions optimally at pH4.0 whereas β-Galactosidase in senescent cells is functional also at suboptimal pH 6.0 and therefore staining for Sa-β-Gal is commonly used for detection of senescence cells (Dimri et al. 1995). However, it has been shown that confluency and even locally increased cell density produce positive staining in proliferating cell cultures (Dimri et al. 1995; Severino et al. 2000). As I also observed falsely positive results with proliferative H28 cell culture, it was crucial to perform this analysis under sub-confluent/medium density conditions.

Cells were grown on 12-well plate to 30-40 % confluency, then washed twice with PBS and fixed with 0,5% glutaraldehyde solution at room temperature for 15 minutes. After fixation cells were washed twice with 1mM $MgCl_2$ in PBS (pH 6.0), then incubated with 1x X-Gal staining solution (overnight, in non-CO_2 incubator, at 37 °C) and then washed three time with H_2O. Images were captured by fluorescent microscope (DM IL LED, Leica).

4.6 Cell cycle arrest measurement

Cell cycle arrest measurement was designed in need to process large quantities of samples and provide quick information about proliferative vs. non-proliferative/hindered state of cells in proliferation fraction of cells in cell culture.

It is based on PI staining of DNA content, assessing ratio of diploid (2N) vs. S phase/Tetraploid (S/4N) fraction of cell population, either with or without incubation with nocodazole, which blocks exit from G2/M phase of the cell cycle. Ratio of 2N:S/4N cells in proliferating cell culture without nocodazole is around 60:40. In same proliferative cell culture with nocodazole, the ratio shifts to 0:100 meaning all cells accumulated in G2/M phase. Presence of non-proliferative/hindered fraction of cells in cell culture, especially in G1 phase, would be reflected by smaller shift of 2N:S/4N ratio (2N:S/4N > 0:100, e.g. 20:80) when nocodazole is added, as cells arrested/hindered in G1 state would not be able to progress into latter cell phases. As senescent and arrested cell ought to not proliferate/hinder proliferation, this is suitable tool to delineate on time scale, when does the cell population as whole ceases to proliferate or when it significantly hinders proliferation.

Experimental design for cell cycle arrest measurement:

Comparison of:

 (A) control (proliferating) samples without nocodazole

 (B) control (proliferating) samples with nocodazole

 (C) experimental samples (with induced expression of GoI) without nocodazole

 (D) experimental (with induced expression of GoI) samples with nocodazole.
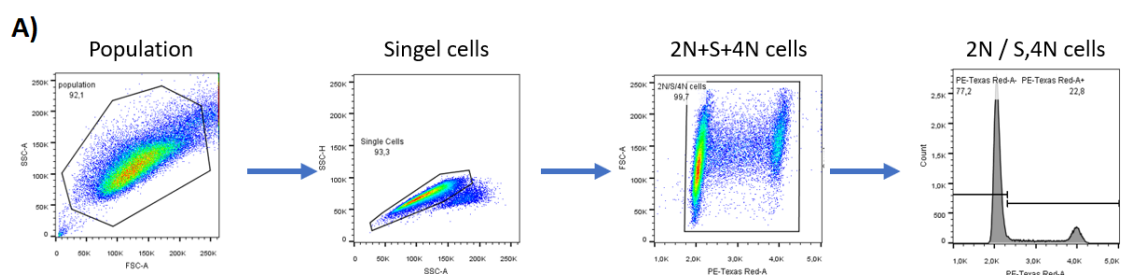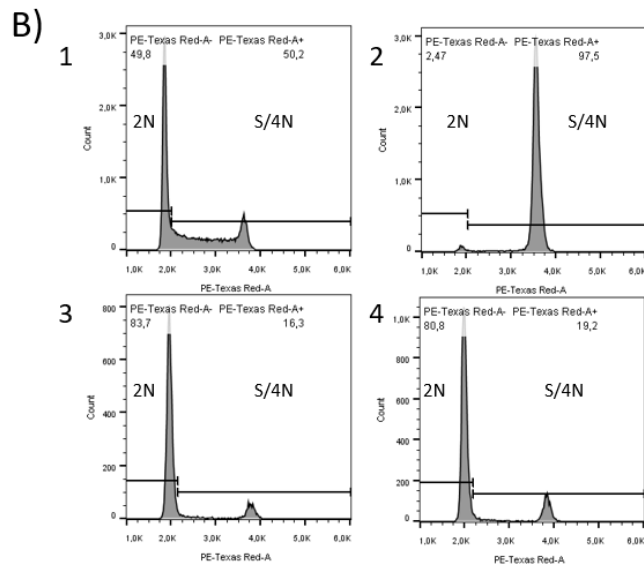
Figure 13. Gating strategy (A) + Cell cycle arrest-comparison (B): DNA content was stained with PI (PE-Texas Red-A) and distribution of G1(2N) and S/G2/M (S/4N) phases was visualized on histogram. 1) Normal cell cycle distribution in full proliferative culture, 2) Distribution of cell cycle of proliferating cells after 24hour incubation with nocodazole. 3) Distribution of cell cycle of cell with senescent phenotype. 4) Distribution of cell cycle of cell with senescent phenotype after 24hour incubation with nocodazole.

Cells were cultivated in 6-well plates and 24 hours prior to analysis were divided into two groups Nocodazole- and Nocodazole+. Cultivating media were replaced in all wells of Nocodazole- group with fresh cultivating medium (+/- doxycycline) and in Nocodazole+ set were exchanged for fresh cultivating media (+/- doxycycline) with 10uM Nocodazole (Sigma). After 24hr incubation cells were harvested:

- washed once with 1x PBS and incubated with 0,5ml of trypsin in CO_2 incubator, at 37°C for 5 minutes. Following incubation with trypsin, the cell suspension was neutralized by addition 0,5ml of cultivating media and cells from each well were collected and centrifugated (400 x g, 4°C, 5 minutes).

The supernatant was discarded and the cell pellet was washed with cold PBS and again centrifuged (500 x g, 4°C, 5 minutes). The supernatant was discarded and cells were fixed with 400ul of ice-cold 70% ethanol. After fixation, cells were centrifuged (850 x g, 25°C, 5 minutes), the supernatant was discarded and pellets were washed twice with 1xPBS. Cells were then resuspended in 100ul of 100ug/ml of RNAse with 50ug/ml Propidium Iodide in PBS and transferred into FACS tubes. Samples were analysed by flow cytometer (BD LSRFortessa, BD Biosciences) and the data were evaluated using software FlowJo v10.

4.7   5-ethynyl-2′-deoxyuridine (Edu) incorporation

Cells were seeded on 6 well plate ($2*10^5$cells/well) prior to experiment and then after 24 hours later the cultivating medium was replaced with fresh 10uM EdU/cultivating media (+/-doxy) and incubated for 24 hours. After incubation cells were harvested as described in chapter 4.6. The cell pellets were resuspended in 1ml 1%BSA/PBS and transferred into 5ml polystyrene FACS tube. Subsequently 2ml of 1%BSA/PBS was added to each sample and the cell suspension was centrifuged (300 x g, 4°C, 5 minutes). Pellets were resuspended in 200ul 1% BSA/PBS and then 300ul of 4%PFA/PBS solution was dropwise used for fixation. After 30 minutes cells were washed (1x) with 3ml of 1% BSA/PBS and centrifuged (300 x g, 25°C, 5 minutes). Cells were resuspended in 1% BSA/PBS and cell membrane was permeabilized with ice-cold 70% EtOH while incubating on ice for 30 minutes. Permeabilized cells were then rehydrated twice with 3ml of 1% BSA/PBS. After rehydratation, pellets were resuspended in 100ul of 1x Click-iT® Plus saponin based permeabilization and wash reagent (Click-IT® Plus EdU Cytometry Assay Kits, 100 tests, Invitrogen™) and Click-iT reaction was performed according to the manufacturer manual. After 30 minutes incubation (25°C) cells were washed twice with 1% BSA/PBS, then resuspended in 500ul 3uM DAPI in 1% BSA/PBS and filtered through 70um cell strainer. DNA content and EdU incorporation was measured using flow cytometer (BD LSRFortessa, BD Biosciences) and the data were analysed with software FlowJo v10.

4.8   Indirect immunofluorescence

Cells cultivated on 12mm round coverslips were washed with 1x PBS, fixed by -20C methanol (5 minutes) in freezer (-20°C) and permeabilized by 0,25% TX-100/PBS. Then cells were washed with PBS (3x, 5 minutes), incubated with blocking agent FBS 10% in DMEM for 60 min and then washed once with 1x PBS. Cells were incubated overnight in primary antibodies which were diluted in DMEM according to manufacturer recommendations. After incubation with primary antibody, cells were washed with 0,01% TX-100/PBS, then with 1x PBS (4x, 5minutes) and incubated in secondary antibody conjugated with fluorophore diluted in 10%FBS/DMEM for 60 min. After incubation with the secondary antibody cells were washed again with 0,01% TX-

100/PBS (1x), then with 1x PBS (3x) and mounted into DAPI containing mowiol. Cells were viewed by confocal microscope (TCS SP8, Leica). Images were processed with LAS X Life Science Microscope software (Leica).

List of primary antibodies used for immunofluorescence:

- Ki67 (Abcam, ab15580)
- γH2AX (Millipore, 05-636),

List of secondary antibodies used for immunofluorescence

- GAM Alexa Fluor® 488 (Jackson, 111-545-008)
- GAM Alexa Fluor® 594 (Jackson, 115-585-008)
- GAR Alexa Fluor® 594 (Jackson, 111-585-008)

4.9 SDS-PAGE and Western blotting

a) Sample preparation

Cells were cultivated in 100mm dish and upon reaching 80% confluency they were washed twice with cold 1x PBS and lysed in 2x Laemmli lysis buffer. Lysates were transferred into 1,5ml safe-lock microcentrifuge tubes denatured by heating (98°C, 2 minutes), and filtered through 200ul filter pipette tips.

b) Measurement of protein concentration

Protein concentration was quantified using Pierce™ BCA Protein Assay Kit (Thermo Fisher Scientific) following manufacturer instructions and samples were diluted in 2x Laemmli lysis buffer and adjusted to the same concentration. Dithiothreitol and Bromophenol blue were then added to the final concentrations 0,05% and 0,02% and the samples were again heated (98°C, 15 minutes).

c) SDS – PAGE electrophoresis

Wells of polyacrylamide gels (8%, 12%) were equally loaded with protein samples (15-30ug) along with protein ruler and proteins were resolved by electrophoresis. Electrophoresis using 1x Laemmli electrophoresis running buffer was initially run at 80V for 30minutes and subsequently at 120V for 90 minutes.

d) Western Blot - Protein transfer

Protein from the SDS PAGE gels in 1x Transfer Buffer were transferred at constant current 0,8mA per cm² onto nitrocellulose membrane (Bio-Rad) using semi-dry transfer units (Hoefer SemiPhor). Quality and efficiency of transfer was visualized by non-selective protein staining with ponceau red.

e) Immunodetection

Nitrocellulose membrane was blocked in 5% milk/PBST for 60minutes, washed with PBST for 10 minutes and incubated overnight with a primary antibody, diluted in non-fat 1% milk/PBST. After incubation with distinct primary antibody, the membrane was washed with PBST (3x, 10 minutes) and incubated with appropriate secondary antibody conjugated with horseradish-peroxidase for 60 minutes. Membrane was again washed (3x, 10minutes) and then the immuno-stained proteins were visualized using Pierce™ ECL Western Blotting Substrate (Thermo Fisher Scientific) or SuperSignal™ West Femto Maximum Sensitivity Substrate (Thermo Fisher Scientific) following manufacturers manual. Bioluminiscence was determined using Azur c600 imaging system (Azure Biosystems).

List of primary antibodies - Immunodetection

β-Actin	Santa Cruz, sc-1615
ANT2	Cell Signalling, #14671
Bak	BD Pharmingen, 556382
Bax	Cell Signaling, 2772
Bcl-2	Cell Signaling, 2870S
Bcl-XL	Cell Signaling, 2764
Bcl-W	Cell Signaling, 2724
Bid	Cell Signaling, 9239

Bim	Cell Signaling, 2933
Caspase-3	Enzo, ALX-804-305-C100
Caspase-8	BD Pharmingen, 551243
Catalase	Abcam, ab1877
c-Flip	Enzo, ALX-804-961
Gpx1	Abcam, ab108427
Mcl-1	Santa Cruz,sc-819
p16	Santa Cruz,sc-817
p21	Invitrogen MA5-17093
p53	Cell Signalling, 9282
pRb	Pharmigen, 554136
Prx3	Santa Cruz, sc-23973
SDHA	Abcam, ab14715
Sod1	Santa Cruz, sc-11407
Sod2	Acris, AP03024-PU-N
Trx2	Abcam, ab185544
XIAP	BD Trans-Lab,610762

List of secondary antibodies conjugated with horse radish peroxidase - immunodetection

GAM	Jackson ImmunoReasearch, 115-035-174
GAM IgG1	Jackson ImmunoReasearch, 115-035-205
GAR	Jackson ImmunoReasearch, 111-035-144
RAG	BIO-RAD, 5160-2104

4.10 Visualizing of mitochondrial content

Cells were cultivated in 100mm dishes and 24 hours prior to experiment ($1x10^4$ cells) were seeded into 35mm dish with 10mm round glass coverslips. Cultivating medium was replaced with fresh one containing 15nM Mitotracker Red (Invitrogen) and incubated for additional 30 minutes in CO_2 incubator. After incubation the cultivation medium was again replaced with fresh one containing 2,5ug/ml Hoechst 33342 (Sigma) and cells were then viewed by confocal microscope (TCS SP8, Leica) under 5% CO_2 atmosphere at 37 °C. Images were processed with LAS X Life Science Microscope software (Leica).

4.11 IncuCyte – measurement of cell proliferation.

IncuCyte® S3 is a device for measuring confluency increment of cell population on growth area of each well of 96-well plate. Measurement is based on: unassisted capturing images in each well of 96-well plate every two hours by device, and software analysing captured images and calculating percentage of its occupancy.

Cells were initially cultivated in 100mm dishes and 24 hours prior to experiment were seeded ($1x10^3$ cells) into 96-well plate and left in flowbox for an hour, assuring even adhesion over the growth surface. Plate was then placed into IncuCyte® S3 accommodated in cell culture incubator (5% CO_2, 37°C). Cells remained in InuCyte® for 5-8 days and cell culture media were exchanged every 3 days.

4.12 Detection and quantification of cell death

Cell death was assessed using Annexin V 647/ Hoechst 33258. (Koopman et al, 1994)

Cells were cultivated on 100mm dishes and 24 hours prior to experiment were seeded onto 12 or 24 well plates in duplicates as described in table 4 reaching 70% just before apoptogenic treatments. Cells were treated with apoptogens and then the cell culture media were collected into 1,5ml microcentrifuge tubes and kept on ice. 500µl of

cold 1x PBS was added into the wells with adherent cells and then was also collected into same microcentrifuge tubes and kept on ice. Remaining adherent cells were harvested as described in chapter 4.6 and transferred to the same microcentrifuge tubes as conditioned media with 1x PBS. The suspended cells were then centrifuged (700 x g, 4°C, 8 minutes), supernatant was aspirated, and pellets were washed (1x) with cold 1x PBS, vortexed and again centrifuged (700 x g, 4°C, 8 minutes). Pellets were washed with 1x Annexin V binding buffer, vortexed and centrifuged (700 x g, 4°C, 8 minutes). Cells were then resuspended in 100ul of 1x Annexin V binding buffer (Apronex) containing 0,3ul Annexin V Dyomics 647 (Apronex) and incubated on ice for 15 minutes. Just before measurement Hoechst 33258 (Sigma) was added to final concentration 2ug/ml. Cell populations were analysed using flow cytometer (BD LSRFortessa, BD Biosciences) and the data were evaluated with software FlowJo v10.

GoI expressing cells	Proliferative state		Arrested Phenotype		Senescent Phenotype	
	Cell count	Final confluency	Cell count	Final confluency	Cell count	Final confluency
p16 expressing clones	$9{,}5*10^4$	70%	$1{,}2*10^5$	70%	$1{,}1*10^5$	70%
p21 expressing clones	$9{,}5*10^4$	70%	$9{,}0*10^4$	70%	$9{,}0*10^4$	70%
Empty Vector	$9{,}5*10^4$	70%				
Plasticware	24wp		12wp		12wp	

Table 4. Overview of cell count, final confluency and plasticware used for seeding cells on well plates.

4.13 Assessment of cells energetic metabolism

Cellular respiration was assessed using Seahorse XFe96 Analyzer (Agilent). Seahorse is a device that measures oxygen consumption rate (OCR) and extracellular acidification rate (ECAR) of cells, adhered to the growth area of specifically designed 96-well plate upon different conditions. Scheme of typical OCR experiment is shown in figure 11. And elaborated in Table 5.
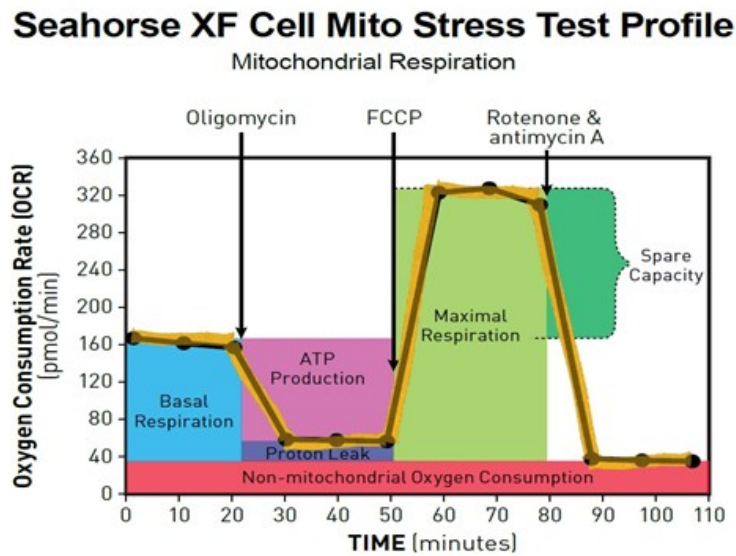
Figure 14. Scheme of Cell Mitostress Test analysis. Black arrows indicate an addition of chemicals conditioning cell environment at certain time points. (Agilent, 2018)

Parameter Value	Equation
Non-mitochondrial Oxygen Consumption	Minimum rate measurement after Rotenone/antimycin A injection
Basal Respiration	(Last rate measurement before first injection) – (Non-Mitochondrial Respiration Rate)
Maximal Respiration	(Maximum rate measurement after FCCP injection) – (Non-Mitochondrial Respiration)
H+ (Proton) Leak	(Minimum rate measurement after Oligomycin injection) – (Non-Mitochondrial Respiration)
ATP Production	(Last rate measurement before Oligomycin injection) – (Minimum rate measurement after Oligomycin injection)
Spare Respiratory Capacity	(Maximal Respiration) – (Basal Respiration)
Spare Respiratory Capacity as a %	(Maximal Respiration) / (Basal Respiration) × 100
Acute Response	(Last rate measurement before oligomycin Injection) – (Last rate measurement before acute injection)
Coupling Efficiency	ATP Production Rate) / (Basal Respiration Rate) × 100

Table 5. Explanation of Cell Mitostress Test scheme from figure 11. (Agilent, 2018)

Time schedule of the typical experiment

Day before experiment

a) Plate coating

Into each well of Seahorse XF96 Cell Culture Microplates (Agilent) was added 25ul of Poly-lysine (Sigma) solution followed by 15 minutes incubation at the room temperature. The poly-lysin solution was recollected and the wells were washed twice with warm cell culture water and left open in flow box for 2 hours to dry out. If the plates were not intended for immediate usage, it could be stored in a fridge for up to 3 days.

b) Cell seeding

Cells were grown on 100mm dish, harvested, counted, diluted to appropriate cell count, as in table 6. (reaching 80% confluency just prior to analysis) within 50ul of cultivating media (doxy+/-), seeded into coated Seahorse XF96 Cell Culture Microplates and left in a flowbox for 60 minutes to ensure even and proper attachment to the well surface. Following this 60minutes incubation, 150ul of cultivating media (doxy+/-) was added into each cells-containing well. Unoccupied wells (blanks and wells without cells) were filled with 200ul of cultivating media. Then plate was placed overnight into a CO_2 incubator (5% CO_2, 37°C).

c) Cartridge hydratation

Assembled cartridge consists of utility plate and sensor part that inserts into utility plate. Cartridge was disassembled and into each well of utility plate was added 200ul of XF Calibrant solution (Agilent). Sensor part was then inserted into utility plate repeatedly (3x) to eliminate bubbles formed under senzors.

d) Setting Seahorse XF96 analyzer for measurement

Seahorse XF96 analyzer was switched on an evening before experiment in order to temper it. Wave software 2.6 (Agilent) was initialized and "Cell Mitostress test" setting was selected.

GoI expressing cells	Proliferative state		Arrested Phenotype		Senescent Phenotype	
	Cell count	Final confluency	Cell count	Final confluency	Cell count	Final confluency
p16 expressing clones	$1*10^4$	80%	$6{,}6*10^3$	80%	$6{,}6*10^3$	80%
p21 expressing clones	$1*10^4$	80%	$5{,}5*10^3$	80%	$5{,}5*10^3$	80%
Empty Vector	$1*10^4$	80%				

Table 6. Overview of cell count and confluency used measuring of respiration in Seahorse XF96 Cell Culture Microplates

The Day of experiment

a) Preparing Cell Mito stress test media (Mito-Media)

Into 100ml of SBM (specified in chapter 4.2) was added pyruvate, L-glutamin and glucose to final concentrations: pyruvate 1mM, L-glutamin 2mM and glucose 10mM. pH 7.4 was optimized using NaOH. 15ml of such a prepared Mito-Media was separated and 850ul of 20%FAF/BSA/ddH$_2$O was added into the rest of the Mito-Media.

b) Preparing cells

From each well of Seahorse plate, 180ul of media was discarded, leaving 20ul of Mito-media in wells. Cells were washed twice with 180ul of SBM and then 160ul was finally added into each well. Plate was then placed in non-CO$_2$ incubator for 60 minutes.

c) Loading cartridge

For each well of a Seahorse plate there are allocated 4 ports on the cartridge. Ports were loaded with chemicals used in Cell Mito stress test as follows:

PORT A: 20ul of 10uM Oligomycin

PORT B: 22ul of 10uM CCCP

PORT C: 25ul of 5uM/5uM Rotenone/Antimycin

PORT D: 28ul of 2ug/ml Hoechst 33342

d) Assessment of cell energy metabolism

As mention above, for analysis, "Cell Mito Stress test" was selected in Wave software and following instructions of selected program, cartridge and plate was inserted into Seahorse. After insertion Wave software autonomously performed the analysis.

e) Microscopy evaluation of cell concentration and normalization

After analysis cell concentration was determined via microscopical detection of cell nuclei in each well by ImageXpress® Widefield system (Molecular Devices) and analysis and quantifications of images in MetaXpress® High-Content Image Acquisition and Analysis Software.

Acquired values by Seahorse were normalized to cell count of each sample and expressed as mean value per $1*10^4$ cells

4.14 Quantification of ROS production

Cells were seeded in duplicates 24 hours prior to analysis on 24 and 12 well plate (described in table 4.) and 1ml of cultivating media was added into each well. 24 hours later MitoSOX™ Red (Invitrogen) Red was added into each well to the final 2,5mM concentration. Cells were incubated with MitoSOX Red for 15 minutes then harvested as described in chapter 4.6. Cells were then collected into microcentrifuge tubes and centrifuged (450 x g, 4°C, 5 minutes). Pellets were resuspended in 100ul of PBS, signal intensity was measured by flow cytometer (BD LSRFortessa, BD Biosciences) and data were analysed with software FlowJo v10.

4.15 Determination of mitochondrial content

Cells were seeded in duplicates 24 hours prior to analysis on 24 and 12 well plate (described in table 4.) and divided into two categories CCCP- and CCCP+. For CCCP- group, cultivating media were replaced with fresh cultivating medium containing 10nM of MitoTracker deep red (Invitrogen) and for group CCCP+ with fresh cultivating medium containing 10nM MitoTracker deep red + 20nM CCCP. Cells were then harvested as described in chapter 4.6 and collected into microcentrifuge tubes and centrifuged (450 x g, 4°C, 5 minutes). Pellets were resuspended in 100ul of PBS, signal intensity was measured by flow cytometer (BD LSRFortessa, BD Biosciences) and data were analysed with software FlowJo v10.

5 Results

5.1 Inducible expression of cell cycle inhibitors in mesothelioma cancer cells H28 induces growth arrest with subsequent senescence-like phenotype

Human mesothelioma cell line H28, was transduced with recombinant lentiviruses, expressing either p16 or p21 proteins in doxycycline-inducible manner and clonal selection was used for selecting several, best performing clones (low background, high inducibility and stability of expression – performed by former PhD. student Gita Novaková).

5.1.1 P16-expressing H28 cells require 15 days to achieve senescence-like phenotype

P16-expressing clonal cultures No. 5 and No. 34 upon doxycycline treatment efficiently induce and maintain expression of p16 protein (Fig. 15). Strong and stable p16 expression led to a senescence-like phenotype (assessed by SA-associated b-Gal activity) in time-dependent manner with first signs of Sa-β-Gal positivity observed in H28 clonal culture No. 5 on day 6, however, enlarged cell morphology was evident already from the day 4 (Figure 16A). Sa-β-Gal staining gradually intensified and reached its maximum on the day 12 and remained so up to day 15 (Fig. 16A) and further (data not shown). Doxycycline-treated clonal cultures No. 5 and 34 behaved very similarly, therefore only representative photos of clone 5 from one the experiments are shown in Fig. 16A. In control H28 cells harbouring just the empty vector doxycycline treatment did not lead to any senescence-like phenotype (enlarged cells, SA-b-Gal activity, Fig. 16B).
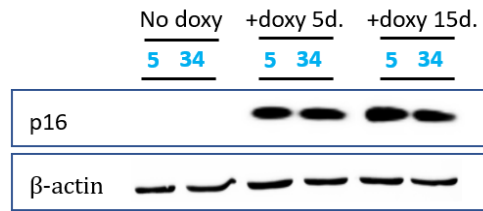
Figure 15. Expression of p16 in clones 5 and 34 after their incubation with doxycycline for 5 and 15 days. Untreated and Doxy-treated cells for 3 and 15 days were analysed by Western blotting for expression of p16 protein. β-actin was used as loading control.
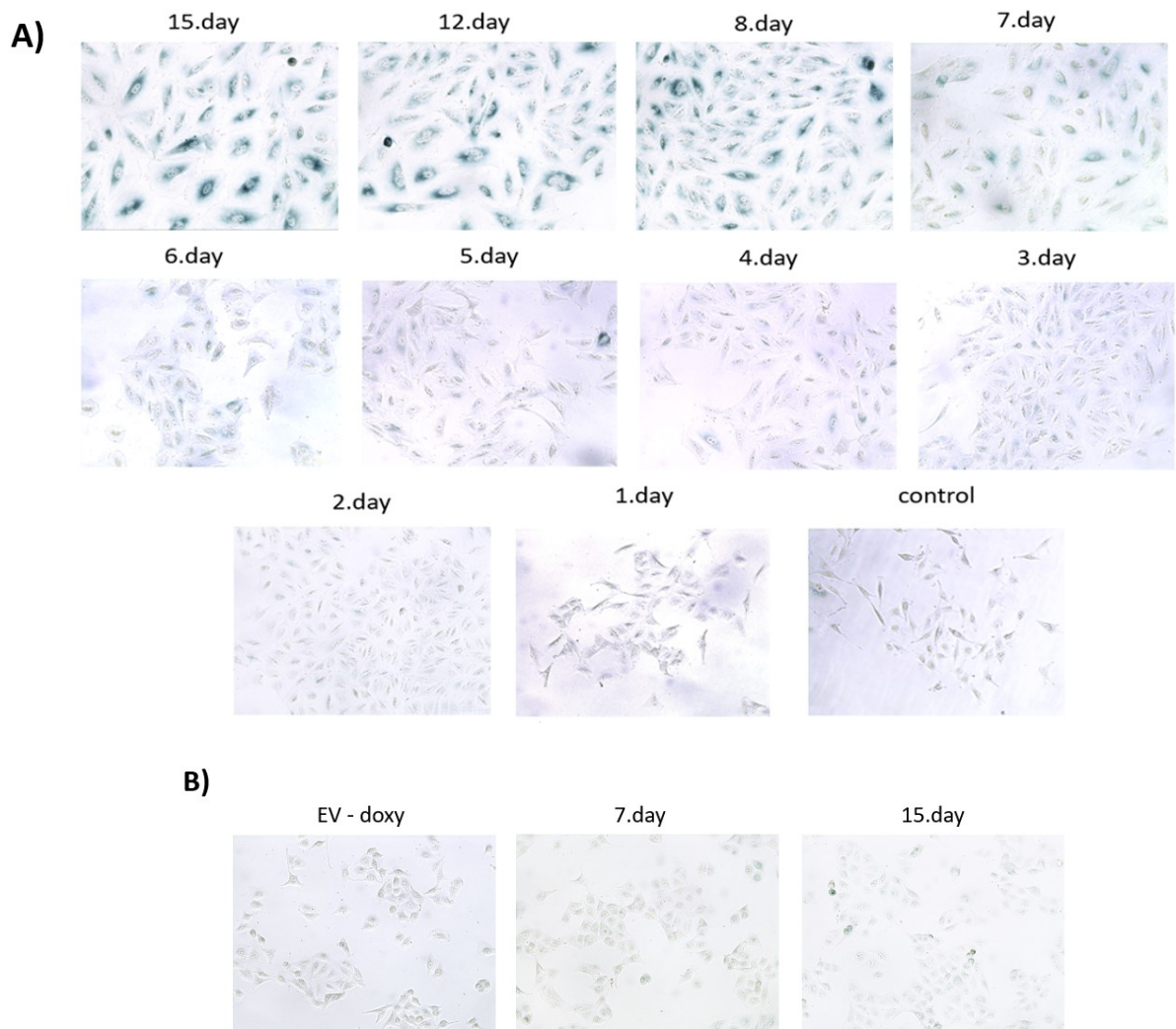
Figure 16. A) Kinetics of Sa-β-Gal staining in p16 expressing clonal culture No. 5. Cells were incubated in time-dependent manner with doxycycline or without doxycycline (control) and then stained over-night in β-Gal staining solutions. **B)** Control EV-harbouring H28 cells were treated with doxycycline for 7 and 15 days. The treatment was performed using reversed kinetics and repeated twice**. (**Magnification200x)

Concurrent cell cycle analysis of p16-expressing cultures revealed significant cell cycle suppression already on day 5 of doxycycline treatment, that from day 8 dropped to only marginal values and remained so till day 15 and further (Fig. 17).
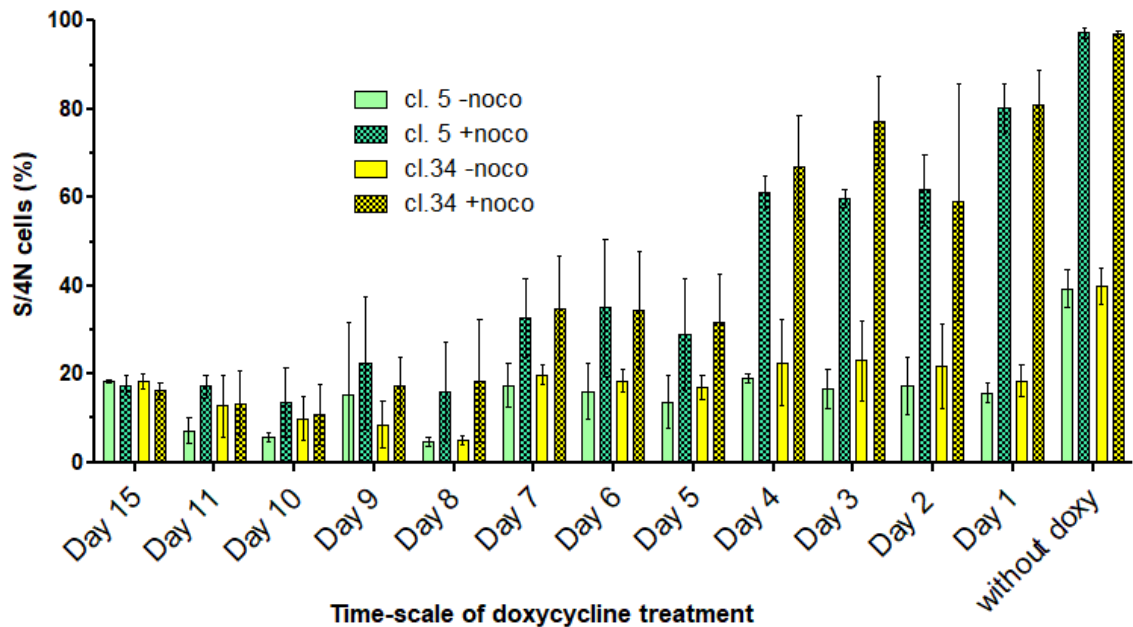

Figure 17. Kinetics of cell cycle arrest in p16 expressing clones 5 and 34. Cells were incubated in time dependent manner with doxycycline using reverse kinetic. Noco + groups (patterned) were also co-incubated for last 24hours of doxycycline treatment with 10uM nocodazole whereas group Noco- (non-patterned) were not. Increment in S/4N cells between group Noco- and Noco+ of the same clone reflects proliferative fraction of cell population. Results are means of 4 independent biological experiments. Bars indicate mean and error bars represent standart deviation.

Taking together the cell appearance, SA-b-Gal positivity and the data from cell cycle analysis, we selected day 5 of the doxycycline treatment as a point of cellular arrest (markedly decreased proliferation and still negative for Sa-β-Gal staining) and day 15 was chosen as a time point of established senescent-like phenotype (for simplicity called only "senescent").

5.1.1 H28 cells expressing protein p21, enter senescent-like state faster than p16-expressing cells

Doxycycline treatment induced efficient and stable expression of protein p21 in H28 clonal cultures No. 33 and 36 (day2 and day 7, Fig. 18). Time-course of SA- β -Gal staining revealed that SA- β -Gal activity largely increased already at day 3 of doxycycline treatment with steadily increasing intensity until day 5, that was stable from day 7 (Fig. 19) even up to day 15 (data not shown) in both clonal cultures. Size of the cells dramatically increased already on day 2, yet without Sa-β-Gal positivity. No. 33 and 36 behaved very similarly, therefore only representative photos of clone 33 from one the experiments are shown in Fig. 19.
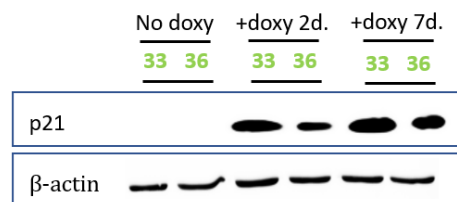
Figure 18. Expression of p21 in clones 33 and 36 after incubation with doxycycline. Untreated and for 2 and 7 days doxycycline-treated cells were analysed by western blotting. β-actin was used as loading control.
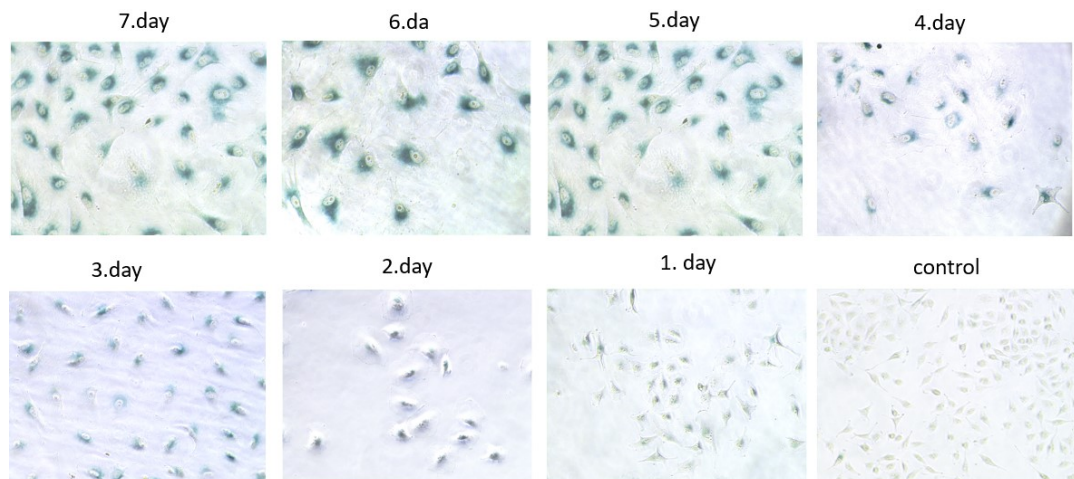
Figure 19. Time-course of Sa-β-Gal staining in p21-expressing clonal culture No. 33. Cells were incubated with doxycycline or without doxycycline (control) for up to 7 days and then stained over-night in β-Gal staining solutions. Experiment was performed using reversed kinetic **(**200x magnification).

Similarly as for p16-expressing cells, the suppression of proliferation in H28 cells expressing p21 was assessed by cell cycle arrest analysis, which uncovered, that already after 2 days of Doxy treatment cells contained only negligible fraction of proliferating cells (Fig. 20). As p21-expressing H28 cells enter the growth arrest much faster than p16-expressing cells, we aimed to determine timing of this process into more detail. A fine 48hrs titration revealed gradual decrease of proliferative rate between 24hrs and 36hrs of the treatment with effective cell cycle suppression between 36th and 40th hr of the treatment. As both p21-expressing clones behaved identically, only clone 33 was subjected to fine titration (Fig. 21).
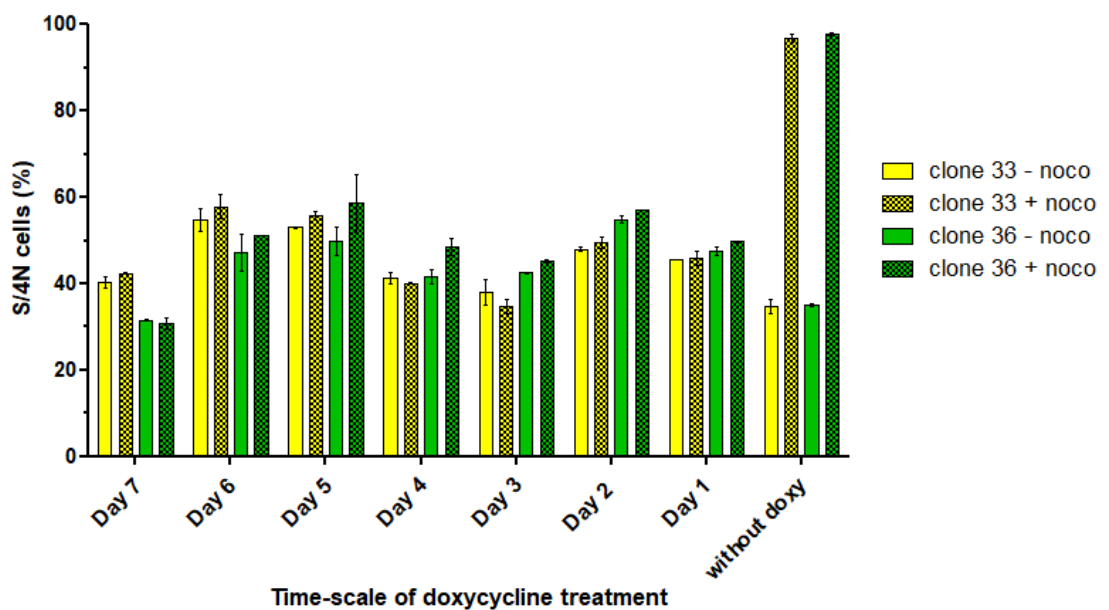
Figure 20. Kinetics of cell cycle arrest of H28 clonal cultures 33 and 36 expressing p21. Cells were incubated in time dependent manner with doxycycline using reverse kinetic. Noco + groups (patterned) were also co-incubated for last 24hours of doxycycline treatment with 10uM nocodazole whereas group Noco- (non-patterned) were not. Increment in S/4N cells between group Noco- and Noco+ of the same clone reflects proliferative fraction of cell population. Results are means of 3 independent biological experiments. Bars indicate mean and error bars represent standard deviation.
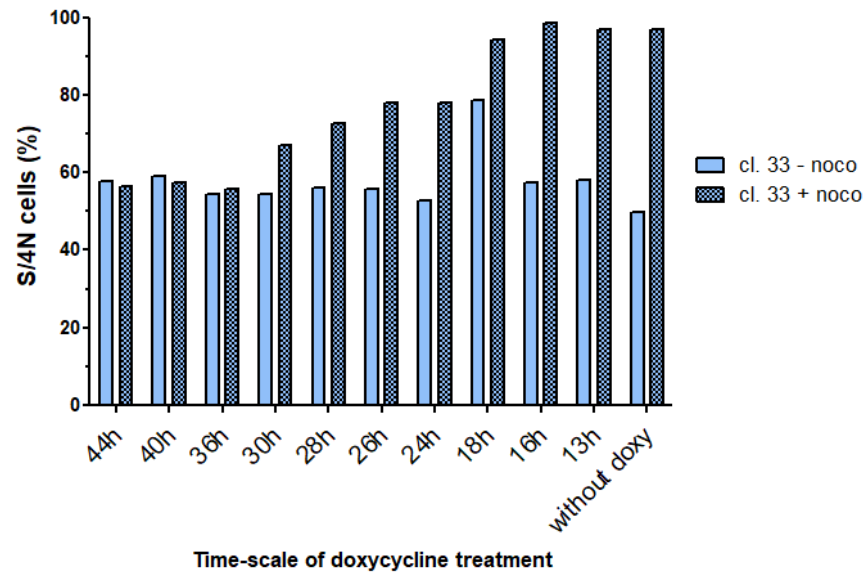
Figure 21. Fine kinetics of cell cycle arrest of p21 expressing clone 33. Experiment followed the same setup as in figure 20 and was performed only once.

Though growth arrest and pro-senescence phenotype appeared already on 2. resp. 3. day of the doxycycline treatment, we did (similarly as for p16 expressing cells) choose longer 7day treatment to firmly ensure full establishment of cellular senescence or senescence-like phenotype (further called "senescent state"). For the establishment of arrested phenotype, 48hours long incubation period was selected as the cells already manifested almost completely ceased proliferation, increased size and at the same time were still negative for Sa-β-Gal staining.

Diminished proliferative capacity of clones in arrested and senescent states was further indirectly confirmed by examining the phosphorylation status of the tumour suppressor and cell cycle regulator retinoblastoma protein (pRb). While in proliferating H28 clonal cultures (i.e. cells cultivated without doxycycline) was as expected majority of pRb in slower, phosphorylated band, both arrested and senescent clonal cultures showed expression of only faster, hypo-phosphorylated protein (Fig. 22).
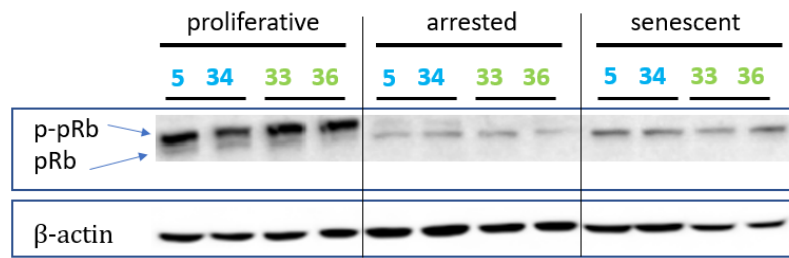
Figure 22. Western blotting analysis of pRb expression in p16 and p21 expressing H28 cells. Comparison pRb expression in proliferating, arrested and senescent p16 (blue) and p21 (green) H28 clonal cultures. (representative image from three independent experiments, β-actin was used as a loading control).

Notably, phenotypically p16- and p21-expressing cells looked rather differently. P16 cells were smaller and intensity of Sa-β-Gal staining was not as pronounced as in p21 cells (Fig. 23). P16- also in contrast to p21-expressing cells apparently proliferated, though at low rate (as they had to be passaged throughout the incubation time).
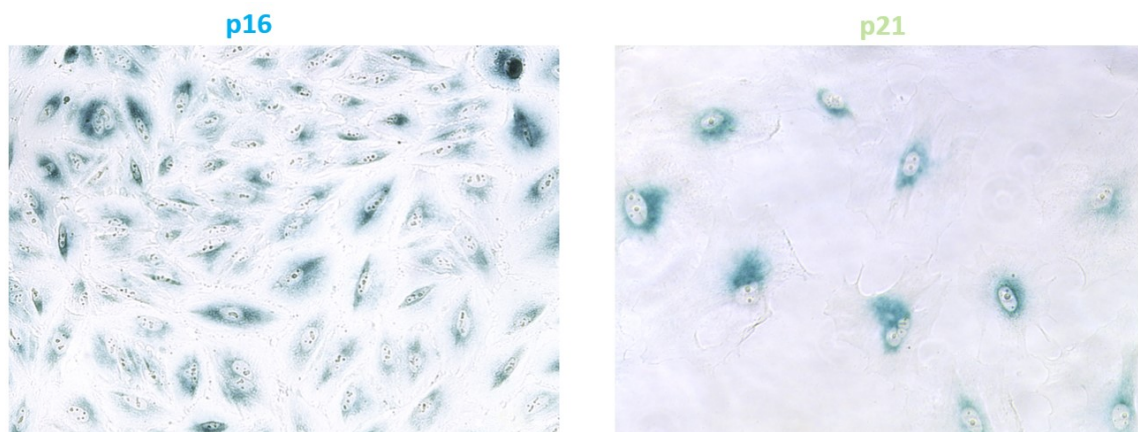

Figure 23. Comparison of p16- vs. p21-expressing H28 cells. P16-expressing cells (on the left) are smaller and display heterogeneity in Sa-β-Gal staining. P21-expressing cells (on the right) are notably bigger with homogenous intensity of Sa-β-Gal. (200x magnification)

5.2 Senescent phenotype is reversible in both p16 and p21 expressing cells upon doxycycline withdrawal and senescence-like p16 clones even exhibit steady low proliferation

In order to better characterize senescent phenotype in p16- and p21-expressing we employed several other assays and tests. Senescence-accompanying damage of chromosomal DNA was evaluated by histone γH2Ax immunocytodetection (Lawless et al. 2010), possible proliferation was assessed by immunostaining of proliferative marker Ki67 (Lawless et al. 2010), by assessment of EdU incorporation and by online visualization and quantification of cellular proliferation using cell analysis system Incucyte S3 (Sartorius).

The results showed, that while histone γH2AX staining was absent in senescent-p16 cells, about 1/3 of p21-expressing senescent cells were positive for γH2AX specific foci (Fig. 24). In contrast, Ki67 staining revealed that about half of the senescent p16-expressing cells were Ki67 positive, while Ki67 staining was almost negative in senescent-p21 cells (Fig. 25). Homogenous distribution of senescent-p16 Ki67 positive cells also excluded possibility that few clones escaped senescence and overgrew neighbouring cells.
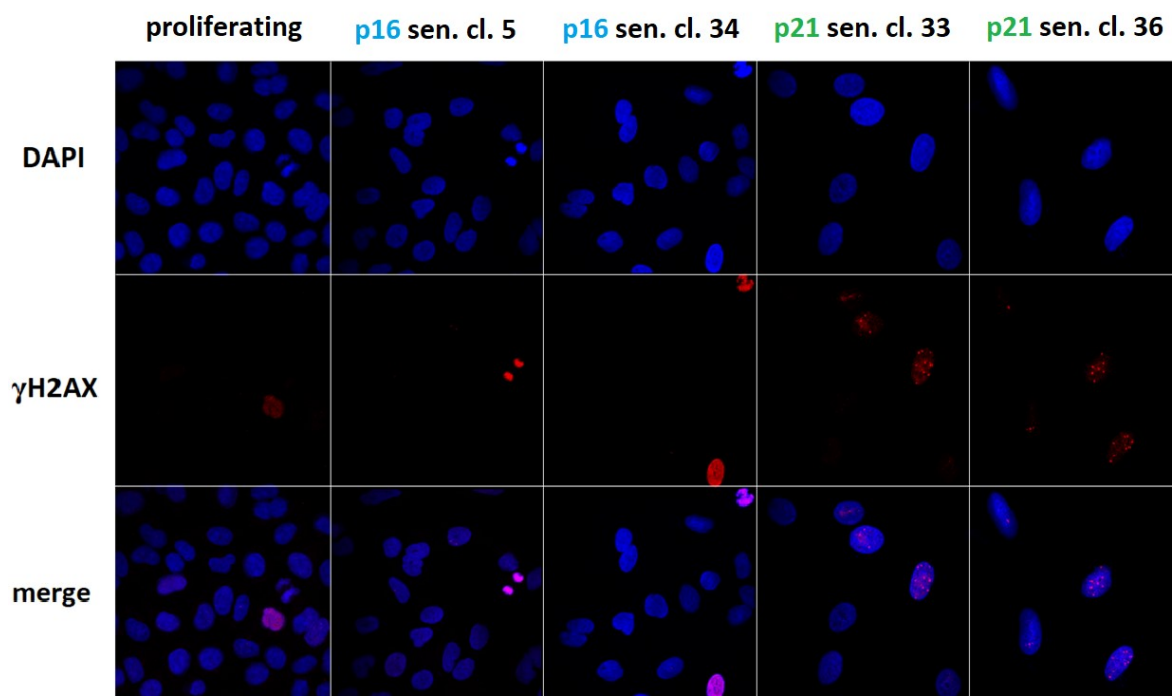
Figure 24. Detection of γH2AX foci. Representative pictures of senescent-p16, -p21 and proliferating control cells stained by γH2AX antibody (Red). Cell´s nuclei were visualised with DAPI (Blue). Only senescent p21 clones stained partly positively for senescent specific γH2AX foci. Non-specific diffuse or punctuated pattern of γH2AX signal associates with dying or dividing cells.
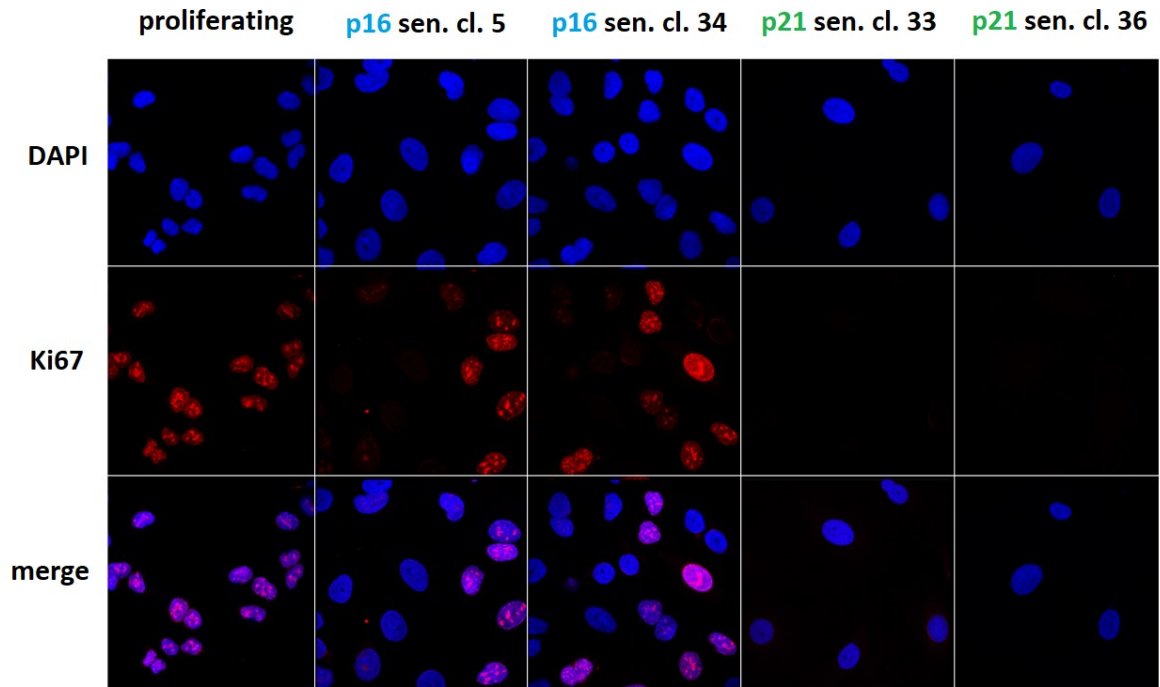
Figure 25. Detection of Ki67. Representative pictures of proliferating and senescent-p16, -p21 cells stained by Ki67 antibody (Red). Cell´s nuclei were visualised with DAPI (Blue). All control cells stain positively for Ki67. Around the half of the senescent-p16 cell stained positively whereas almost all senescent-p21 cells were negative.

For further assessment of proliferation-like phenotype of senescent p16-expressing H28 cells, we employed EdU incorporation test. 24hrs incubation of senescent cells with the reagent revealed, that while up 60% of p16-expressing cells incorporated EdU, only up to 2% of p21-cl.33 and up to 10% of p21-cl.36 incorporated EdU over the same time period (Fig. 26B).
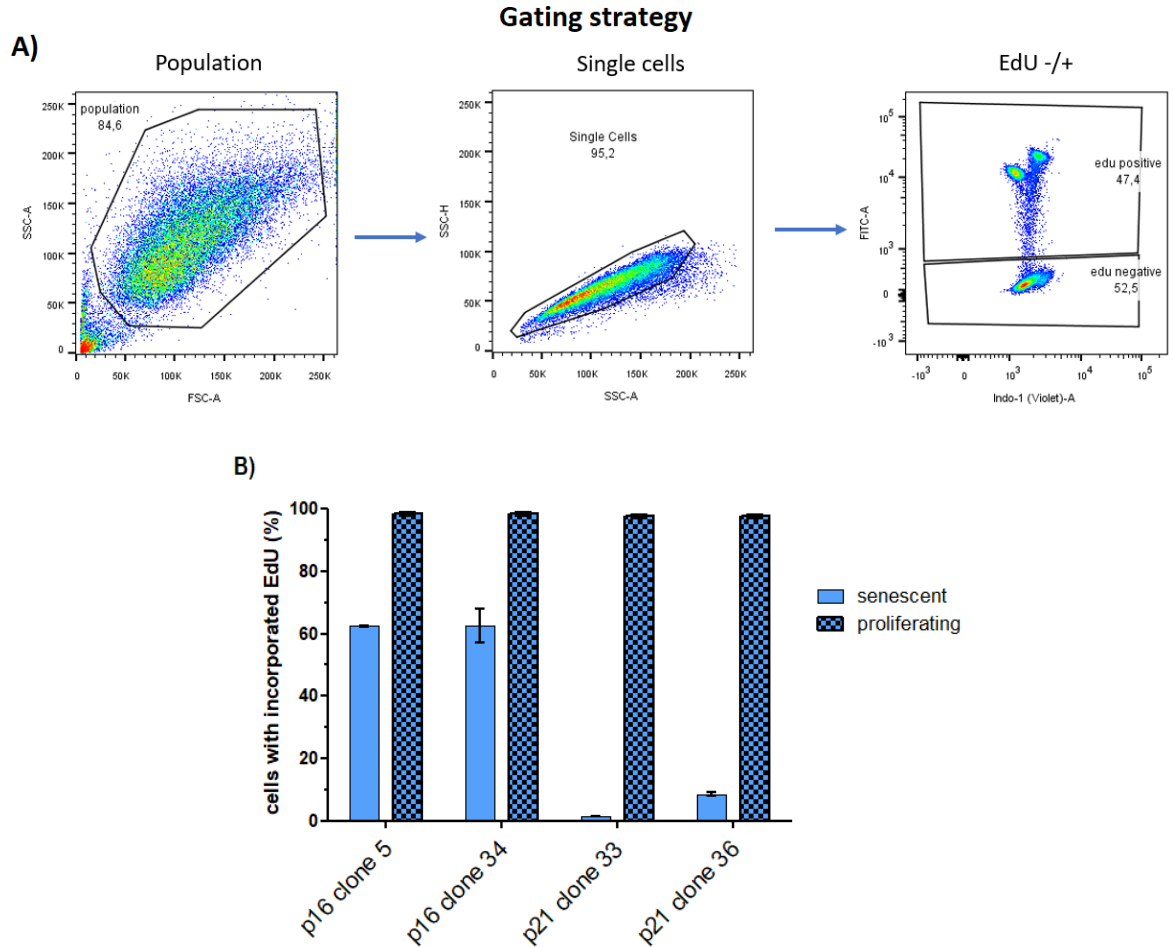
Figure 26. Detection of EdU incorporation. A) Gating strategy used for EdU incorporation test B) All clones in both senescent (patterned) and proliferative (non-patterned) states were co-incubated with EdU for 24hours. Bars are mean results of 2 independent experiment and error bars represent standard deviation.

Apparent proliferation of p16-expressing H28 cells prompted us to analyse this phenomenon further, using live cell analysis system Incucyte S3. Cells (proliferating, arrested, and senescent) were cultivated with and without doxycycline on 96 well plates for up to 7 days and their growth was every 2 hrs monitored and captured by an image acquisition system. The data revealed very similar proliferation rate of H28 clonal cultures with no expression of p16 or 21 reaching confluency between 90-100 hr of cultivation (Fig. 27A). Growth arrested and senescent cells expressing p21 or p16 (plated as already arrested/senescent cells i.e. after 2/7 or 7/15 days of their treatment with doxycycline) cultivated in doxy-containing medium behaved differently from the proliferating cells as well as from each other. While p21-expressing growth arrested and senescent clones 33 and 36 did not show almost any signs of proliferation, p16-

expressing clones 5 and 34 were apparently proliferating/dividing though at very slow rate (Fig. 27A, B). Thus, these data from IncuCyte analyser confirmed our previous results that pointed to low proliferation rate in p16-expressing clones (Ki67 and EdU staining) even though they displayed other signs of senescence such as cell enlargement and SA-b-Gal staining. The 3rd employed setup was release of arrested/senescent cells, i.e. their further cultivation without doxycycline and thus rapid drop of p16 or p21 expression (expression data not shown). These cultivation conditions led after a short (p21-expressing clones) or longer delay (p16-expressing clones) to restoration of their proliferation, eventually reaching confluency (Fig. 27A).

Video file (Suppl. data vid.1, figure 27B) composed of images captured by IncuCyte revealed, that despite having senescent phenotype, senescent-p16 cells (with doxycycline during test) were able to proliferate with various speed, which differed among individual cells. However, some of cells remained in non-proliferative state. Video also documents that once doxycycline is removed from media, majority of senescent cells p16 (Suppl. data vid.2, figure 27B) and p21 (Suppl. data vid.3, figure 27B) shrunk, and restored their proliferative capacity. Needlessly to say, that almost all p16 cells reverted their phenotype while approximately ¼ of senescent p21 cells remained large and did not divide.
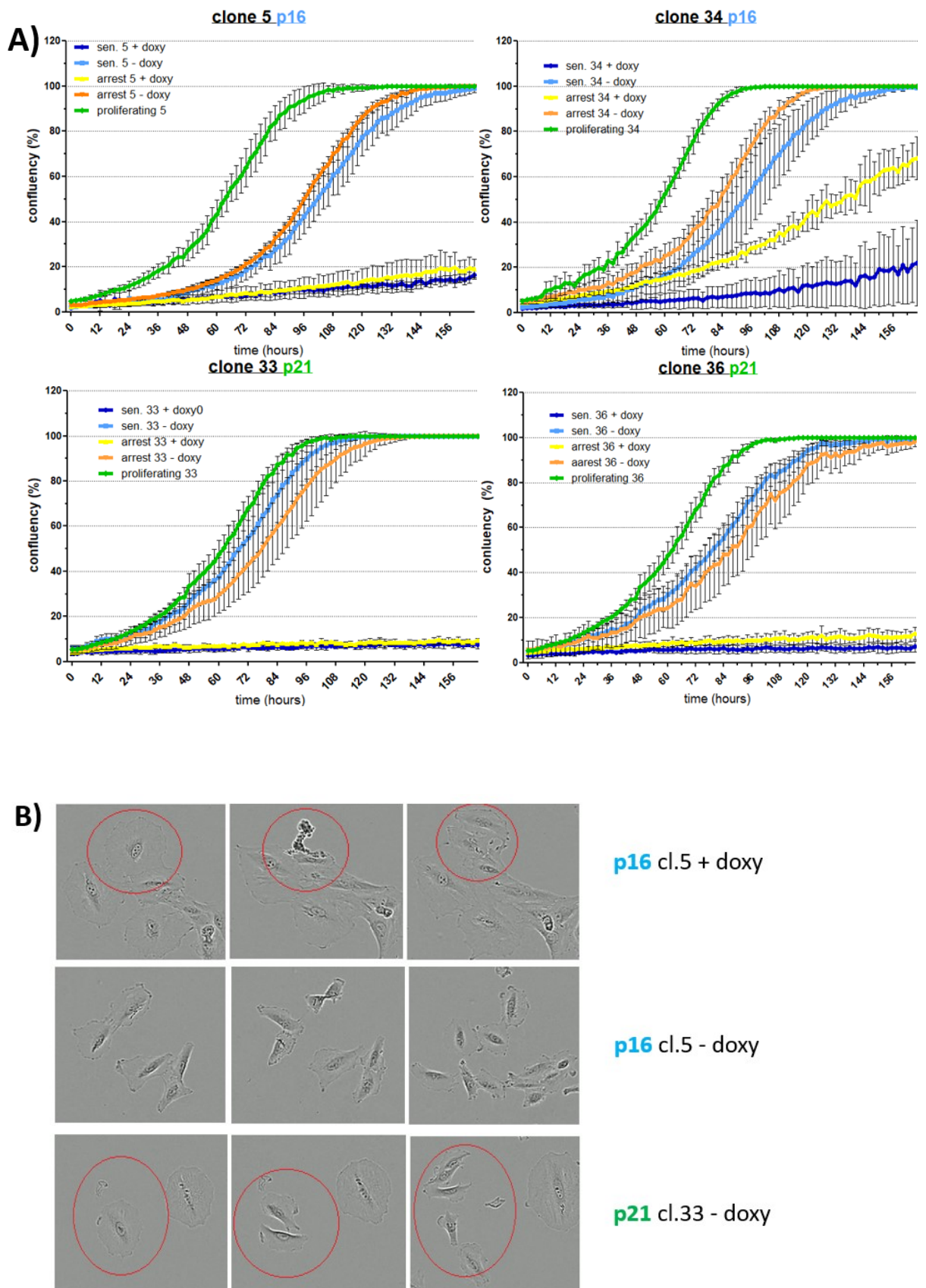
Figure 27. IncuCyte – measurement of proliferation. A) Proliferating curves reflect increment of confluency (%) over time (hours). Data from each clone were acquired from proliferating cells (no doxy, green), arrested state with or without doxycycline (yellow/orange) and senescent state with or without

doxycycline (violet/blue). Representative data from one out of three individual biological experiment are shown. B) Representative photos of senescent-p16 clones (blue) cultured during experiment with doxycycline (+doxy) or without (-doxy) and senescent-p21 clones cultured during experiment without doxycycline showing shrinkage and restoration of proliferation. (Magnification 200x)

All these data indicate that senescence-like phenotype acquired by H28 clonal cultures expression p16 or p21 is upon cessation of p16/p21 expression reversible and that this senescence-like phenotype is more pronounced in p21-expressing cells then in p16-expressing cells, which upon p16 expression still slowly albeit steadily proliferate.

5.3   Response of proliferating, arrested and senescent H28 cells expressing protein p16 or p21 to apoptotic stimuli

P16- and p21-expressing (arrested and senescent) cells and their non-expressing, proliferating counterparts were subjected to time and concentration dependent treatments with various apoptogens (see below) and their combinations targeting both extrinsic and intrinsic apoptotic signalling pathways. For evaluation and quantification of apoptosis we used flow cytometry - late apoptotic/necrotic cells were stained with Hoechst 33258 (Indo-1 violet detector) and apoptotic cells with Annexin V- Dy647 (APC detector). Population of cells and singlets were gated as shown in figure 28 A. Total number of Apoptotic cells was determined as a sum of late apoptotic cells represented by quadrant 2 (Q2, Annexin V, Hoechst 33258 double positive) and early apoptotic cells represented in quandrant 3 (Q3, Annexin V positive, Hoechst 33258 negative).

Due to large variability in cell size of different states (figure 28B - size: proliferative<arrested<senescent) voltages for detection of forward (FSC-A) and side scatter (SSC-A) - population gate, were re-adjusted for each clone in arrested and senescent state (but for clones in proliferative state) to resemble localization of events within plot area as shown on population gate depicted in figure 28 A). Due to different sizes and states, cells also displayed different values of autofluorescence, thus also shifting localization of event within plotting area of "Apoptotic gate" (shown in figure 28A). Each individual clone in each state was therefore evaluated and gated as distinct cell type according to its own negative controls.

Apoptogens used for the treatments (concentration, incubation time):

- Fas ligand – 70ng/ml, 24 hours

- mitochondrially-targeted vitamin E succinate (mitoVES) – 16µM, 24 hours

- mitochondrially-targeted tamoxifen (mitoTAM) - 7µM, 24 hours

- Homoharringtonine (HHT) + TRAIL – 50ng/ml, 4 hours + 50ng/ml, 3 hours

- Homoharringtonine + ABT737 – 50ng/ml, 3 hours + 15µM, 2 hours
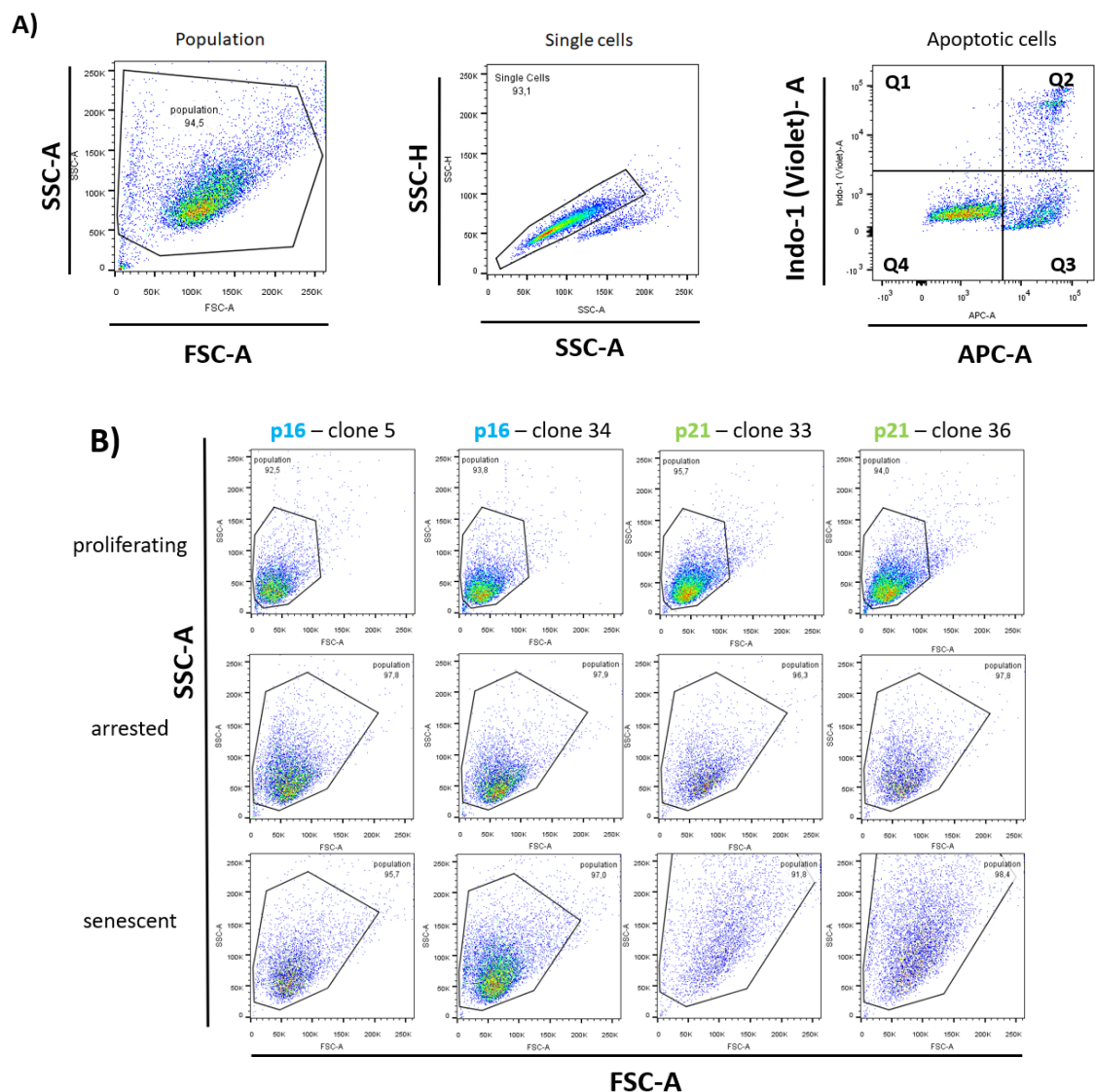
Figure 28. Gating strategy for apoptotic tests. A) Illustrative strategy for gating population, singlets and apoptotic cells, common for all apoptotic test and all cell clones in all states. Population is determined based on cell size as indicated and singlets are determined from gated population. Apoptotic cells are determined as sum of Q2 and Q3 B) Visualisation of different cell sizes in different states while using constant voltages for forward and side scatter on flow-cytometer.

5.3.1 H28 p16- and p21-expressing cells are sensitized to FasL mediated apoptosis in doxycycline-dependent manner.

Initial data showed, that both arrested and senescent cells became sensitive to extrinsic, FasL-induced apoptosis (Fig. 29). However, we also found that control H28 cells containing only empty virus (i.e. non-expressing p16 or p21) were sensitized to FasL-triggered apoptosis just by the treatment with 1 ug/ml doxycycline (Fig. 29, right part). Thus, in respect to these data we cannot claim that arrested or senescence-like state enhances FasL-induced apoptosis. Interestingly, both senescent p16 (after 15days) and p21 (after 7days) cells show reproducibly lower sensitivity to FasL in comparison doxycycline-treated H28 cells containing empty virus.
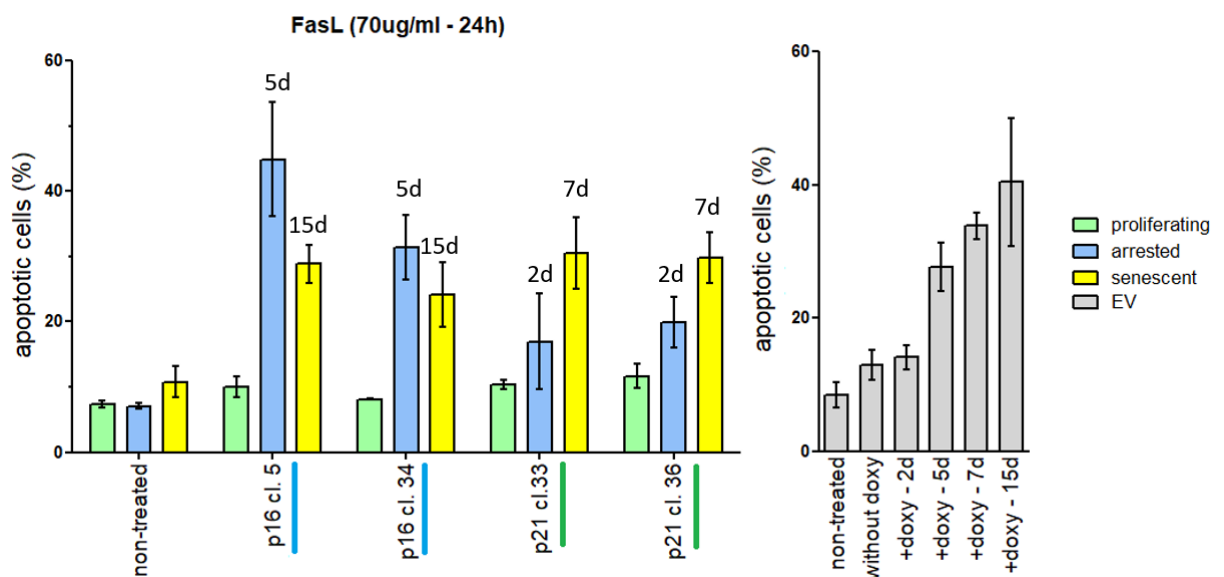
Figure 29. Quantification of apoptosis: Fas ligand treatment. Proliferating (green), arrested (blue), senescent (yellow) and EV (grey) were treated with FasL 70μg/ml for 24 hours. Numbers (5d, 15d etc.) above or under bars indicate number of days incubated with doxy during senescence induction. Results are means of 3 independent biological experiments. Bars indicate means and error bars indicate standard deviation.

5.3.2 Senescent p16- and p21-expressing cells are more resistant to mitoVES treatment.

MitoVES inhibits mitochondrial complex II inducing ROS generation and activates intrinsic apoptotic signalling (Dong et al. 2011)

Both senescent-p16 clones and-p21 cl.33 exhibited significantly increased resistance toward mVES treatment in comparison to proliferative or arrested state (Fig. 30) despite that doxycycline treatment of H28/EV cells significantly enhanced their sensitivity to mitoVES (Fig. 30). Thus, if compared to doxycycline-treated EV-containing cells, it could be debatable, that the arrested state cells also became slightly more resistant mitoVES treatment.
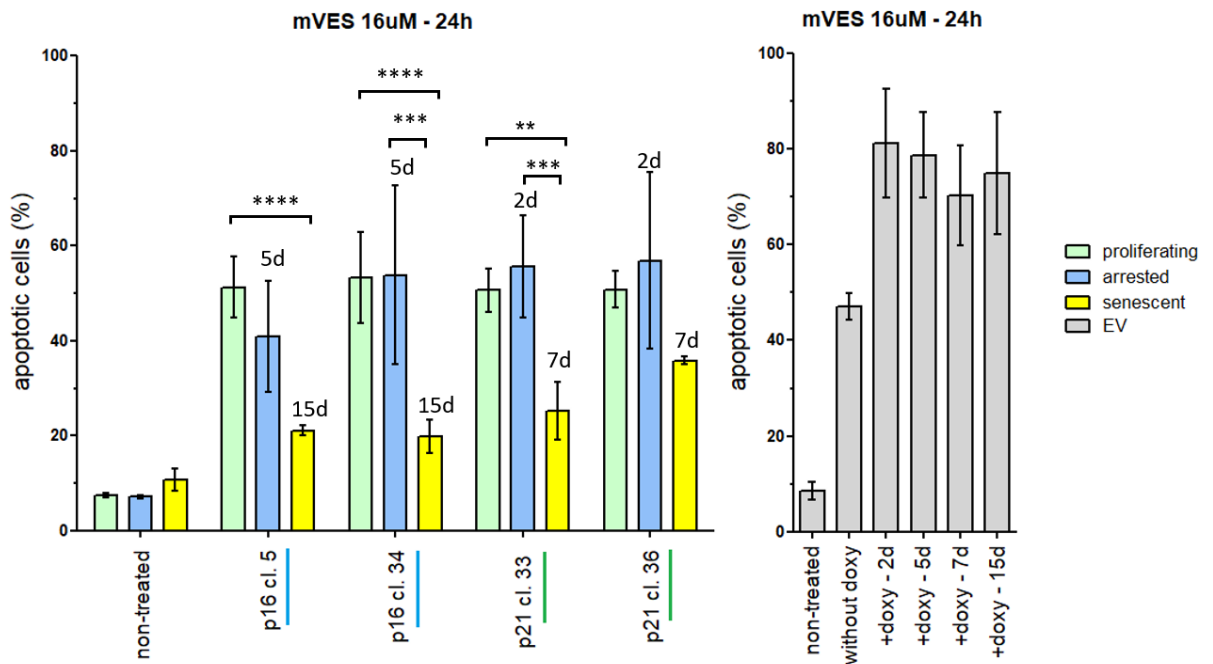
Figure 30. Quantification of apoptosis: mitoVES treatment. Proliferating (green), arrested (blue), senescent (yellow) and EV (grey) were treated with mitoVES 70μg/ml for 24 hours. Numbers (5d, 15d etc.) above or under bars indicate number of days incubated with doxy during senescence induction. Results are averaged of 3 independent biological experiments for proliferating arrested and senescent phenotypes and at least 2 independent experiment in case of EVs. Bars indicate mean and error bars indicate Std. Significance was calculated by two-way ANOVA test, ****: p<0,0001, ***: 0,001>p>0,0001, **: p=0,0013

Senescent p16 and p21 cells increase anti-oxidant defence

Increased resistance of senescent p16- or p21-expressing cells prompted us to examine influence of arrested or senescent state of H28 cells on the expression of anti-oxidant defence proteins. Data from Western blotting revealed increased expression of both mitochondrial and cytoplasmic superoxide dismutases SOD2 and SOD1 as well as glutathione peroxidase 1 (Gpx1), catalase (Cat), mitochondria-specific peroxiredoxin 3 (Prx3) and thioredoxin 3 (Trx3) (Fig. 31), suggesting enhanced ROS-scavenging activity by senescent cells protecting them against acute effects of massively generated ROS. Interestingly, we observed also increased expression of SDHA in senescent cells.
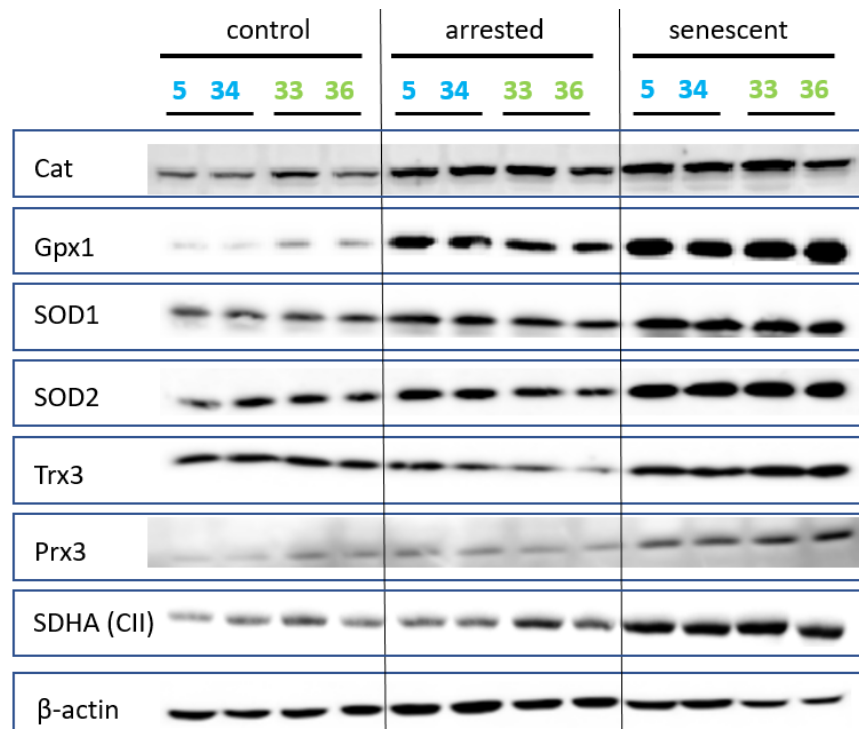
Figure 31. Expression of antioxidant and SDHA proteins in H28 clonal cultures. Comparison of proliferating, arrested and senescent p16 (blue) and p21 (green) cell lysates in expression of indicated antioxidant proteins and SDHA (subunit of mitochondrial complex II). The data shown are representative Western blots from two independent cell lysates. β-actin was used as loading control

5.3.3 Arrested p21-expressing cells exhibit increased sensitivity to mitoTAM treatment.

MitoTAM induces apoptosis of cancer cell by generation of ROS via inhibition of mitochondrial respiratory complex I (Rohlenova et al. 2017). In senescent cells mitoTAM-triggered apoptosis is at least partly connected with dropped levels of Adenine nucleotide translocase 2 (ANT2) in senescent (Hubackova et al. 2018).

Apoptosis assays employing mitoTAM treatment of H28 clonal cultures provided largely inconsistent data, however, there was a trend of higher sensitivity of arrested cells toward mitoTAM, especially observed in p21-expressing clonal cultures (Fig. 32). Doxycycline-treated EV-containing H28 cells were also sensitized to mitoTAM, which was especially pronounced for the 15day long treatment period (Fig. 32). Interestingly, induction of senescent-like phenotype in p16-expressing clones blunted mitoTAM-induced apoptosis by 30-40% (in comparison to doxy-treated EV cells).
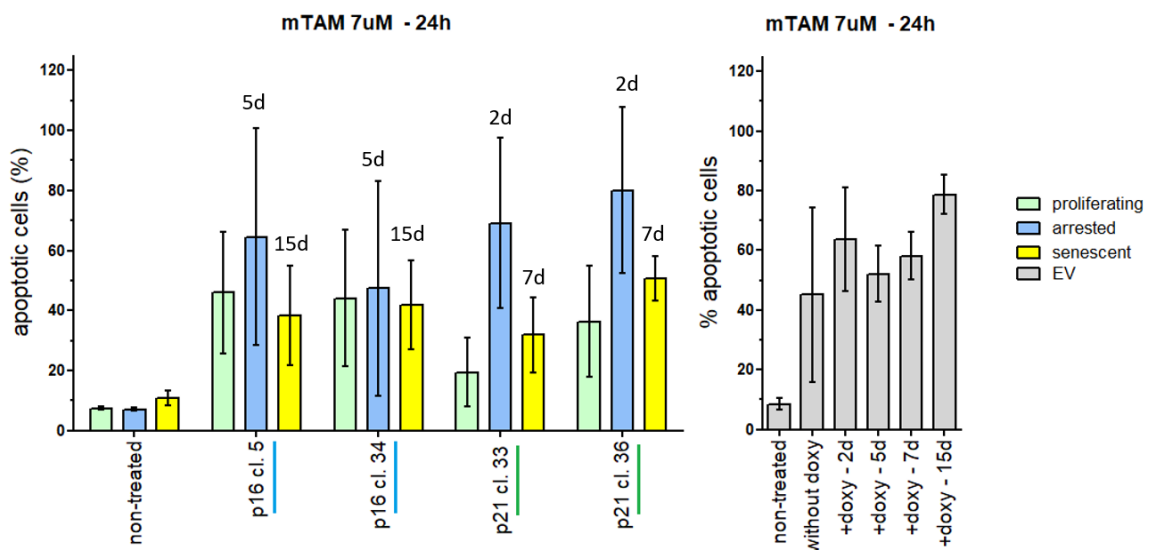
Figure 32. Quantification of apoptosis: mitoTAM treatment. Proliferating (green), arrested (blue), senescent (yellow) and EV (grey) were treated with mitoTAM 7μg/ml for 24 hours. Numbers (5d, 15d etc.) above or under bars indicate number of days incubated with doxycycline during senescence induction. Results are averaged of 6 independent biological experiments in case of senescent and proliferative phenotype and 3 independent results of arrested phenotype and at least 2 independent experiments in case of EVs. Bars indicate means and error bars represent standard deviation.

5.3.4 Both p16 and p21 senescent cells are significantly more resistant to TRAIL-induced apoptotis

TRAIL, similarly to FasL binds to death receptors namely DR4, DR5, and initiate assembly of a DISC. As H28 cells are resistant to TRAIL-induced apoptosis, we employed homoharringtonine (HHT) as already known sensitizer of cancer cells to this death ligand (Beranova et al. 2013). HHT alone similarly as TRAIL alone was unable to induce apoptosis in in proliferating as well as in arrested/senescent clonal cultures (Fig. 33A). However, combined HHT+TRAIL treatment elicited a strong apoptotic response in proliferating H28 cells but both p21- and p16-expressing senescent cells showed significantly increased resistance to this combined treatment (Fig. 33A), though this increased resistance was more pronounced in p21-expressing cells. Sensitivity of arrested cells to HHT+TRAIL was only marginally suppressed. Doxycycline, similarly as for FasL also sensitized EV-containing H28 to even TRAIL alone-induced apoptosis (Fig. 33B) and despite its sensitizing effect senescent cells became resistant to HHT+TRAIL treatment.
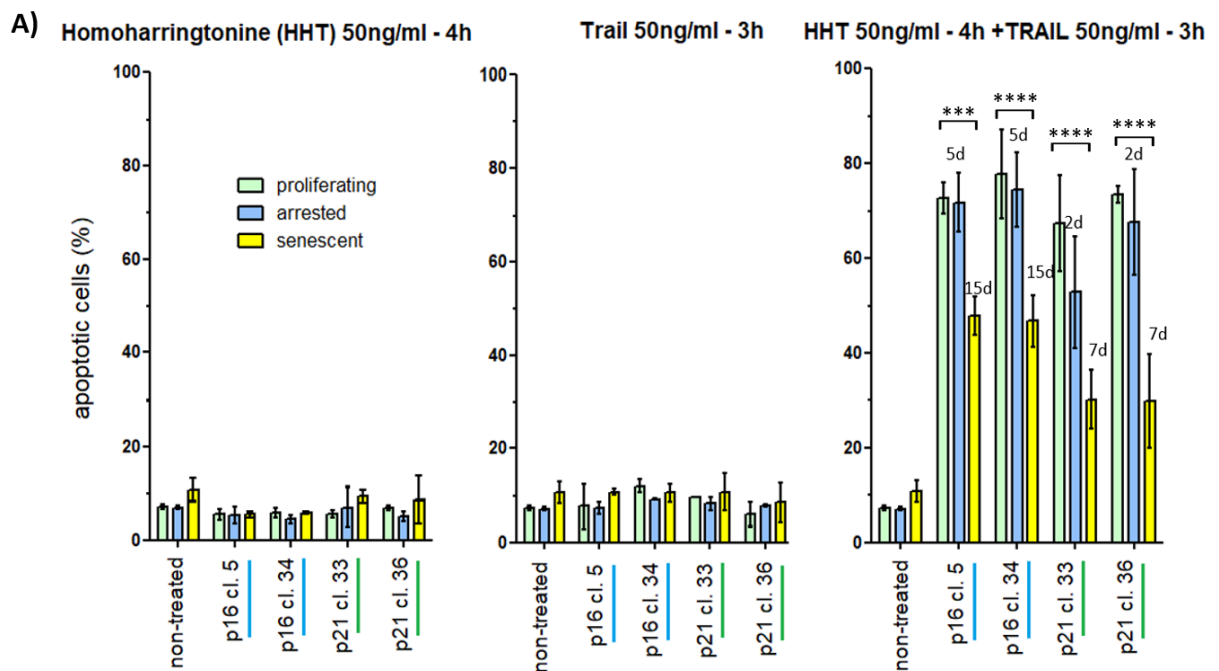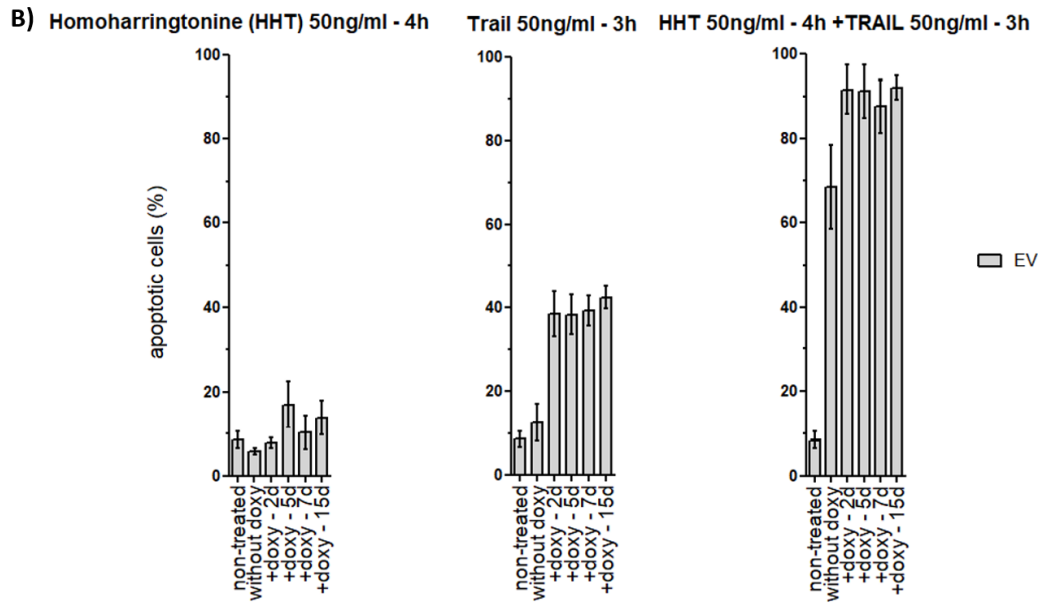
Figure 33. Quantification of apoptosis: HHT+TRAIL treatment. A) Proliferating (green), arrested (blue) and senescent (yellow) were pre-treated with HHT 50ng/ml for 1 hours and then co-incubated together with TRAIL 50ng/ml for additional 3 hours. B) EV cells (grey) were pre-treated with HHT 50ng/ml for 1 hours and then co-incubated together with TRAIL 50ng/ml for additional 3 hours.

Numbers (5d, 15d etc.) above or under bars indicate number of days incubated with doxycycline during senescence induction. Results are means of 4 independent biological experiments in case of senescent phenotype and 3 independent results of arrested phenotype and at least 2 independent experiments in case of EVs. Bars indicate means and error bars represent standard deviation. Significance was calculated by two-way ANOVA test, ****: $p < 0,0001$, ***: $p = 0,0002$.

5.3.5 Senescent H28 clonal cultures became weakly sensitized to Bcl-2 antagonist.

ABT-737 is an BH3-mimicking inhibitor for anti-apoptotic Bcl-2 proteins Bcl-2, Bcl-Xl and Bcl-W, that selectively targets and eliminates senescent cells (Yosef et al. 2016) and HHT is known to suppress expression of short-live Mcl-1 protein from the same family. Co-administration of ABT-737 with HHT enhanced apoptosis promoting ability of ABT-737 (Kuroda et al. 2008).

Single ABT-737 treatment showed marginally increased sensitivity of senescent clonal cultures, which however was not significantly different from increased sensitivity

of EV cells imposed just by doxycycline treatment (Fig. 34B). Joint HHT+ABT-737 treatment was very effective in inducing apoptosis of both proliferating and arrested/senescent clonal cultures as well as in EV-containing cells. Induction of senescence-like state especially in p16-expressing cells apparently enhanced effectivity of this combined treatment - though just marginally in comparison to doxycycline-treated EV-containing cells (Fig. 34A, B). Interestingly, arrested p21-expressiong cells became slightly more resistant this combined treatment than their proliferating counterparts

Figure 34. Quantification of apoptosis: HHT+ABT-737 treatment. A) Proliferating (green), arrested (blue) and senescent (yellow) were pre-treated with HHT 50ng/ml for 1 hours and then co-incubated together with ABT-737 15μM for additional 2 hours. B) EV cells (grey) were pre-treated with HHT 50ng/ml for 1 hours and then co-incubated together with ABT-737 15μM for additional 2 hours
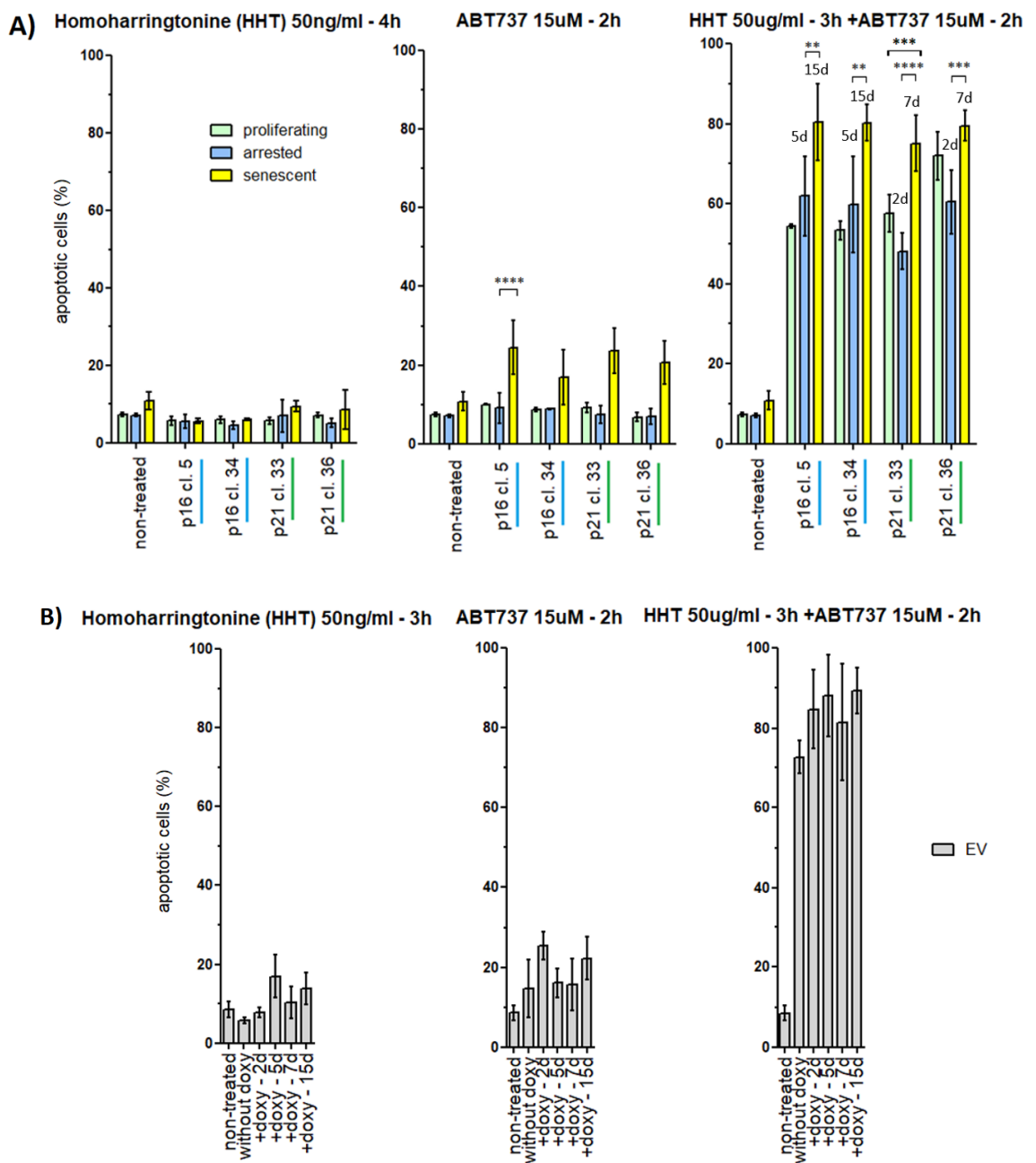
Numbers (5d, 15d etc.) above or under bars indicate number of days incubated with doxycycline during senescence induction Results are means of 3 independent biological experiments in case of senescent phenotype and 3 independent results of arrested phenotype and at least 2 independent experiments in case of EVs. Bars indicate mean and error bars indicate Std. Significance was calculated by two-way ANOVA test, ****: $p < 0,0001$, ***: $0,001 > p > 0,0001$, **: $p > 0,001$

5.4 Cells in senescent and arrested state alter expression of apoptosis-related proteins

Out of a number of proteins involved in the induction, regulation and execution of apoptosis we examined possible differences in protein expression of selected Bcl-2 family proteins, selected caspases, p53 tumor suppressor and inhibitors of caspases activation and activity (Fig. 35).

Comparison of these proteins between their proliferative, arrested and senescent state revealed gradual increase of main anti-apoptotic Bcl-2 proteins expression, Bcl-2, Bcl-Xl and Mcl-1. Level of anti-apoptotic protein Bcl-W remained unchanged. XIAP, inhibitor of activated caspases did not change its expression markedly in arrested state but did in senescent stateShort isoform cFLIP protein is known to have anti-apoptotic abilities and interestingly was downregulated in arrested and senescent state while the long version, which has dual function and can be both anti- and pro-apoptotic under certain situation, displayed increased expression. Unexpectedly, level of p53 was highest in proliferative state and decreased slightly in arrested and markedly in senescent state. Level of pro-apoptotic protein Bak remained unchanged while expression of Bax was elevated in senescent state in comparison to arrested and control cells. The same trend displayed BH3-only inducers of apoptosis protein Bid, and to lesser extent also protein Bim. Levels of Caspase-3 increased marginally only in senescent state and caspase-8 gradually increased its expression in arrested and senescent state.
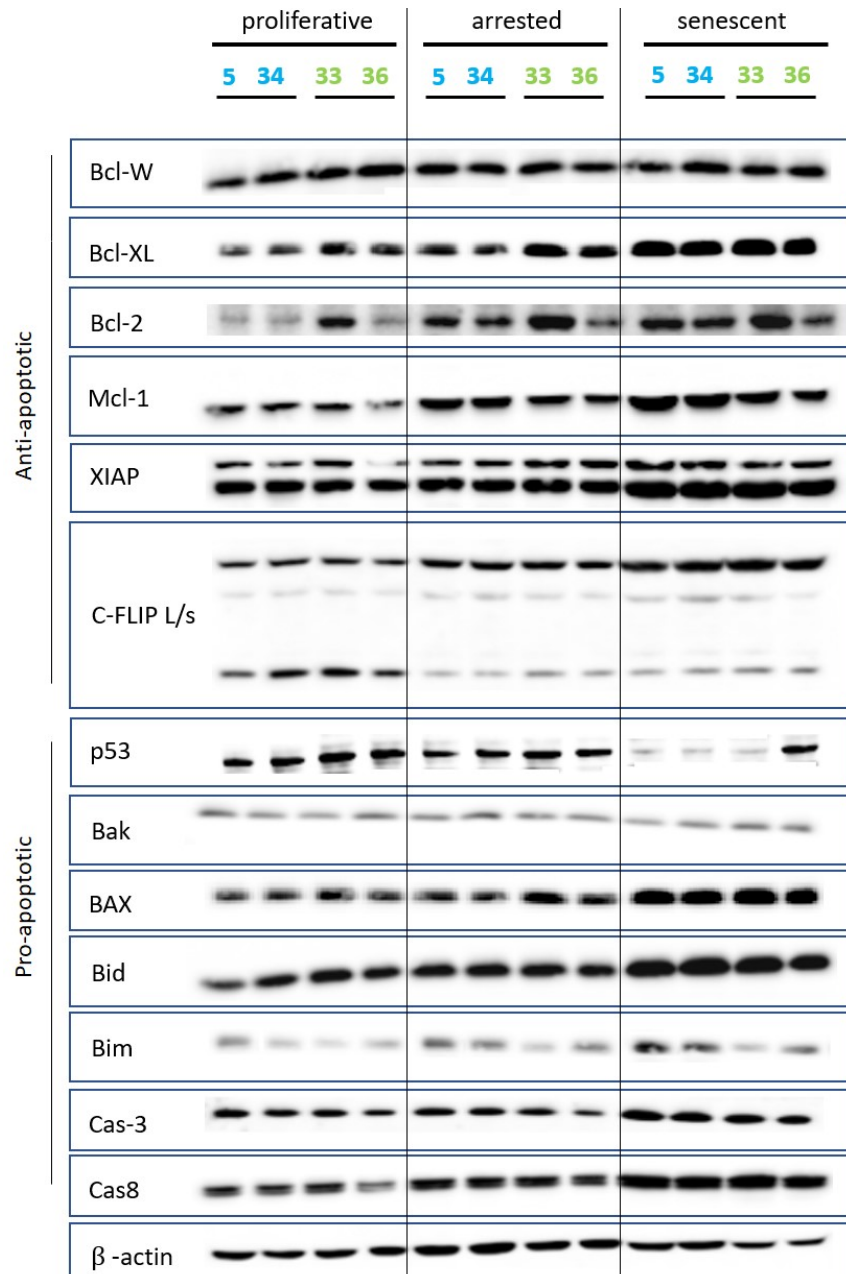
Figure 35. Detection of apoptosis executing and regulating proteins. Comparison of cell lysates of proliferating, arrested and senescent p16 (blue) and p21 (green) states of an expression of indicated antioxidant proteins. Western blots showing representative data from 3 independent experiments. β-actin was used as loading control.

5.5 Arrested and senescent cells have significantly increased mitochondrial content, ROS production and respiration.

As mentioned in literature review, senescent cells accumulate malfunctional mitochondria and elevate production of ROS, which are both related to apoptotic signaling and were furthermore shown to be mediators of senescent phenotype. In this diploma project, I used two apoptogenic substances targeting mitochondria and respiration (mitoVES, mitoTAM), providing senescent and arrest phenotype-specific results showing changes in apoptotic response. For all these reasons, I assessed mitochondrial content, ROS production and respiratory capacity of both p16 and p21 clones in proliferative, arrested and senescent state along with EV without or with doxycycline after 7 or 15 days.

Mitochondrial content and ROS production were quantified using intracellular dyes and flow-cytometry. For both analysis, cells population and singlets were gated as indicated in figure 36A. Non-stained control of each clone in each state were also included to monitor eventual non-specific signal caused by increased autofluorescence of enlarged cells (proliferative<arrested<senescent). Assessment of mitochondrial mass was always determined parallelly in two settings: with (+) and without (-) CCCP. CCCP+ was used as a control for falsely positive mitochondrial membrane potential-dependent increase of a signal. CCCP+ settings displayed only negligible differences (data not shown).

B)

	Sample Name	Subset Name	Count
	Unstained control	Single Cells	7033
	proliferative	Single Cells	8583
	Arrested	Single Cells	8850
	Senescent	Single Cells	8185

C)

	Sample Name	Subset Name	Count
	Prolif. unstained	Single Cells	5492
	Arrest. unstained	Single Cells	6150
	Senesc. Unstained	Single Cells	8872
	Proliferative	Single Cells	8461
	Arrested	Single Cells	12330
	Senescent	Single Cells	8974

Figure 36. A) Gating strategy determining population and singlets for assessment of mitochondrial content and ROS production. B) Illustrative histograms of proliferative arrested and senescent state regarding mitochondrial content (indicated in graph). Unstained samples in all states exhibited zero signal. C) Illustrative histograms of proliferative arrested and senescent state regarding ROS production. Unstained samples of all states for each clone had different value from zero, which directly correlated with cell size. Autofluorescence-dependent nonspecific signal was prior to calculations subtracted from mean signal intensity of corresponding stained samples.

Assessment of mitochondrial mass (Fig. 37A) revealed that p16-expressing cells in arrested and senescent phenotype have both equally significantly 2 to 3-fold increased mitochondrial content in comparison with their proliferating counterparts. Arrested p21-expressing cells also displayed up to 3-fold increased level of mitochondria content while senescent p21 cells had largest quantities of mitochondria about up to 5-fold higher than their proliferative counterparts and almost 2-fold higher than senescent p16 cells.

Production of ROS displayed similar trend as the increase of mitochondrial content (Fig. 37B), which was however less pronounced in p16-expressing cells. ROS production by p21 cell in arrested and senescent cell was significantly elevated. Furthermore, p21-clone 33 exhibited even significant difference between arrested and senescent state.

Interestingly p16-clones in arrested and also in senescent state, both manifested significantly smaller increase in ROS production as p21-clone 33 in corresponding state. Also difference of ROS production between senescent p21-clones 33 and 36 was also significantly increased. In EV-containing H28 cells, there was detected slightly dropping trend of mitochondrial content treated with doxycycline and seemed to directly correlate with the length of incubation with doxycycline (Fig. 37). On the other hand, production of ROS followed opposite trend, steadily increasing. In all cases, changes in in EV-containing H28 cell culture, related to doxycycline, were insignificant.
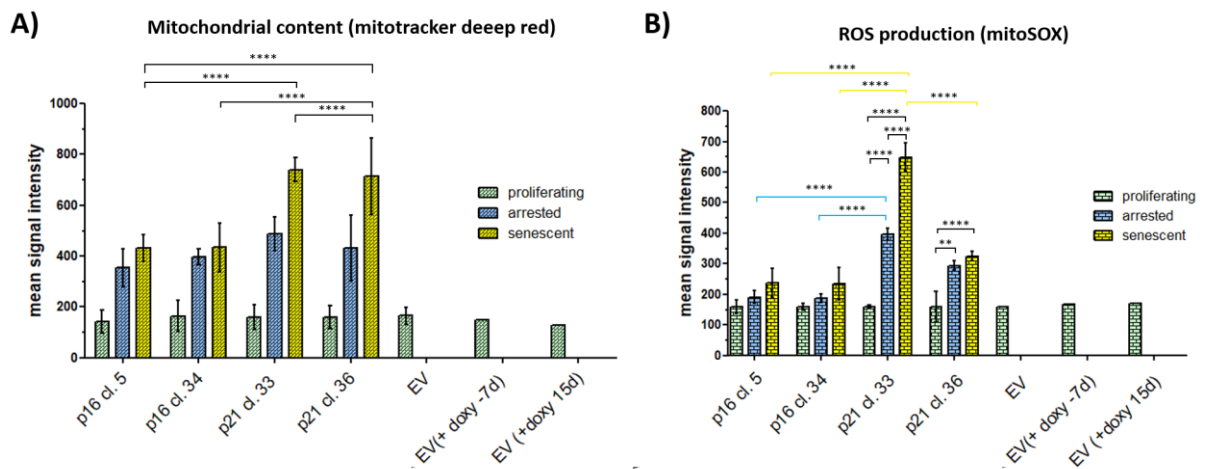
Figure 37. Quantification of mitochondrial content and ROS production. Comparison of proliferating (green), arrested (blue), senescent(yellow) H28 p16- and p21-expressing cells together with H28/EV cells without doxycycline (EV) or with doxycycline for 7days (EV (+ doxy- 7d)) or 15 days (EV(+doxy -15d)) in A) Mitochondrial content. B) ROS production. Results are averaged of 4 independent biological experiments in case of senescent cells and EV (without doxycycline, 3 experiment in case of arrested cells and only 1 experiment in case of EV with doxycycline (+7 or +15days). Bars indicate means and error bars represent standard deviation.

Increase of mitochondrial content in arrested and senescent cells prompted us to analyze mitochondria in these cells also by different approach. Proliferating and senescent cells were stained with MitoTracker deep red and subjected to live-imaging confocal-microscopy (Fig. 38). Captured images demonstrate that senescent cells indeed accumulate mitochondria and they are not fragmented but tubular, forming huge networks. A visible difference in mitochondrial content was also between p16 and p21 senescent clones, which was also in agreement with data from flow cytometry (Fig. 37 A).
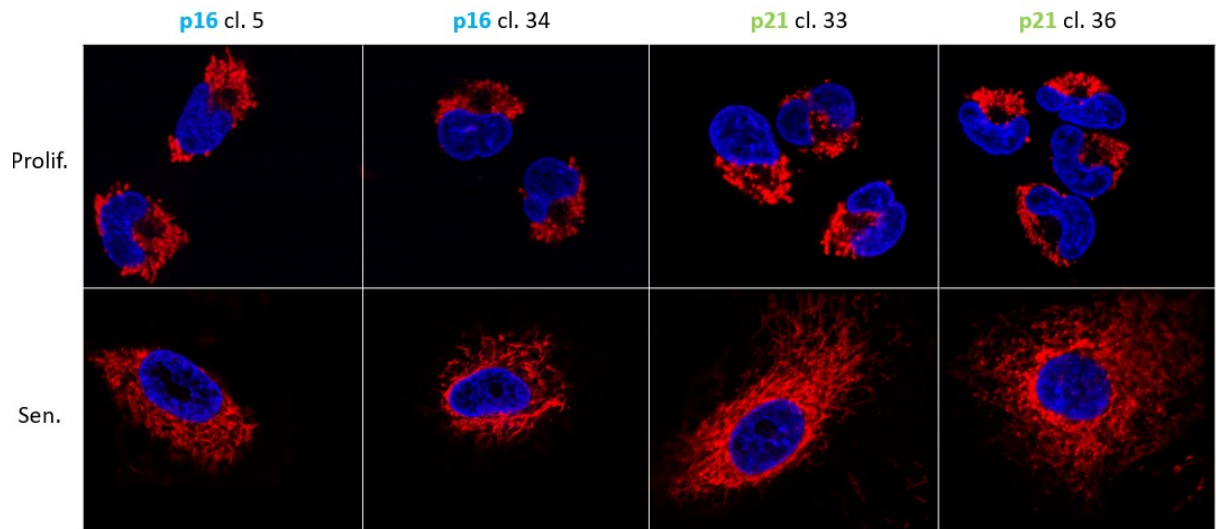
Figure 38. Detection of mitochondrial content by confocal microscope. Cells were incubated with mitotracker DEEP red and subjected to live-imaging microscopy on confocal microscope. Comparison of p16 (blue) and p21 (green) clones between proliferative and senescent state.

Respiration, acidification and ATP production was assessed with Seahorse analyzer. Basal respiration increased only negligibly in all clones in all states however maximal respiration dramatically increased and correspondingly correlated with mitochondrial content and production of ROS (Fig. 39). Ahler et al. (2013) published that doxycycline at concentration of 1µg/ml alter metabolism, markedly lowered OCR and increased lactate production in different cancer cell lines, therefore we also included EV-containing control cells incubated with doxycycline and in contrast with published data we did not observe any changes in OCR or glycolysis (Fig. 39, grey columns). Both arrested and senescent cells increased also acidification rate, again following the same trend as trend of mitochondrial content increment. Figure 40. visually represent time-lapse of both OCR and ECAR measurements with indicated treatments, demonstrating different steepness and rapidness of changes in proliferating arrested and senescent-like states.
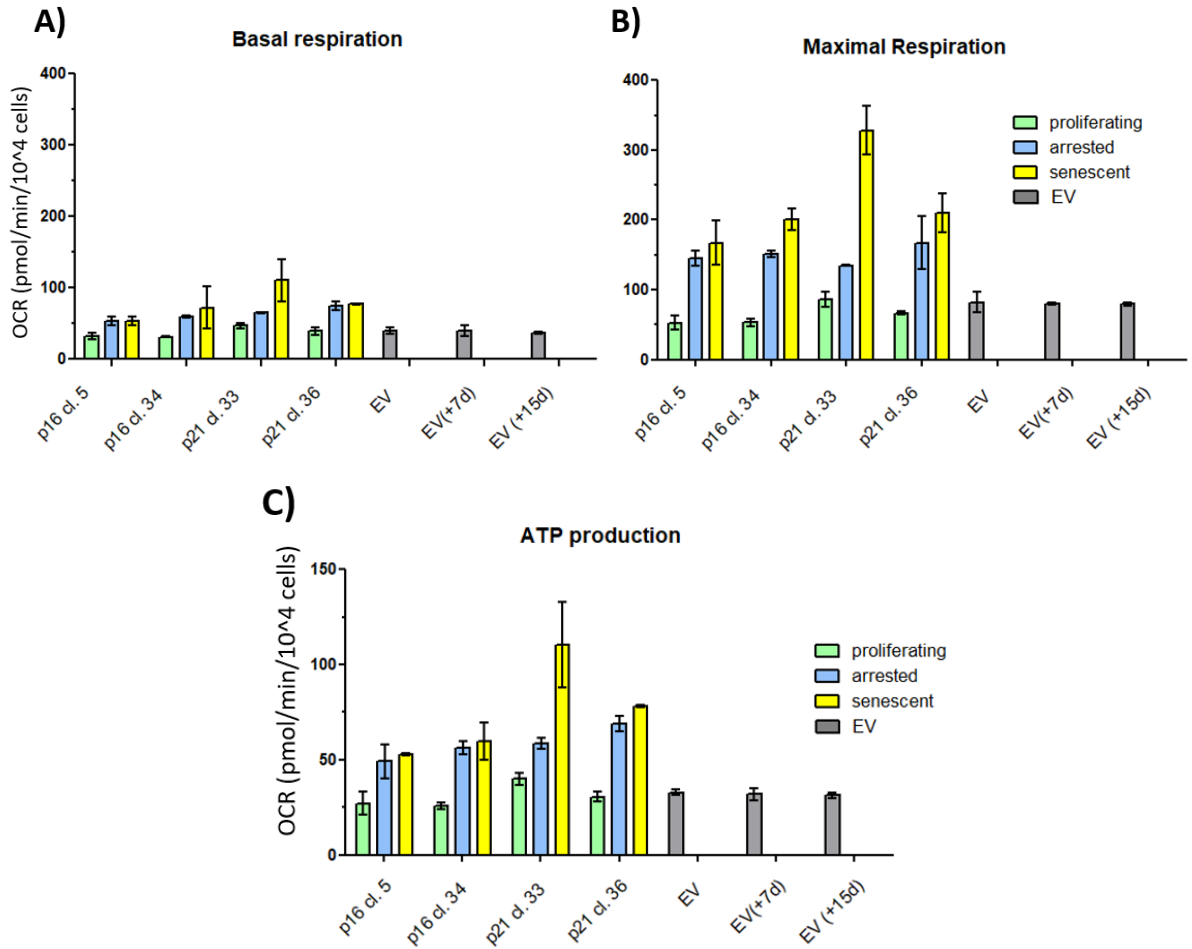
Figure 39. Assessement of mitochondria energy metabolism. Comparison of proliferating (green), arrested (blue), senescent(yellow) H28 p16- and p21-expressing cells together with H28/EV cells (grey) without doxycycline (EV) or with doxycycline for 7days (EV (+ doxy- 7d)) or 15 days (EV(+doxy -15d)).   A) Basal respiration. B) Maximal respiration. C) ATP production. Results are averaged of 2 independent biological experiments and only one experiment in case of EV with doxycycline (+7 or +15days). Bars indicate means and error bars represent standard deviation.

A)

OCR clone 5

OCR clone 34

OCR clone 33

OCR clone 36

B)

ECAR clone 5

ECAR clone 34

ECAR clone 33

ECAR clone 36
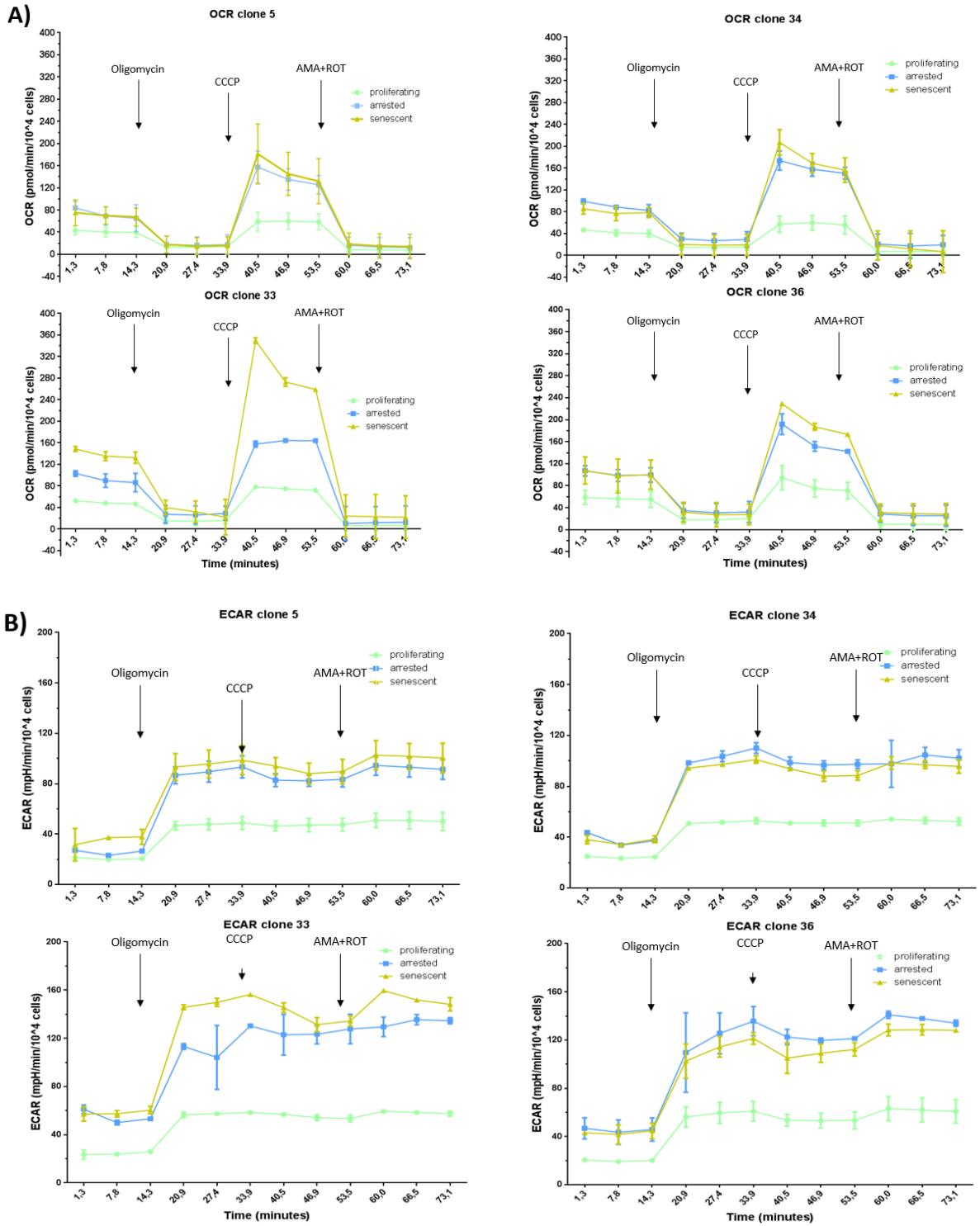
C)
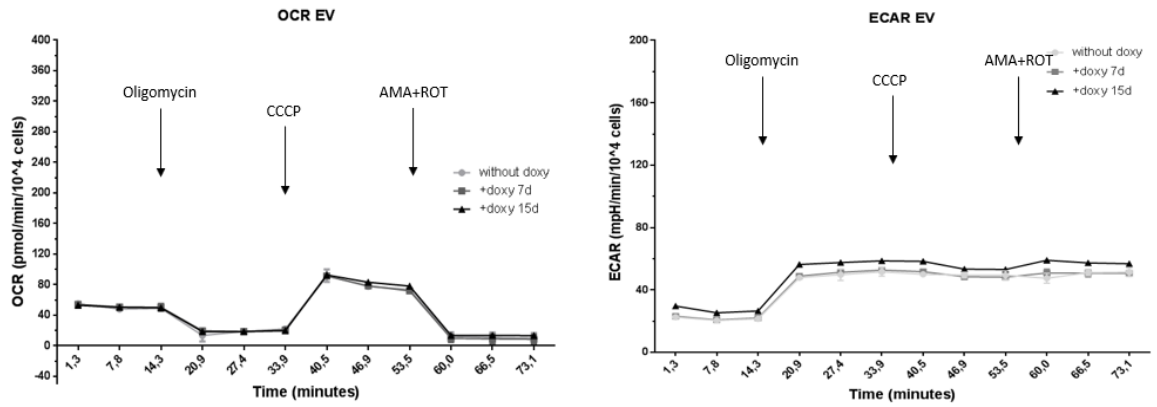
Figure 40. Time-lapse of OCR and ECAR experiments. Cells were seeded into individual well on special seahorse plate and injected in 3 different time points with Oligomycin, CCCP and Antimycin with Rotenone. Each point on curve represent measurement of OCR/ECAR. Comparison of proliferating (green), arrested (blue) and senescent(yellow) states A) OCR. B) ECAR. C) OCR and ECAR of EV without or with doxycyline incubated for 7 (+doxy 7d) or 15(+doxy 15d) days.

6   Discussion

It is already well known, that cyclin-dependent kinase inhibitors (CDKIs) p16 (and related proteins) and p21 are main inducers of the cellular senescence that can be triggered by two main signalling pathways: p16/Rb and p53/p21. Cellular senescence as a state of irreversible cessation of the cell cycle can be triggered by build-up (ageing) or by acute (irradiation, various drugs) cellular stress and is usually accompanied by (persistent) DNA damage and changes in cellular metabolism and cellular secretome (known as SASP – senescence associated secretory phenotype). Generally, senescent state can be imposed in primary and cancer cells by sub-lethal doses of DNA/replication-hampering agents such as bromodeoxyuridine (BrdU). In this diploma project, we employed inducible expression of p16 or p21 CDKIs on a model wild type p53-expressing mesothelioma cancer cell line H28 and characterized respective clonal cell cultures (cellular phenotype, metabolism and particularly their response to various intrinsic and extrinsic apoptogens) and also pointed to notable differences in effects imposed by either of these CDKIs. Moreover, senescent (or senescence-like) and by us defined arrested phenotypes achieved through inducible expression of CDKIs was established without inflicting DNA damage, as it is in case of stress induced senescence models by g.e. DNA stress-inducing drug such as BrdU.   Defining arrested and senescent states also allowed us to map the evolvement of apoptotic responses imposed by various apoptogens.

6.1 Characterisation of H28 clonal cultures with mid- and long-term expression of p16 and p21 CDKIs

Upregulated expression of CDKIs p16 and p21 is a common feature and also a main reason of senescent phenotype. Constitutive ectopic expression of proteins p16 and p21 led to senescence-like phenotype in breast cancer cell line MDA-MB-231 and human fibroblast cells (Capparelli et al. 2012; Coppé et al. 2011; McConnell et al. 1998). In our cellular model we took an advantage of inducible expression either of these two major pro-senescent CDKIs and combining microscopy with biochemical (activation of

senescence-associated b-galactosidase/Sa-β-gal) and cell cycle analyses revealed that p16-expressing cells required much longer induction period then p21-expressing cells to become Sa-β-gal positive, as well as for getting arrested in cell cycle. Moreover, p16-expressing cells did not enlarge to the extent of p21 cells and they also displayed significant heterogeneity in Sa-β-gal staining. Analysis of cell cycle arrest revealed the same trend of slower stepping-out from the cell cycle for p16-expressing cells. However, p21 unlike p16 is capable of arresting cells both in G1 and G2 phase(Ando et al. 2001; Cayrol et al. 1998) and thus can more effectively impose cell cycle arrest. Indeed, we also noticed apparent increased distribution of p21-expressing cells in comparison to p16-expressing cells (Fig. 15) in G2 phase after addition of doxycycline (Fig. 18) confirming a stronger grip of p21 protein on the enforcement of the cell cycle arrest. Based on SA-β-Gal data, microscopic and cell cycle analysis we were able to define arrested or pre-senescent and senescent state of p16- and p21-expressing cells and all our further experiments were based on these findings.

To further address and describe different phenotypes of senescent p16 and p21 cells, these cells were stained cells for another marker of proliferation, protein Ki67 that is expressed only in proliferating cells and together with senescent specific γH2AX foci and Sa-β-gal is used for assessment of cellular senescence (Lawless et al. 2010). Senescent specific γH2AX foci are maintained by increased ROS production and they serve as reservoir for persistent DDR that is required for establishment of a senescence. Ki67 staining revealed, that about the half of the p16-expressing cells display positivity for this marker while manifested negativity for γH2AX. p21 senescent cells on other hand were Ki67-negative and one third of cells exhibited γH2AX foci. These data are in apparent contrast with paper published by Pospelova et. Al (2009) showing, that the mere upregulation of these two CDKi proteins was sufficient to induce senescent specific γH2AX, in mouse embryonal fibroblast. These differences could eventually be accounted to using tumour cell line and not primary cells, which could possibly have mutated (thus non-functional) some of the proteins linked to p16-mediated ROS production. However, protein p21 was also unable to elicit overall positive staining for γH2AX.

For further elucidation of apparent proliferative potential of p16-expressing senescent cells we employed two additional assays - EdU incorporation and assessment of cellular proliferation using IncuCyte live cell analysis system. EdU assay indeed confirmed that over 24hr period there were 50-60% of the senescent p16-expressing cells in a proliferative state and thus confirmed Ki67 positivity. Moreover, homogenous distribution of Ki67 positive cells excluded possibility, that few cells escaped cell cycle arrest and subsequently overgrew the other arrested cells. Long-term growth assay using the IncuCyte system also revealed that the vast majority of senescent p16-expressing cells do proliferate even with senescent phenotype, however at various speed. Length of cell cycle of the p16-expressing cells was observed to increase from 20hours to up to 5 days, possibly explaining why only 50-60% of cells were Ki-67 positive or incorporated EdU over 24hours. IncuCyte-assisted acquisition of cell proliferation also revealed that upon doxycycline withdrawal, senescent phenotype reverted for both p16 and p21 cells. Needlessly to say, that almost all p16 cells reverted their phenotype while approximately ¼ of senescent p21 cells remained large and did not divide. Interestingly, this observation correlates with percentage of γH2AX-positive p21-expressing senescent cells. Moreover, despite stronger phenotype of senescent-p21 cells, data acquired by IncuCyte analysis showed that after doxycycline withdrawal, they return to proliferation noticeably faster than senescent p16-expressing cells. Possible explanation of this phenomenon could be attributed to the fact that p21-expressing cells have up to 50% of the population arrested in G2 phase, so they do not need to replicate DNA and hence can undergo mitosis faster than p16-expressing cells. Despite the acquired markers of cellular senescence (cell spreading, SA-b-Gal positivity and no Ki67 and EdU positivity in p21-clonal cultures) present in both p16- and p21-expressing senescent cells, these cells upon doxycycline withdrawal rapidly restore proliferation (i.e. cessation of p16/p21 expression). Especially for cancer cells was shown that they can escape cellular either spontaneously both in vivo and in vitro or upon exposure to apoptotic stimuli (Roberson et al. 2005; Yang et al. 2017), though in our case it is also possible that just with imposed CDKIs ectopic expression these particular cancer cells just enter only pre-senescent state or undergo incomplete senescent transformation.

ROS and mitochondria apparently important players in in establishing senescent phenotype (Correia-Melo et al. 2016) and also our data indicate mitochondrial participation in p16- and p21-mediated induction of senescence-like phenotype in H28

cells. Both p16- and p21-expressing cells did in their senescence-like state enhanced ROS production and multiplied their mitochondria. Interestingly, p21-expressing clonal cultures showed higher ROS production as well as higher mitochondrial content than p16-expressing cells. These results correlated with observed positivity of γH2AX (linked to ROS production/mitochondrial content), which was detected exclusively in p21 senescent cells. Positivity of Sa-β-Gal activity was also shown to be suppressed in senescent cells upon parkin-mediated clearance of mitochondria (Correia-Melo et al. 2016), suggesting that enlarged size along with more intense Sa-β-Gal staining in p21 cells could also be related to increased mitochondrial mass. As was described in literature review, p53/p21 pathway possesses additional mechanism through which can be increased mitochondrial content and ROS production, thus possibly explaining weaker phenotype of p16 cells (Bartoletti-Stella et al. 2013; Passos et al. 2010). In summary, it looks like that p16-signalling pathway was not sufficient to generate required amount of ROS, necessary for the formation of γH2AX (DDR), thus lacking part of pro-senescent signalling and eventually could partly explain weaker senescent phenotype. Downregulation of the mitochondrial ANT2 transporter was reported as one of the features of e.g. senescent fibroblasts(Kretova et al. 2014). However, in our senescent-like H28 cells expressing p16 or p21proteins we did not notice any downregulation of ANT2 (data not shown), again pointing to a hypothesis, that these cells did not enter fully senescent state.

In respect to continuous proliferation of already senescent or senescence-like cells, there might be several possible reasons for our finding that upregulation of CDKIs was not sufficient to induce irreversible cell cycle arrest and lasting senescence.

1) In cancer cells, that are usually driven to proliferation, simple blocking of the cell cycle without any additional stress like damaged DNA is not enough to impose a full stop senescence. This statement is entirely valid for p16-expressing cells but apparently not for p21-expressing cells, which showed stronger ROS production and likely ROS-mediated DNA damage at least in 20-30% of cells. Also, upon releasing p21 block majority of p21-expressing cells restored proliferation but some of them (maybe those with damaged chromosomal DNA) remained in senescence-like state.

2) Doxycycline-related phenomenon. Proapoptotic stimuli can apparently reverse or mute senescent phenotype in both caspase-3-dependant and -independent manner

(Yang et al. 2017). Caspase-3 cleaves protein Rb, which when degraded, can no longer sequester transcription factor E2F (Jänicke et al. 1996). Degradation of Rb protein would subsequently abolish regulatory effects of CDKs and CDKIs on release of E2F. Moreover, it was shown, that doxycycline itself can activate caspase-3, -9 and cause release of cytochrome C (Onoda et al. 2006). However, this published effect was observed on different cell line (HT-29) using concentration of doxycycline 20times higher as used in for induction of p16 and p21 proteins in our clonal cultures. Despite lower concentration of doxycycline, total level of the Rb protein was indeed lower in both arrested and senescent cells (Fig. 22). Another contribution of doxycycline to incomplete senescent transformation could be related to its known function as an inhibitor of small mitochondrial ribosomal subunit resulting in inhibition of mitochondrial biogenesis (Kroon and Van Den Bogert 1983) (which was indeed observed Fig. 37A, however only negligibly). This would apparently hamper pro-senescent signalling that leads to increased mitochondrial mass.

In compliance with observed increase of mitochondrial mass and ROS production, we detected increased respiration (OCR) in both p16- and p21-expressing arrested and senescent cells. Levels of glycolysis represented by ECAR measurement was also elevated in comparison with proliferative cells. These results were in agreement with published data (Hubackova et al. 2018; Korolchuk et al. 2017) showing both increased OCR and glycolysis in senescent cells.

6.2 Response of the proliferating, arrested and senescent H28 cells expressing p16 or p21 to apoptotic stimuli

Principal initial aim of this Thesis was to compare and analyse eventual alterations of apoptotic signalling between arrested and senescent state imposed by inducible expression of p16 or p21 CDKIs.

We used intrinsic and extrinsic apoptogens and their combinations in specific protocols for the induction of apoptosis in proliferating, arrested and senescent H28 clonal cultures as well as in EV-containing H28 cells and Annexin V/Hoechst 33258 staining and flow cytometry for its detection and quantification. Senescent cells such as

fibroblasts were considered to enhance their resistance to apoptosis through upregulation of antiapoptotic Bcl-2 proteins, modulation of IGF pathway or caspase-3 downregulation(Hampel et al. 2005; Marcotte, Lacelle, and Wang 2004). Though other published data document that senescent cells are more prone to die by FasL-mediated apoptosis and this enhancement is likely caused by upregulation of FasR through NFκb mediated autocrine secretion of IFNγ and TNFα (Crescenzi et al. 2011) and/or by direct Nfκb-mediated enhancement of FasR expression (Liu et al. 2012). However, for FasL-induced apoptosis of our H28 clonal cultures we encountered one technical problem, which hampered our dissection of this extrinsic signalling in arrested and senescent cells. We found that just doxycycline treatment of our control EV-containing H28 cells for various time periods enhanced FasL-triggered apoptosis to even higher extent as we observed in arrested and senescent p16- and p21-expressing clonal cultures thus making our data irrelevant. Effect of doxycycline on Fas-mediated apoptosis was already documented and can be either positive - it increased Fas-mediated apoptosis in Jurkat cells (Liu, Kuszynski, and Baxter 1999) by elevating expression of both FasR and FasL or negative - suppressed sensitivity to FasL in Hela cells (Yoon et al. 2015).

Interestingly, even despite both p16- and p21-expressing senescent cells manifested increased mitochondria mass, increased basal ROS production and elevated levels of mitochondrial complex II (represented by subunit SDHA) markedly increased resistance to mitoVES. However, senescent H28 cells induced by BrdU treatment were in contrast to p16-and p21-expressing clonal cultures more sensitive to mitoVES treatment (Nováková, 2014). Discrepancy could be accounted to different ways of senescence induction, as BrdU inflicts massive DNA damage. Combined effect of massive DNA damage together with acutely increased ROS production caused by mitoVES treatment, could then eventually explain higher sensitivity to mitoVES in case of Nováková (2014). Enhanced anti-oxidant defence was recently described as an efficient tool in protecting epithelial and quiescent endothelial cells from ROS-mediated cell death (Blecha et al. 2017; Haendeler et al. 2004). Normally, Nrf2-Keap1 pathway functions as sensor of oxidative stress activating expression of antioxidant proteins and in agreement both p16 and p21 senescent cells with increased ROS production displayed elevated levels of antioxidant proteins. Needlessly to mention that senescent p16-expressing cells produced markedly less ROS then p21 cells, but it was apparently enough to induce equally strong (or maximal) antioxidant response as in senescent p21 cells. Arrested

and again especially senescent p16- and p21-expressing cells upregulate expression of anti-apoptotic proteins (Fig. XX), that might be together with elevated antioxidant defence responsible for increased resistance to mitoVES-triggered apoptosis. Moreover, both arrested cells p16- and p21-expressing cells that with exception of Gpx1 and slightly elevated Bcl-2 and Mcl-1 levels do not express anti-apoptotic and anti-oxidant proteins to such levels as do senescent cells and correspondingly did not show any enhanced resistance to mitoVES-triggered apoptosis.

MitoTAM as new apoptosis-inducing agent targeting complex I was proven as efficient cell death inducer in a number of cancer cells both in vitro and in vivo (Rohlenova et al. 2017). However, in H28 cells and derived arrested/senescent clonal cultures we had great difficulties to explain variations in its effectivity with tendency being more efficient in inducing apoptosis of arrested cells especially of p21-expressing cells. This our observation contrasts with the current study of Hubáčková et. al. (2018) where they showed that replicative senescent fibroblasts or stress-induced-senescent (BrdU or Doxorubicin) cells are significantly more sensitive to mitoTAM treatment. They proved, that cell death induced by mitoTAM in senescent cell is mediated by destabilization of mitochondrial potential, which is linked downregulated levels of ANT2 in senescent cells (Kretova et al. 2014). However, as already mentioned in previous part of the discussion, we did not detect any changes in expression of ANT2, which could be one of the reasons behind relatively low sensitivity of senescent H28 clonal cultures to this agent. Hubáčková et. al. (2018) also claimed that cell death of senescent cells is independent of ROS production induced by blockage of mitochondrial complex I. They suggested that this could be due to abilities of senescent cells to cope more effectively with oxidative stress, which agrees with our data showing upregulation of antioxidant proteins along with decreased sensitivity of senescent cell to ROS-mediated cell death by mitoVES.

ABT-737 and its just Bcl-2-targeting sibling ABT-199 are very efficient in inducing apoptosis and eliminating tumour cells and ABT-199 was recently under trademark venetoclax approved for treatment of chronic leukemia patients (Scheffold et al. 2014) Interestingly, ABT-737 was also effective in eliminating senescent cells (Yosef et al. 2016), which could be related to upregulated levels of Bcl-W and Bcl-XL in senescent state (in their study in both replicative and stress-induced senescence). We also observed relatively low enhancement of ABT-737-induced apoptosis in senescent p16-

and p21-expressing clones that express higher levels of Bcl-Xl, but these data were partly blunted by results from control EV-containing H28 cells – those were also sensitized to ABT-737 treatment just by doxycycline. Combined HHT+ABT-737 treatment induced massive apoptosis in all treated cells partly also enhanced by doxycycline treatment and again with a trend of stronger HHT+ABT-737 pro-apoptotic effect in senescent clonal cultures.

Senescent cells, regardless of p16 or p21 proteins induction, manifested increased resistance to TRAIL alone, and also to HHT + TRAIL combination. These results are this time in agreement with results of Nováková (2014) where she demonstrated that senescent cell induced by BrdU are also more resistant to both of these treatments. She also demonstrated 50% downregulation of surface expression of DR4 and DR5 receptors, and also showed elevated levels of both Long and Short isoforms of protein c-FLIP, which, however, did not play role in this resistance. Counter-intuitively to increased resistance, we observed downregulation of anti-apoptotic short isoform of protein c-FLIP together with increasing levels of its long ambiguous isoform. Likely, resistance of senescent p16- and p21-expressing cells toward HHT+TRAIL seems to be a cumulative effect of generally elevated levels of anti-apoptotic proteins together with possibly decreased expression of DR4, DR5.

Despite increased expression of both pro-apoptotic and anti-apoptotic proteins, senescent P16- and p21-expresing cells apparently enforced their resistance to ROS-dependent intrinsic and TRAIL-participating extrinsic stimuli. Notably, significantly increased ROS production together with mitochondrial mass in senescent p21 cells in comparison to senescent p16 cells did not seem to manifest in response to apoptogenic treatments despite directly affecting key players of intrinsic apoptotic pathway. As the p16- and p21-expressing cells manifesting only senescent-like phenotype and not true senescence (characterised by permanent cell cycle arrest), it is apparent, that changes in apoptotic response are not consequence of senescent state per se, but are rather result of a pro-senescent-signalling itself, leading to a senescent state.

7 Summary

1. We established conditions for the induction of arrested and senescent-like phenotype in H28 cells by doxycycline-mediated upregulation of CDKIs p16 and p21 expression.

2. We characterized senescent-like phenotype of p16 and p21 proteins-expressing H28 cells. We found that senescent-like phenotype of p21-expressing cells is more pronounced then of p16-expressing cells. Additionally, we observed that, senescent-like phenotype, as well as arrested phenotype, is reversible upon doxycycline withdrawal.

3. We analysed and compared response of p16- and p21-expressing H28 cells in proliferative, arrested and senescent state to apoptotic stimuli. We found that both p16- and p21-expressing senescent clones are more resistant to mitoVES, HHT+TRAIL, while are more sensitive to Bcl-2 antagonist ABT-737.

4. We uncovered that both p16 and p21-expressing H28 cells in arrested and especially in senescent state elevate expression of antioxidant-defence proteins such as Catalase, Gpx1, SOD1, SOD2, Prx3.

5. We discovered that senescent p21-expressing clones harbour larger mitochondrial mass and increase ROS production in comparison to senescent p16-expressing clones as well as to their proliferative counterparts. In correlation with these findings, we also observed increased overall energy metabolism represented by increased basal respiration, maximal respiration by mitochondria and also elevated levels of glycolysis represented by extracellular acidification rate.

6. We compared the expression of apoptosis related proteins in p16- and p21-expressing H28 cells in arrested and senescent state. We detected significant increased levels of Bcl-XL, Bcl-2, Mcl-1, XIAP, Bax, Bid, Caspase-8 and slight increase of protein Bim, Caspase-3 and long isoform of c-FLIP. We also noticed attenuated expression of a short isoform of c-FLIP, p53 and steady levels of pro-apoptotic protein Bak.

7. Our results indicate, that altered apoptotic responses of senescent cells linked to senescent phenotype are independent of the terminal cell cycle arrest.

8 References

Acosta, Juan C. et al. 2008. "Chemokine Signaling via the CXCR2 Receptor Reinforces Senescence." *Cell* 133(6):1006–18.

Agilent, (2018). Wave software 2.6: „Software." Retrieved from: Seahorse XF Cell Mitostress. Test Equations & Example Calculations. "

Ahmad, Tanveer et al. 2015. "Impaired Mitophagy Leads to Cigarette Smoke Stress-Induced Cellular Senescence: Implications for Chronic Obstructive Pulmonary Disease." *FASEB Journal* 29(7):2912–29.

Akin, Serkan, Taner Babacan, Furkan Sarici, and Kadri Altundag. 2014. "A Novel Targeted Therapy in Breast Cancer: Cyclin Dependent Kinase Inhibitors." *Journal of B.U.ON.* 19(1):42–46.

Allen, George F. G., Rachel Toth, John James, and Ian G. Ganley. 2013. "Loss of Iron Triggers PINK1/Parkin-Independent Mitophagy." *EMBO Reports* 14(12):1127–35.

Ando, Tomoaki et al. 2001. "Involvement of the Interaction between P21 and Proliferating Cell Nuclear Antigen for the Maintenance of G2/M Arrest after DNA Damage." *Journal of Biological Chemistry* 276(46):42971–77.

Ashkenazi, Avi. 2002. "Targeting Death and Decoy Receptors of the Tumour-Necrosis Factor Superfamily." *Nature Reviews Cancer* 2(6):420–30.

Baar, Marjolein P. et al. 2017. "Targeted Apoptosis of Senescent Cells Restores Tissue Homeostasis in Response to Chemotoxicity and Aging." *Cell* 169(1):132–147.e16.

Barradas, Marta et al. 2009. "Histone Demethylase JMJD3 Contributes to Epigenetic Control of INK4a / ARF by Oncogenic RAS." *Genes & Development* 1177–82.

Bartoletti-Stella, A. et al. 2013. "Gamma Rays Induce a P53-Independent Mitochondrial Biogenesis That Is Counter-Regulated by HIF1α." *Cell Death and Disease* 4(6):e663-11.

Beranova, Lenka et al. 2013. "The Plant Alkaloid and Anti-Leukemia Drug Homoharringtonine Sensitizes Resistant Human Colorectal Carcinoma Cells to TRAIL-Induced Apoptosis via Multiple Mechanisms." *Apoptosis* 18(6):739–50.

Bey, E. A. et al. 2004. "Protein Kinase C Is Required for P47phox Phosphorylation and Translocation in Activated Human Monocytes." *The Journal of Immunology* 173(9):5730–38.

Blecha, Jan et al. 2017. "Antioxidant Defense in Quiescent Cells Determines Selectivity of Electron Transport Chain Inhibition-Induced Cell Death." *Free Radical Biology and Medicine* 112:253–66.

Bracken, Adrian P. et al. 2007. "The Polycomb Group Proteins Bind throughout the INK4A-ARF Locus and Are Disassociated in Senescent Cells." *Genes and Development* 21(5):525–30.

Bringold, Frank and Manuel Serrano. 2000. "Tumor Suppressors and Oncogenes in Cellular Senescence." *Experimental Gerontology* 35(3):317–29.

Capparelli, Claudia et al. 2012. "CDK Inhibitors (P16/P19/P21) Induce Senescence and Autophagy in Cancer-Associated Fibroblasts, 'Fueling' Tumor Growth via Paracrine Interactions, without an Increase in Neo-Angiogenesis." *Cell Cycle* 11(19):3599–3610.

Cayrol, C., M. Knibiehler, and B. Ducommun. 1998. "P21 Binding to PCNA Causes G1 and G2/M Cell Cycle Arrest in P53-Deficient Human Colon Cancer Cells." *Oncogene* 16(3):311–20.

Chang, Bey Dih et al. 1999. "A Senescence-like Phenotype Distinguishes Tumor Cells That Undergo Terminal Proliferation Arrest after Exposure to Anticancer Agents." *Cancer Research* 59(15):3761–67.

Chen, Lin et al. 2005. "Differential Targeting of Prosurvival Bcl-2 Proteins by Their BH3-Only Ligands Allows Complementary Apoptotic Function." *Molecular Cell* 17(3):393–403.

Chen, Qin M. et al. 2000. "Involvement of Rb Family Proteins, Focal Adhesion Proteins and Protein Synthesis in Senescent Morphogenesis Induced by Hydrogen Peroxide." *Journal of Cell Science* 113 (Pt 2:4087–97.

Childs, B. G., D. J. Baker, J. L. Kirkland, J. Campisi, and J. M. van Deursen. 2014. "Senescence and Apoptosis: Dueling or Complementary Cell Fates?" *EMBO Reports* 15(11):1139–53.

Clontech, (2014). Tet One Technology: "Product overview." Retrieved from http://www.clontech.com/US/Products/Inducible_Systems/TetSystems_Product_Overview/Tet-One_Overview

Coppé, Jean Philippe et al. 2011. "Tumor Suppressor and Aging Biomarker P16 INK4a Induces Cellular Senescence without the Associated Inflammatory Secretory Phenotype." *Journal of Biological Chemistry* 286(42):36396–403.

Coppé, Jean Philippe et al. 2010. "A Human-like Senescence-Associated Secretory Phenotype Is Conserved in Mouse Cells Dependent on Physiological Oxygen." *PLoS ONE* 5(2).

Coppé, Jean Philippe et al. 2008. "Senescence-Associated Secretory Phenotypes Reveal Cell-Nonautonomous Functions of Oncogenic RAS and the P53 Tumor Suppressor." *PLoS Biology* 6(12).

Correia-Melo, Clara et al. 2016. "Mitochondria Are Required for Pro-ageing Features of the Senescent Phenotype." *The EMBO Journal* 35(7):724–42.

Crescenzi, E. et al. 2011. "NF-KB-Dependent Cytokine Secretion Controls Fas Expression on Chemotherapy-Induced Premature Senescent Tumor Cells." *Oncogene* 30(24):2707–17.

Czabotar, Peter E., Guillaume Lessene, Andreas Strasser, and Jerry M. Adams. 2014. "Control of Apoptosis by the BCL-2 Protein Family: Implications for Physiology and Therapy." *Nature Reviews Molecular Cell Biology* 15(1):49–63.

D'Alessio, M. 2005. "Oxidative Bax Dimerization Promotes Its Translocation to Mitochondria Independently of Apoptosis." *The FASEB Journal* 25:1–25.

Dalle Pezze, Piero et al. 2014. "Dynamic Modelling of Pathways to Cellular Senescence Reveals Strategies for Targeted Interventions." *PLoS Computational Biology* 10(8).

Demaria, Marco et al. 2014. "An Essential Role for Senescent Cells in Optimal Wound Healing through Secretion of PDGF-AA." *Developmental Cell* 31(6):722–33.

Devadas, Satish et al. 2006. "Granzyme B Is Critical for T Cell Receptor-Induced Cell Death of Type 2 Helper T Cells." *Immunity* 25(2):237–47.

Deveraux, Q. L. and J. C. Reed. 1999. "IAP Family Proteins [Mdash] Suppressors of Apoptosis." *Genes Dev.* 13:239–52.

Dimri, G. P. et al. 1995. "A Biomarker That Identifies Senescent Human Cells in Culture and in Aging Skin in Vivo." *Proceedings of the National Academy of Sciences of the United States of America* 92(20):9363–67.

Dixon, Scott J. et al. 2013. "NIH Public Access." 149(5):1060–72.

Dong, Lan Feng et al. 2011. "Mitochondrial Targeting of Vitamin E Succinate Enhances Its Pro-Apoptotic and Anti-Cancer Activity via Mitochondrial Complex II." *Journal of Biological Chemistry* 286(5):3717–28.

Garbe, James C. et al. 2009. "Molecular Distinctions between Stasis and Telomere Attrition Senescence Barriers Shown by Long-Term Culture of Normal Human Mammary Epithelial Cells." *Cancer Research* 69(19):7557–68.

Gewirtz, David A., Shawn E. Holt, and Lynne W. Elmore. 2008. "Accelerated Senescence: An Emerging Role in Tumor Cell Response to Chemotherapy and Radiation." *Biochemical Pharmacology* 76(8):947–57.

Gil, Jesús, David Bernard, Dolores Martínez, and David Beach. 2004. "Polycomb CBX7 Has a Unifying Role in Cellular Lifespan." *Nature Cell Biology* 6(1):67–72.

Guo, Zhi, Sergei Kozlov, Martin F. Lavin, Maria D. Person, and Tanya T. Paull. 2010. "ATM Activation by Oxidative Stress." *Science* 330(6003):517–21.

Haendeler, Judith, Verena Tischler, Jörg Hoffmann, Andreas M. Zeiher, and Stefanie Dimmeler. 2004. "Low Doses of Reactive Oxygen Species Protect Endothelial Cells from Apoptosis by Increasing Thioredoxin-1 Expression." *FEBS Letters* 577(3):427–33.

Hampel, Barbara et al. 2005. "Apoptosis Resistance of Senescent Human Fibroblasts Is Correlated with the Absence of Nuclear IGFBP-3." *Aging Cell* 4(6):325–30.

Harismendy, Olivier et al. 2011. "9p21 DNA Variants Associated with Coronary Artery Disease Impair Interferon-γ 3 Signalling Response." *Nature* 470(7333):264–70.

Hayflick, L. and P. S. Moorhead. 1961. "The Serial Cultivation of Human Diploid Cell Strains." *Experimental Cell Research* 25(3):585–621.

Hubackova, Sona et al. 2018. "Selective Elimination of Senescent Cells by Mitochondrial Targeting Is Regulated by ANT2." *Cell Death & Differentiation* 1.

Hubackova, Sona, Katerina Krejcikova, Jiri Bartek, and Zdenek Hodny. 2012. "IL1-and TGFβ-Nox4 Signaling, Oxidative Stress and DNA Damage Response Are Shared Features of Replicative, Oncogene-Induced, and Drug-Induced Paracrine 'Bystander

Senescence.'" *Aging* 4(12):932–51.

Iannello, A. and D. H. Raulet. 2013. "Immune Surveillance of Unhealthy Cells by Natural Killer Cells." *Cold Spring Harb Symp Quant Biol* 78:249–57.

Iannello, Alexandre, Thornton W. Thompson, Michele Ardolino, Scott W. Lowe, and David H. Raulet. 2013. "P53-Dependent Chemokine Production by Senescent Tumor Cells Supports NKG2D-Dependent Tumor Elimination by Natural Killer Cells." *The Journal of Experimental Medicine* 210(10):2057–69.

Itahana, K. et al. 2003. "Control of the Replicative Life Span of Human Fibroblasts by P16 and the Polycomb Protein Bmi-1." *Molecular and Cellular Biology* 23(1):389–401.

J. F. R. KERR*, A. H. WYLLIE AND A. R. CURRIEt. 1972. "Apoptosis: A Basic Biological Phenomenon With Wide- Ranging Implications in Tissue Kinetics." *Journal of Internal Medicine* 258(6):479–517.

Jänicke, R. U., P. A. Walker, X. Y. Lin, and A. G. Porter. 1996. "Specific Cleavage of the Retinoblastoma Protein by an ICE-like Protease in Apoptosis." *The EMBO Journal* 15(24):6969–78.

Jeyapalan, Jessie C., Mark Ferreira, John M. Sedivy, and Utz Herbig. 2007. "Accumulation of Senescent Cells in Mitotic Tissue of Aging Primates." *Mechanisms of Ageing and Development* 128(1):36–44.

Kang, Tae Won et al. 2011. "Senescence Surveillance of Pre-Malignant Hepatocytes Limits Liver Cancer Development." *Nature* 479(7374):547–51.

Kaplon, Joanna et al. 2013. "A Key Role for Mitochondrial Gatekeeper Pyruvate Dehydrogenase in Oncogene-Induced Senescence." *Nature* 498(7452):109–12.

Kim, Young Hwa et al. 2017. "Senescent Tumor Cells Lead the Collective Invasion in Thyroid Cancer." *Nature Communications* 8(May):1–14.

Korolchuk, Viktor I., Satomi Miwa, Bernadette Carroll, and Thomas von Zglinicki. 2017. "Mitochondria in Cell Senescence: Is Mitophagy the Weakest Link?" *EBioMedicine* 21:7–13.

Kosar, Martin et al. 2011. "Senescence-Associated Heterochromatin Foci Are Dispensable for Cellular Senescence, Occur in a Cell Type- And Insult-Dependent Manner, and Follow Expression of P16ink4a." *Cell Cycle* 10(3):457–68.

Kretova, Miroslava et al. 2014. "TGF-β/NF1/Smad4-Mediated Suppression of ANT2 Contributes to Oxidative Stress in Cellular Senescence." *Cellular Signalling* 26(12):2903–11.

Krishnamurthy, Janakiraman et al. 2004. "Ink4a/Arf." *Journal of Clinical Investigation* 114(9):1299–1307.

Krizhanovsky, Valery et al. 2008. "Senescence of Activated Stellate Cells Limits Liver Fibrosis." *Cell* 134(4):657–67.

Kroon, Am and C. Van Den Bogert. 1983. "Antibacterial Dugs and Their Interference with the Biogenesis of Mitochondria in Animal an Human Cells." *Pharmaceutisch Weekblad Scientific Edition* 5(Table I).

Krtolica, A., S. Parrinello, S. Lockett, P. Y. Desprez, and J. Campisi. 2001. "Senescent Fibroblasts Promote Epithelial Cell Growth and Tumorigenesis: A Link between Cancer and Aging." *Proceedings of the National Academy of Sciences* 98(21):12072–77.

Kuroda, Junya et al. 2008. "ABT-737 Is a Useful Component of Combinatory Chemotherapies for Chronic Myeloid Leukaemias with Diverse Drug-Resistance Mechanisms." *British Journal of Haematology* 140(2):181–90.

Lawless, Conor et al. 2010. "Quantitative Assessment of Markers for Cell Senescence." *Experimental Gerontology* 45(10):772–78.

Li, Tongyuan et al. 2012. "Tumor Suppression in the Absence of P53-Mediated Cell-Cycle Arrest, Apoptosis, and Senescence." *Cell* 149(6):1269–83.

Liu, Feiyan et al. 2012. "NF-??B Directly Regulates Fas Transcription to Modulate Fas-Mediated Apoptosis and Tumor Suppression." *Journal of Biological Chemistry* 287(30):25530–40.

Liu, Jian, Charles A. Kuszynski, and B. Timothy Baxter. 1999. "Doxycycline Induces Fas/Fas Ligand-Mediated Apoptosis in Jurkat T Lymphocytes." *Biochemical and Biophysical Research Communications* 260(2):562–67.

Liu, Xing et al. 2016. "Inflammasome-Activated Gasdermin D Causes Pyroptosis by Forming Membrane Pores." *Nature* 535(7610):153–58.

Liu, Y. et al. 2013. "Autosis Is a Na+,K+-ATPase-Regulated Form of Cell Death Triggered by Autophagy-Inducing Peptides, Starvation, and Hypoxia-Ischemia." *Proceedings of the National Academy of Sciences* 110(51):20364–71.

van Loo, G. et al. 2002. "The Serine Protease Omi/HtrA2 Is Released from Mitochondria during Apoptosis. Omi Interacts with Caspase-Inhibitor XIAP and Induces Enhanced Caspase Activity." *Cell Death and Differentiation* 9(1):20–26.

Lujambio, Amaia et al. 2013. "Non-Cell-Autonomous Tumor Suppression by P53." *Cell* 153(2):449–60.

Mantovani, Alberto, Subhra K. Biswas, Maria Rosaria Galdiero, Antonio Sica, and Massimo Locati. 2013. "Macrophage Plasticity and Polarization in Tissue Repair and Remodelling." *Journal of Pathology* 229(2):176–85.

Marcotte, Richard, Chantale Lacelle, and Eugenia Wang. 2004. "Senescent Fibroblasts Resist Apoptosis by Downregulating Caspase-3." *Mechanisms of Ageing and Development* 125(10–11 SPEC. ISS.):777–83.

McConnell, Beth B., Maria Starborg, Sharon Brookes, and Gordon Peters. 1998. "Inhibitors of Cyclin-Dependent Kinases Induce Features of Replicative Senescence in Early Passage Human Diploid Fibroblasts." *Current Biology* 8(6):351–54.

Michishita, E. et al. 1999. "5-Bromodeoxyuridine Induces Senescence-like Phenomena in Mammalian Cells Regardless of Cell Type or Species." *Journal of Biochemistry* 126(6):1052–59.

Milanovic, Maja et al. 2018. "Senescence-Associated Reprogramming Promotes Cancer Stemness." *Nature* 553(7686):96–100.

Muñoz-Espín, Daniel et al. 2013. "XProgrammed Cell Senescence during Mammalian Embryonic Development." *Cell* 155(5).

Muñoz-Espín, Daniel and Manuel Serrano. 2014. "Cellular Senescence: From Physiology to Pathology." *Nature Reviews Molecular Cell Biology* 15(7):482–96.

Nakahira, Kiichi et al. 2011. "Autophagy Proteins Regulate Innate Immune Responses by Inhibiting the Release of Mitochondrial DNA Mediated by the NALP3 Inflammasome." *Nature Immunology* 12(3):222–30.

Nováková 2014." Characterization of a role of senescence in the induction and regulation of cancer cell death" *Master Thesis, Charles University, Faculty of Science*

Ohtani, Naoko et al. 2001. "Opposing Effects of Ets and Id Proteins on P16INK4a Expression during Cellular Senescence." *Nature* 409(6823):1067–70.

Onoda, Toshinao, Takashi Ono, Dipok Kumar Dhar, Akira Yamanoi, and Naofumi Nagasue. 2006. "Tetracycline Analogues (Doxycycline and COL-3) Induce Caspase-Dependent and -Independent Apoptosis in Human Colon Cancer Cells." *International Journal of Cancer* 118(5):1309–15.

Ovadya, Yossi and Valery Krizhanovsky. 2014. "Senescent Cells: SASPected Drivers of Age-Related Pathologies." *Biogerontology* 15(6):627–42.

Passos, João F. et al. 2010. "Feedback between P21 and Reactive Oxygen Production Is Necessary for Cell Senescence." *Molecular Systems Biology* 6(347):1–14.

Pospelova, Tatyana V. et al. 2009. "Pseudo-DNA Damage Response in Senescent Cells." *Cell Cycle* 8(24):4112–18.

Roberson, Rachel S. et al. 2005. "Escape from Therapy-Induced Accelerated Cellular Senescence in P53-Null Lung Cancer Cells and in Human Lung Cancers." *Cancer Research* 65(7):2795–2803.

Rohlenova, Katerina et al. 2017. "Selective Disruption of Respiratory Supercomplexes as a New Strategy to Suppress Her2 [High] Breast Cancer." *Antioxidants & Redox Signaling* 26(2):84–103.

Rytomaa, M., P. Mustonen, and P. K. J. Kinnunen. 1992. "Reversible, Nonionic, and PH-Dependent Association of Cytochrome c with Cardiolipin-Phosphatidylcholine Liposomes." *Journal of Biological Chemistry* 267(31):22243–48.

Sagiv, A. et al. 2013. "Granule Exocytosis Mediates Immune Surveillance of Senescent Cells." *Oncogene* 32(15):1971–77.

Sagiv, Adi et al. 2016. "NKG2D Ligands Mediate Immunosurveillance of Senescent Cells." *Aging* 8(2):328–44.

Salminen, Antero, Kai Kaarniranta, and Anu Kauppinen. 2012. "Inflammaging: Disturbed Interplay between Autophagy and Inflammasomes." *Aging* 4(3):166–75.

Scheffold, Annika, Billy Michael, Chelliah Jebaraj, and Stephan Stilgenbauer. 2014. *Small Molecules in Oncology*. Vol. 201. Springer International Publishing.

Schleich, Kolja et al. 2012. "Stoichiometry of the CD95 Death-Inducing Signaling Complex: Experimental and Modeling Evidence for a Death Effector Domain Chain

Model." *Molecular Cell* 47(2):306–19.

Serrano, Manuel, Athena W. Lin, Mila E. McCurrach, David Beach, and Scott W. Lowe. 1997. "Oncogenic Ras Provokes Premature Cell Senescence Associated with Accumulation of P53 and P16(INK4a)." *Cell* 88(5):593–602.

Severino, Joseph, R. G. Allen, Samuel Balin, Arthur Balin, and Vincent J. Cristofalo. 2000. "Is β-Galactosidase Staining a Marker of Senescence in Vitro and in Vivo?" *Experimental Cell Research* 257(1):162–71.

Shidoji, Yoshihiro, Katsuhiro Hayashi, Sadaaki Komura, Nobuko Ohishi, and Kunio Yagi. 1999. "Loss of Molecular Interaction between Cytochrome c and Cardiolipin Due to Lipid Peroxidation." *Biochemical and Biophysical Research Communications* 264(2):343–47.

Sikora, Ewa, Grazyna Mosieniak, and Malgorzata Alicja Sliwinska. 2016. "Morphological and Functional Characteristic of Senescent Cancer Cells." *Current Drug Targets* 17(4):377–87.

Skouta, Rachid et al. 2014. "Ferrostatins Inhibit Oxidative Lipid Damage and Cell Death in Diverse Disease Models." *Journal of the American Chemical Society* 136(12):4551–56.

Takahashi, Akiko et al. 2006. "Mitogenic Signalling and the P16INK4a-Rb Pathway Cooperate to Enforce Irreversible Cellular Senescence." *Nature Cell Biology* 8(11):1291–97.

Taylor, Rebecca C., Sean P. Cullen, and Seamus J. Martin. 2008. "Apoptosis: Controlled Demolition at the Cellular Level." *Nature Reviews Molecular Cell Biology* 9(3):231–41.

Thiery, Jerome et al. 2011. "Perforin Pores in the Endosomal Membrane Trigger the Release of Endocytosed Granzyme B into the Cytosol of Target Cells." *Nature Immunology* 12(8):770–77.

Umar, Asad et al. 1996. "Requirement for PCNA in DNA Mismatch Repair at a Step Preceding DNA Resynthesis." *Cell* 87(1):65–73.

Verhagen, Anne M. et al. 2000. "Identification of DIABLO, a Mammalian Protein That Promotes Apoptosis by Binding to and Antagonizing IAP Proteins." *Cell* 102(1):43–53.

Wang, Eugenia. 1995. "Senescent Human Fibroblasts Resist Programmed Cell Death , and Failure to Suppress Bcl 2 Is Involved Senescent Human Fibroblasts Resist Programmed Cell Death , and Failure to Suppress Bctl Is Involved1." *Cancer Research* 2284–92.

Wang, Huayi et al. 2014. "Mixed Lineage Kinase Domain-like Protein MLKL Causes Necrotic Membrane Disruption upon Phosphorylation by RIP3." *Molecular Cell* 54(1):133–46.

Wang, Xianghong et al. 1998. "Evidence of Cisplatin-Induced Senescent-like Growth Arrest in Nasopharyngeal Carcinoma Cells Advances in Brief Growth Arrest in Nasopharyngeal." *Cancer Research* 5019–22.

Wiley, Christopher D. et al. 2016. "Mitochondrial Dysfunction Induces Senescence with a Distinct Secretory Phenotype." *Cell Metabolism* 23(2):303–14.

Xiong, Yue et al. 1993. "P21 Is a Universal Inhibitor of Cyclin Kinases." *Nature* 366(6456):701–4.

Yang, Leixiang, Jia Fang, and Jiandong Chen. 2017. "Tumor Cell Senescence Response Produces Aggressive Variants." *Cell Death Discovery* 3(June):17049.

Yoon, Jung Mi, Sushruta Koppula, Se Jong Huh, Sun Jin Hur, and Chan Gil Kim. 2015. "Low Concentrations of Doxycycline Attenuates FasL-induced Apoptosis in HeLa Cells." *Biological Research* 48:1–9.

Yosef, Reut et al. 2016. "Directed Elimination of Senescent Cells by Inhibition of BCL-W and BCL-XL." *Nature Communications* 7.

Zhang, Yu et al. 2011. "DNMT3a Plays a Role in Switches between Doxorubicin-Induced Senescence and Apoptosis of Colorectal Cancer Cells." *International Journal of Cancer* 128(3):551–61.

Supplementary data

Supplementary data find on the attached CD.

Video 1

Creator

MUDr. Lukáš Lacina, Ph.D.

Description

IncuCyte - live cell analysis of senescent p16-expressing clone No. 5 with doxycycline. Cells proliferate despite exhibiting senescent-like phenotype.

File name:

Vid.1 p16 cl. 5 + doxy

Video 2

Creator

MUDr. Lukáš Lacina, Ph.D.

Description

IncuCyte - live cell analysis of senescent p16-expressing clone No. 5 without doxycycline. Cells shrunk and restore proliferative capacity.

File name:

Vid.2 p16 cl. 5 - doxy

Video 3

Creator

MUDr. Lukáš Lacina, Ph.D.

Description

IncuCyte - live cell analysis of senescent p21-expressing clone No. 33, without doxycycline during analysis. Cells shrunk and restore proliferative capacity.

File name

Vid.3 p21 cl.33 -doxy